LBNL-40993
UC-100

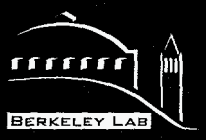

ERNEST ORLANDO LAWRENCE
BERKELEY NATIONAL LABORATORY

Selenium Fractionation and Cycling in the Intertidal Zone of the Carquinez Strait

Annual Report

October 1, 1995–December 31, 1996

P.T. Zawislanski, A.E. McGrath,
S.M. Benson, H.S. Mountford,
T.M. Johnson, E. Gabet, S.C.B. Myneni,
T.K. Tokunaga, S. Chau, and H. Wong

Earth Sciences Division

October 1997

DISCLAIMER

Portions of this document may be illegible electronic image products. Images are produced from the best available original document.

LBNL-40993
UC-100

SELENIUM FRACTIONATION AND CYCLING IN THE INTERTIDAL ZONE OF THE CARQUINEZ STRAIT

Annual Report

October 1, 1995 through December 31, 1996

P.T. Zawislanski, A.E. McGrath, S.M. Benson, H.S. Mountford, T.M. Johnson, E. Gabet, S.C.B. Myneni, T.K. Tokunaga, S.Chau, and H. Wong

Earth Sciences Division
Lawrence Berkeley National Laboratory
University of California
Berkeley, CA 94720

October 1997

This work was supported by the Assistant Secretary for Fossil Energy, National Petroleum Technology Office, of the U.S. Department of Energy, under Contract Number DE-AC03-76SF00098, and by the San Francisco Bay Regional Water Quality Control Board.

Table of Contents

List of Figures

List of Tables

Acknowledgments

The authors thank Kim Taylor and Michael Carlin of the San Francisco Bay Regional Water Quality Control Board, and Art Hartstein, Ernie Zuech, and Alex Crawley of the Department of Energy for their support. We thank Mark Conrad of LBNL for a thorough and insightful review. We also thank Greg Cutter of Old Dominion University for advice on low-level selenium analysis and cycling; Tom Bullen of USGS Menlo Park for assistance in stable isotope research; Sam Luoma of the USGS Menlo Park for consultation on selenium cycling by benthic organisms; Joan Oldfather and Claude Drugan of LBNL for analytical support; Tom Orr of LBNL for the making of custom glassware; and Jim Phillips of California State Parks, and Bill Nichols and Ron Russo of the East Bay Regional Park District for permission to collect field samples at Benicia State Park and Martinez Shoreline Regional Park, respectively.

1 Introduction

Selenium geochemistry in tidal wetlands is a topic of continuing study at Lawrence Berkeley National Laboratory. The program of studies described in this report was initiated in the fall of 1994 in response to concerns about elevated Se concentrations in waters, sediments, and biota in the Carquinez Strait. Processes by which selenium is introduced and potentially released from the sediment system have been the focus of research in 1996.

The Carquinez Strait connects the Suisun Bay and San Pablo Bay in the northern reaches of the San Francisco Estuary. Releases of effluent containing selenium (Se) by local oil refineries, San Joaquin Valley agricultural discharge, as well as natural inputs of Se over geologic time, have resulted in higher-than-average Se levels in local waters (Cutter, 1989), sediment (Johns et al., 1988), bivalves (Johns et al., 1988; Luoma et al., 1996), diving ducks (CDFG, 1988; 1989), and nonmarine birds, such as the endangered Clapper rail (Lonzarich et al., 1991). The highest Se levels in bivalves have been found near the outfall point for a refinery in eastern San Pablo Bay (SFBRWQCB, 1992). Similarly, the areas in which the highest sediment-Se levels have been observed are near oil refineries in the Carquinez Strait (SFBRWQCB, 1992). Such findings are not surprising given that, at present, oil refineries contribute as much as 75% of the total Se loading to the San Francisco Bay during low riverine flow periods, and approximately 50% of the Se load during high riverine flow periods (SFBRWQCB, 1992).

Although there have been no Se-related adverse effects observed to date, there is concern that chronic exposure to elevated Se concentrations will result in bioaccumulation and eventual toxicosis, especially in birds and fish. Recently, the clam *Potamocorbula amurensis*, an invader species from eastern Asia, was found to accumulate high levels of Se and other trace elements (Brown and Luoma, 1995). This may be due to the species high feeding rate and efficiency in bioaccumulating Se (Luoma et al., 1996), and is probably not indicative of higher Se levels in the clam's food source (phytoplankton). However, the fact remains that *P. amurensis* is now the dominant clam species in the Estuary and may cause increased Se levels in its

predators. Since bivalves, which are the primary food source for diving ducks, reside either at, or just below the sediment-water interface, the importance of understanding Se cycling and concentrations in shallow sediments is evident.

The studies described in this report fall into three categories:

- development of methodologies for Se analysis (Chapters 3, 7, 8, and 9),
- characterization of Se speciation, fractionation, and distribution (Chapters 2, 3, 5, and 8), and
- characterization and quantification of Se fluxes (Chapters 2, 4, and 6).

The ongoing research has shed light on the Se cycle in the intertidal wetlands of the Carquinez Strait. Of particular interest are the results of process-oriented studies which have helped identify the most important Se fluxes in this environment. The implications of these and other findings are discussed in detail in Chapter 10.

1.1 Summary of Previous Findings

Field and laboratory research conducted in 1994 and 1995 was described in Zawislanski et al. (1995) and the resultant preliminary conclusions are summarized below. Preliminary conclusions reached at that time were used to guide the design of research activities in 1996.

- Preliminary analyses of sediment cores, on a fairly coarse scale, indicated that there were no significant depth-trends in total Se concentrations. A more detailed sampling and analysis was recommended, including the identification of an oxic layer, in order to better define gradients in both total Se and Se fractions with depth.
- Reduced forms of Se dominate, with residual Se being an important fraction in the marsh. This was postulated to be due to an association with organic matter, and/or the presence of pyrite-Se.
- Higher Se concentrations in the sediments of the marsh relative to the mudflat were interpreted as being primarily the result of *in-situ* reduction and immobilization.
- Sudden increases in interstitial Se concentrations at the mudflat-marsh boundary were observed, but no explanation was offered.
- Interstitial Se concentrations were found to be much higher than dissolved Se concentrations in the Bay, resulting in an upward Se gradient.
- Given the observed dissolved Se concentration in the marsh, an estimate of plant tissue Se on the order of 0.5 $\mu g\ g^{-1}$ was made.

2 Selenium Distribution and Fractionation in Intertidal Sediments

Selenium distribution in the sediments of mudflats and marshes in the Carquinez Strait provides valuable information on the past and present modes of selenium deposition in these environments. Horizontal Se gradients are indicative of various mechanisms which control Se accumulation. Se fractionation and speciation in the sediment system are further clues as to the rates of Se transformations as well as its biological availability.

2.1 Site Selection

Two sites were selected in the Carquinez Strait area (Fig. 2.1). The primary criterion for this selection was the presence of an undisturbed intertidal zone, including a well developed mudflat and marsh. The sites had to be accessible but not used by the public for hiking, fishing, etc. The sites needed to be downstream of the local refineries. Both sites are described in greater detail in the 1995 Annual Report (Zawislanski et al., 1995). That description is summarized below.

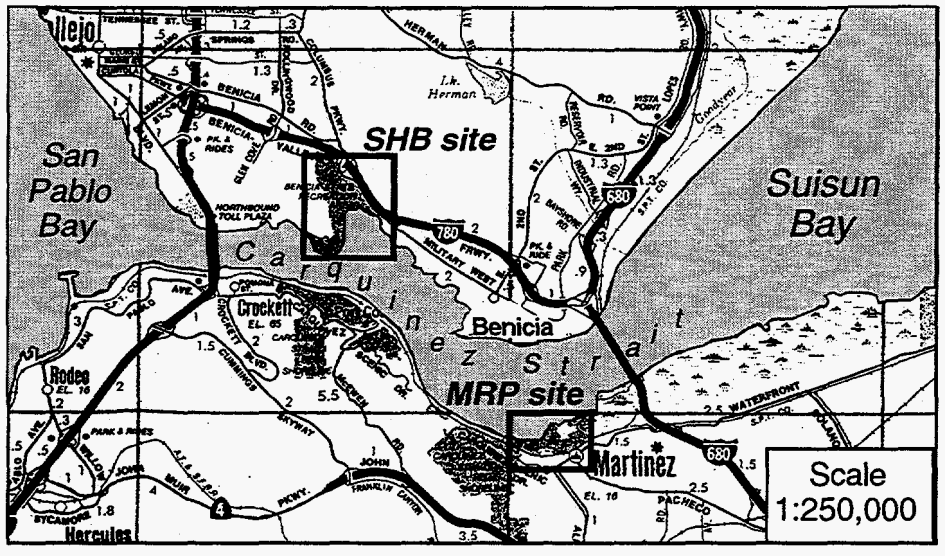

Figure 2.1 Location of field sites within the Carquinez Strait.

2.1.2 The Martinez Regional Shoreline Park Site

The Martinez Regional Park site ("MRP site") is located in the mudflats and marsh roughly 300 to 400 m west of the Martinez Marina (Fig. 2.2). This area falls under East Bay Regional Park District jurisdiction and the appropriate permits have been obtained for performing field research. The specific site from which samples were taken is some 100 to 150 m west of Arroyo Del Hambre, a creek which flows through the city of Martinez and cuts through the marsh.

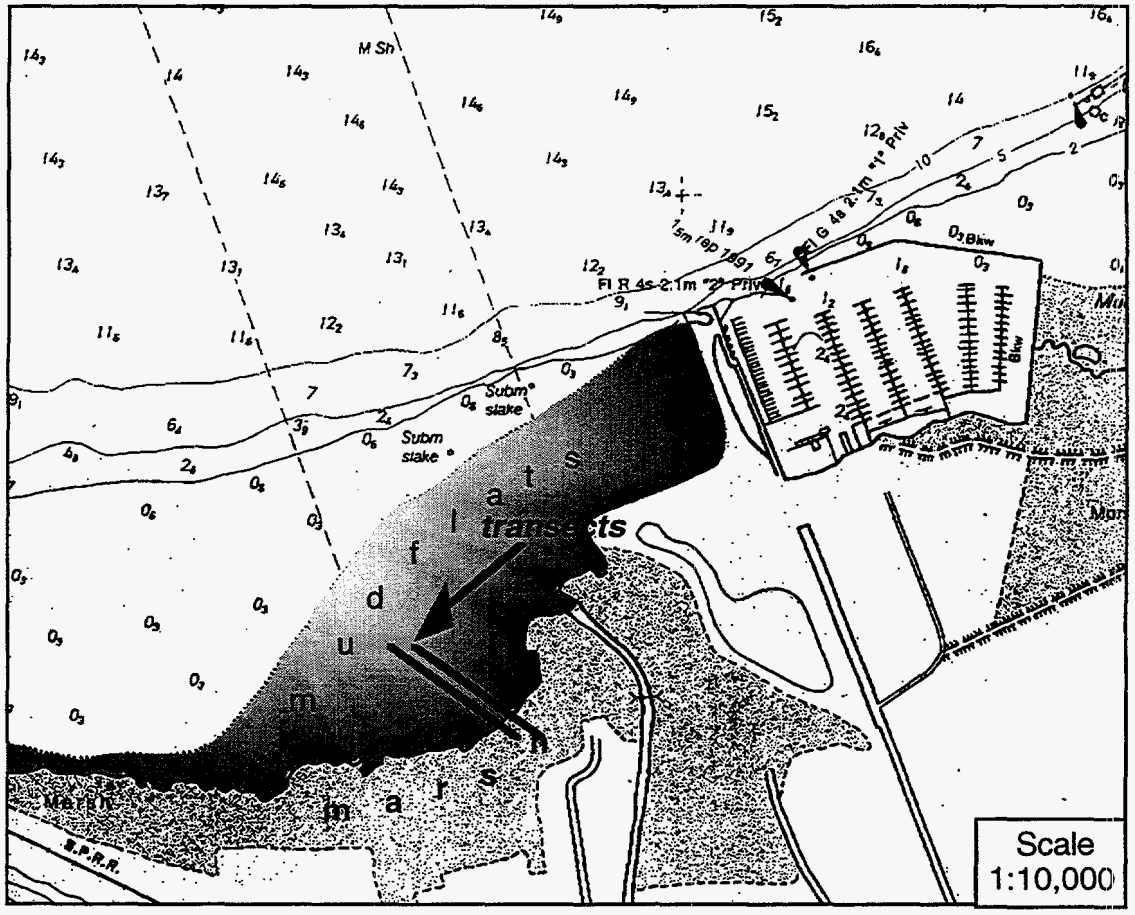

Figure 2.2 Location of sampling transects within the mudflats and marshes of Martinez Regional Park.

The MRP site is a relatively undisturbed shoreline surrounded by largely developed areas to the east and south. To the west it is bounded by a developed shoreline and the cliffs of the Carquinez Strait Regional Park. The area to the east is a popular marina and the shoreline there is rip-rap reinforced. According to Ogden Beeman and Associates (1992), the area immediately surrounding the marina, including the site, experienced significant sedimentation between 1955 and 1990 (0 to 6 ft, with the higher rates found

in subtidal and mudflat areas). The areas west of the marina, and possibly including the western edge of the site, experienced very modest net erosion over the same period of time (0 to 1 ft). The MRP site is a relatively high-energy shoreline because of its location on the Strait and its proximity to shipping channels. Strong winds out of the northwest produce high-energy waves on a regular basis, and passing ships, primarily refinery-related, can cause foot-high waves on occasion.

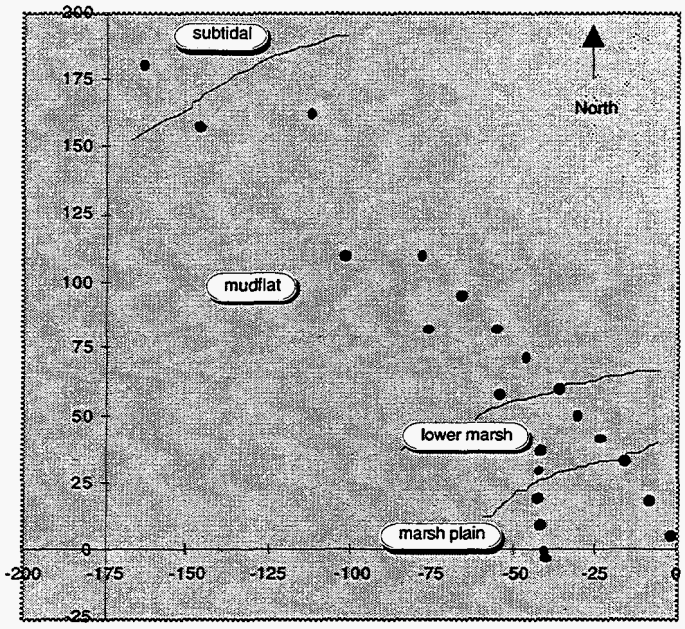

Figure 2.3 Close-up view of MRP site and sample locations. Axes units in meters.

At extremely low tide, approximately 150 m of mudflats are exposed. They are covered seasonally by a thin film of light brown diatoms. The mudflats are sandy and can be easily traversed and sampled. Because this area is open to waves and tidal flow, deposited layers are interrupted and heterogeneous in texture. Therefore, generalizations about the three-dimensional physical description of the sediment profile cannot be made. The interface between the mudflats and the marsh is well defined by a distinct rise in elevation and the appearance of plants. In the marsh, sediments are of finer texture and more homogeneous. At the surface, dead plant material forms a litter layer between 0 and 5 cm in depth.

In 1995, the interface between marsh and mudflat was sparsely vegetated by cordgrass (*Spartina foliosa*), up to 1 m tall. In the early spring of 1996, the number and

density of *Spartina* plants increased as much as ten-fold. About 2 or 3 m inland, cordgrass is intermixed with California bulrush (*Scirpus californicus*), which grows up to 2 m tall. About 10 m into the marsh, cordgrass is no longer found and the plant community is dominated by bulrush and cattails (*Typha latifolia*). Here the bulrush can grow to nearly 3 m tall while the cattails are generally 2 m tall. The density of plants here increases to as many as 100 per m^2. Mixed in with the bulrush and cattails are occasional patches of higher elevation with a variety of more upland plants, including saltgrass (*Distichlis spicata*) and pickleweed (*Salicornia* sp.). Saltgrass and pickleweed completely dominate the marsh plain, which extends for about 25 to 50 m upgradient from the lower marsh.

2.1.3 The Southampton Bay Site

The Southampton Bay site ("SHB site") is located in the southwest quadrant of the Benicia State Recreation Area, northeast of Dillon Point (Fig. 2.4). This area is part of the California State Park system. The SHB site is within a system of marshes, upland areas, and very extensive mudflats. The shoreline is undisturbed except for ship wrecks which are submerged and not visible. According to Ogden Beeman and Associates (1992), the part of Southampton Bay which contains the site experienced moderate sedimentation between 1955 and 1990 (0 to 3 ft, with the higher rate measured in the subtidal region). The area between the site and Dillon Pt. experienced very modest net erosion over that same period (0 to 1 ft). The SHB shoreline is a relatively low-energy regime, probably because it is nestled within the bay.

At extremely low tide, over 200 m of mudflats are exposed (Fig. 2.5). The surface sediments of the mudflats, from 0-2 cm, are lighter in color than the lower layers, which are black. They are covered seasonally by a film of light brown diatoms, and on occasion by a layer of green algae. The 0-2 cm layer is light brown color and very loose. From 2-20 cm the sediment is very fine, dominated by clays, and organic carbon. Overall, the mudflats are fine-textured and remain near saturation even at lowest tide. Much like the MRP site, the interface between the mudflats and the marsh is well defined by a distinct rise in elevation and the appearance of plants. Marsh sediments have less color differentiation in the upper 2 cm, and the sediments contain higher concentrations of reduced carbon throughout the profile, making the color of all the sediments darker. The surface of the marsh has a poorly defined layer of decomposing plant tissue. There are numerous channels and irregularities in the surface of the lower marsh, some with relief on the order of 0.25 to 0.5 m.

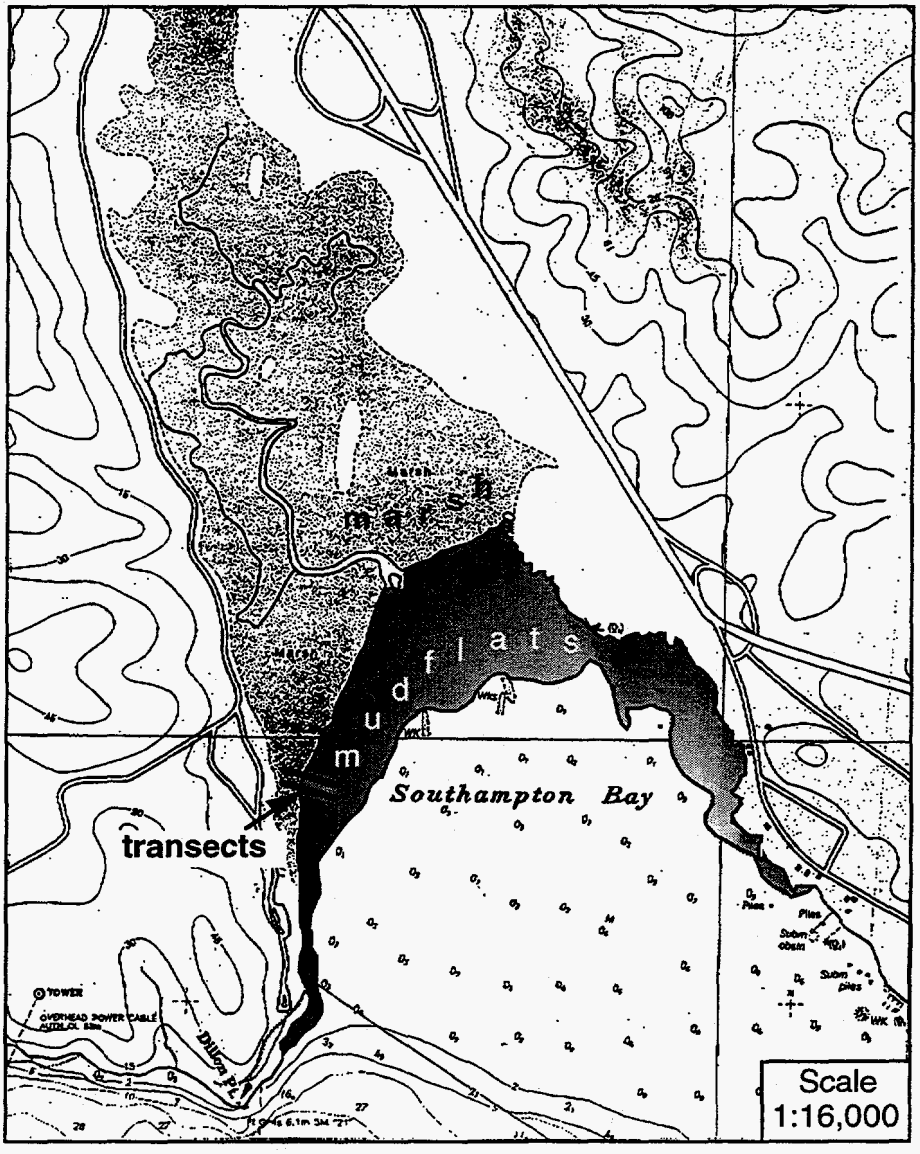

Figure 2.4 Location of sampling transects within the marshes and mudflats of Benicia State Park.

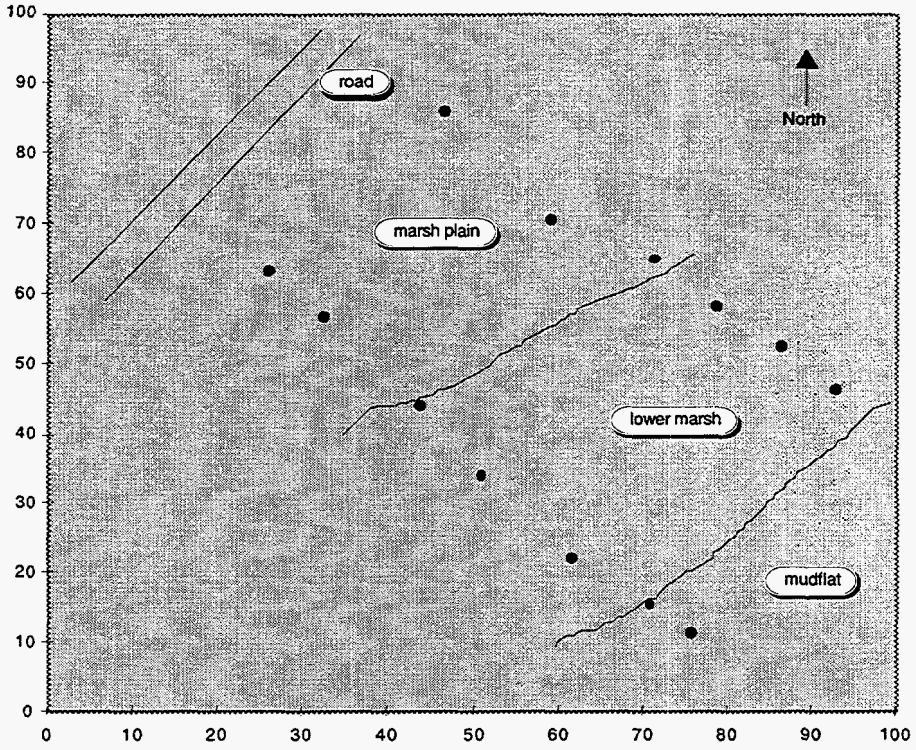

Figure 2.5 Close-up view of SHB site and sample locations. Axes units in meters.

The interface between marsh and mudflat is sparsely vegetated with cordgrass, up to 1 m tall. About 3 m inland, cordgrass is intermixed with two *Scirpus* species: California bulrush (*S. californicus*, up to 2.5 m tall), and alkali bulrush (*S. robustus*, up to 2 m tall). Also within this zone, but less common, are cattails, generally no taller than 1.5 m. The density of plants here is somewhat smaller than at the MRP site. About 25 m inland, a transition to shorter plants occurs, a zone dominated by alkali bulrush (here up to 1 m tall), with less common California bulrush and pickleweed (*Salicornia virginica* or *S. subterminalis* or both). About 30 to 35 m further inland, there is a transition to the marsh plain, which is dominated by a mixture of pickleweed and saltgrass. At 35 m and beyond, saltgrass is dominant. The marsh plain continues to a distance of approximately 90 m from the mudflat/marsh interface. Beyond 90 m, the elevation rises abruptly to about 5 m above marsh level.

2.2 Field Sampling

Intensive sampling of soil and sediment at both the Martinez Regional Park (MRP) site and the Southampton Bay (SHB) site took place in early December 1995.

Additional samples were collected in July of 1996. The goal was to characterize Se distribution and speciation as a function of depth, distance from shore, pH, Eh (redox potential), and organic carbon (TOC, total organic carbon). Previous sampling had been done with hand augers which may have caused some disturbance and cross-contamination between different depth levels. A new sampling tool was designed and constructed at LBNL to accommodate the sampling of both very wet, almost flowing mudflat sediments and root-dominated marsh soils. This tool is shown in Fig. 2.6 and described in Zawislanski et al. (1996a).

Samples were taken along two transects perpendicular to shore at each site (Figs. 2.3 and 2.5). Sample locations were chosen to represent each of the three environments: mudflats, lower marsh, and the marsh plain. Twenty-one locations were sampled at each site, with locations being generally 10 to 20 m apart. At each sample point, a 20 cm-deep core was collected and free water was sampled from the resultant hole when available. The location and elevation of the sample point was surveyed using a Hewlett Packard total station. This was done for both mapping purposes and to facilitate the correlation of physical and chemical characteristics of the sample with relative effects of tidal flooding. Samples were taken close to low tide, in order to be able to sample the largest expanse of mudflat possible.

2.3 Sample Processing and Extraction

In the laboratory, 1-mm-diameter holes were drilled in every core at depths of 0.5, 1.5, 2.5, 4.0, 6.25, 8.75, 12.5, and 17.5 cm, in order to accommodate the insertion of Eh and pH electrodes. Banks of platinum and antimony electrodes were used to measure Eh and pH, respectively. Both Eh and pH were recorded directly in mV. Subsequently, Eh, which was measured referenced to a calomel electrode, was adjusted by adding 245 mV to reference it to a standard hydrogen electrode (Light, 1972). Eh was calibrated to saturated quinhydrone solutions (Bohn, 1971). pH was calculated using a linear correlation derived by Schaller and Fischer (1981) and calibrated to readings taken with a glass pH electrode in pH 7 and 10 buffers. After the measurement, the cores were re-sealed and frozen for further processing. Frozen cores were cut into thin horizontal slices: 0-1 cm; 1-2 cm; 2-3 cm; 3-5 cm; 5-7.5 cm; 7.5-10 cm; 10-15 cm; and 15-20 cm. These intervals coincide with the depths at which Eh and pH were measured. The frozen sediment sections were thawed immediately prior to sequential extraction. The sequential extraction procedure is described in detail in Appendix A and testing of this procedure is described in Chapter 3. In addition,

moisture content of each sample was measured. Total C and N were determined on dry subsamples using a Carlo Erba NA 1500 C and N Analyzer. Generally, organic C is determined by difference between total C and inorganic C. In this case, the carbonate content of the marsh sediments is low, and the total C is estimated to be primarily comprised of reduced, or organic C.

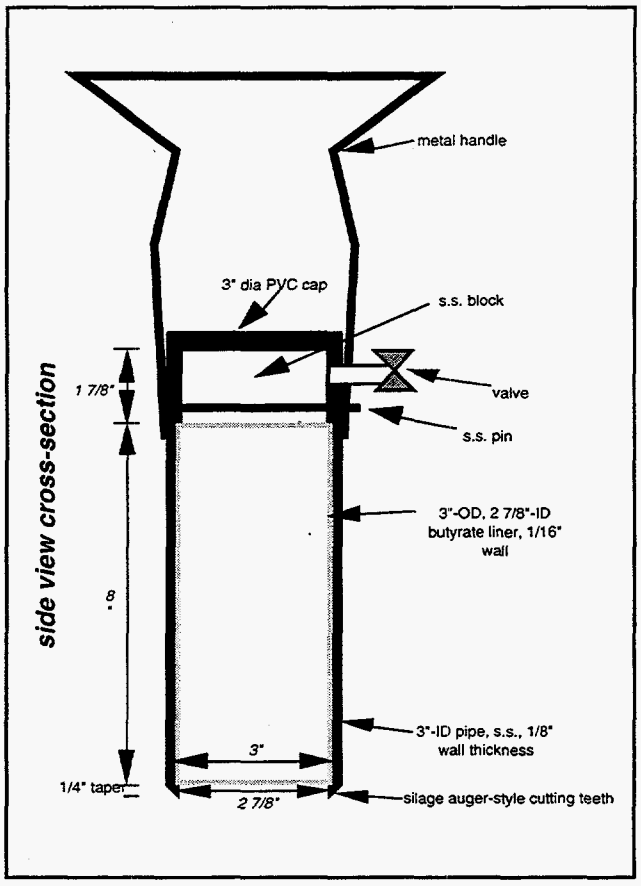

Figure 2.6 Schematic diagram of new marsh core sampler design.

2.4 Results of Se Fractionation and Eh and C Measurements

The results of Se fractionation and other analyses are presented in terms of vertical distribution within the top 20 cm of sediment and by wetland environment: marsh plain, lower marsh, and mudflat. Each value is an arithmetic mean of samples from a number of cores, specified in parentheses in the legend. The error bars shown in Figs. 2.7 through 2.20 represent one standard deviation of the mean, thereby giving some idea of the spatial variability of each parameter. Error bars are generally shown on only one side of the mean in order to improve clarity and legibility of the graph.

2.4.1 Total Carbon Distribution

Organic carbon, as an electron donor, is one of the most important variables controlling the redox potential and therefore is an indication of the potential for maintaining reducing conditions or further reduction. Equally important is the fact that organic matter is a potential site for Se immobilization.

The distribution of total C is shown in Figs. 2.7 and 2.8, for sites MRP and SHB, respectively. As expected, the marsh plain is most carbon-rich, followed by the lower marsh, followed by the mudflats. The main difference between the two sites is the higher C in the mudflats and lower marsh at SHB. This is clearly related to the low-energy conditions at SHB which are more conducive to the presence of algae and settling of organic material (see discussion in Chapter 4). There is a strong vertical gradient in the C within the marsh plain, with C at the MRP site decreasing from near 15% at the surface to 5% at 20 cm. This suggests the progressive mineralization of organic matter with depth, meaning that on average, decomposition dominates over carbon production (Zwolsman et al., 1993). Alternatively, such a gradient could be explained by a change in environment from mudflat to marsh as a result of accretionary processes, i.e., the deeper sediments may represent older mudflat sediments. The exception is the profile in the lower marsh at MRP, where total C increases somewhat with depth. It is possible that the primary productivity in this area is relatively higher.

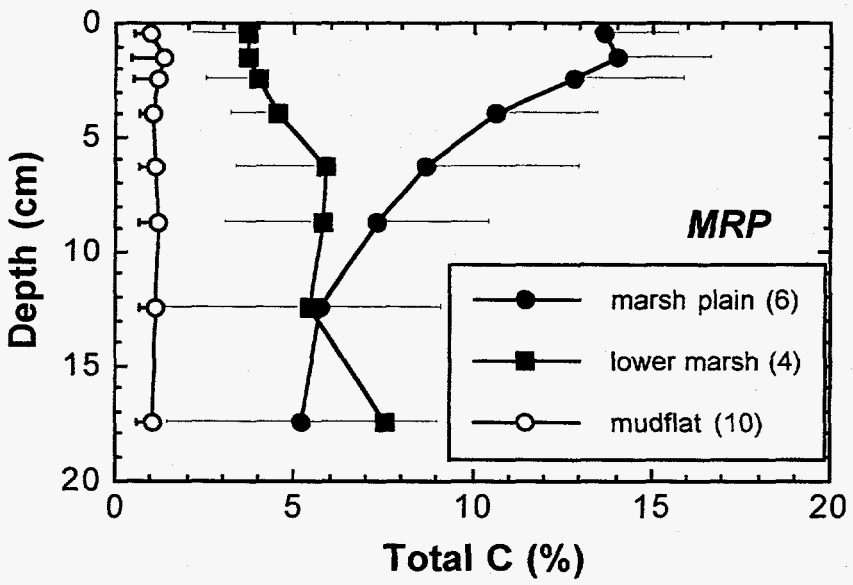

Figure 2.7 Total carbon distribution in intertidal sediments from site MRP.

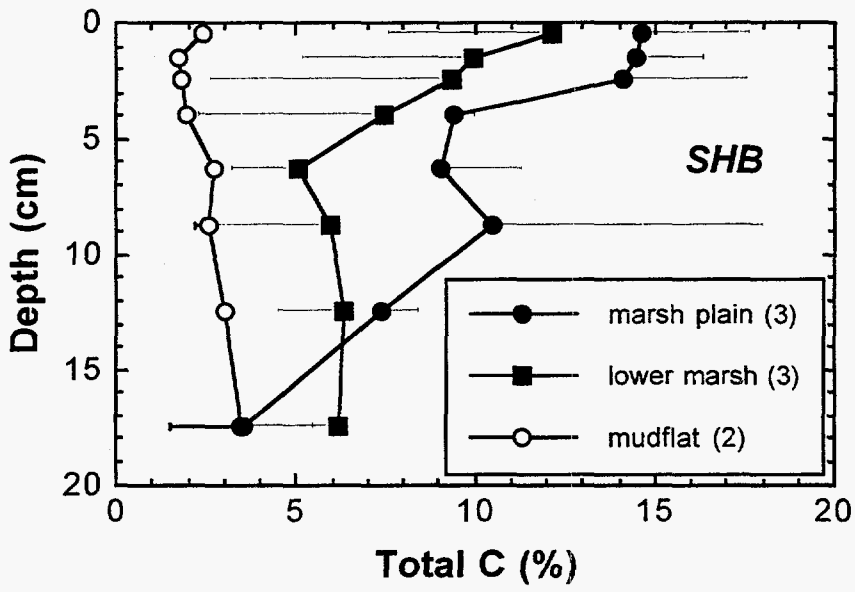

Figure 2.8 Total carbon distribution in intertidal sediments from site SHB.

2.4.2 Redox Potential Distribution

Although its measurement in sediments is somewhat ambiguous and equilibrium conditions cannot be assumed, redox potential is useful in the general description of oxic/suboxic/anoxic zones within the sediment.

The vertical and spatial distribution of Eh measured in the sediment cores is shown in Figs. 2.9 and 2.10, for sites MRP and SHB, respectively. Several unexpected trends can be seen. Redox potential is highest in the marsh plain and lower in the mudflats and lower marsh. The range of redox potentials is fairly narrow and almost always positive. For instance, Eh at site MRP is almost always higher than 100 mV. The fact that the top 2 cm of sediment in the mudflats at MRP are significantly more oxidized than underlying sediments was anticipated, but otherwise there is no distinct oxidized zone in the other profiles.

The relatively oxidized nature of the organic-rich marsh plain suggests that this environment is not inundated by water for periods long enough to result in anoxic conditions. On the other hand, despite being much lower in total C, the mudflats are covered with water most of the time, resulting in suboxic conditions.

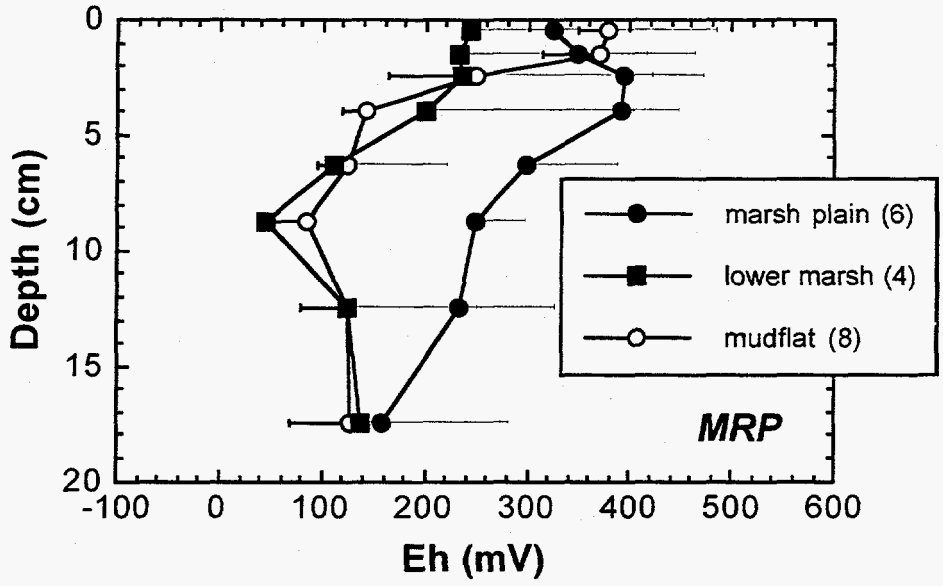

Figure 2.9 Redox potential distribution in intertidal sediments from site MRP.

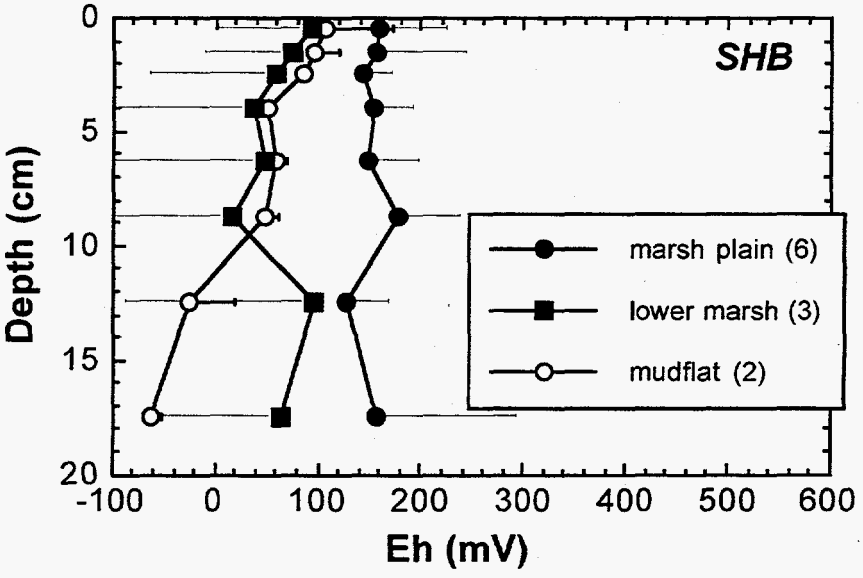

Figure 2.10 Redox potential distribution in intertidal sediments from site SHB.

2.4.3 Total Se Distribution

Total Se distribution is shown in Fig. 2.11 and 2.12, for sites MRP and SHB, respectively. The most apparent feature of both these plots is the relatively lower Se concentrations in the mudflat sediments compared with marsh sediments. Mudflat

sediments generally contain between 0.5 and 0.9 mg Se kg^{-1}, while marsh sediments contain between 0.9 and 1.3 mg Se kg^{-1}. At MRP, there is a further distinction between lower marsh and marsh plain sediments, with the lower marsh containing intermediate Se concentrations. The wider range of concentrations at the MRP site may be related to a wider range of sediment textures (see Chapter 4) and related C content. Aside from slight decreases of Se with depth in the marsh and slight increases with depth in the mudflats, there are no dramatic changes with depth, i.e., time. At this point, the correlation between depth and time deserves some discussion.

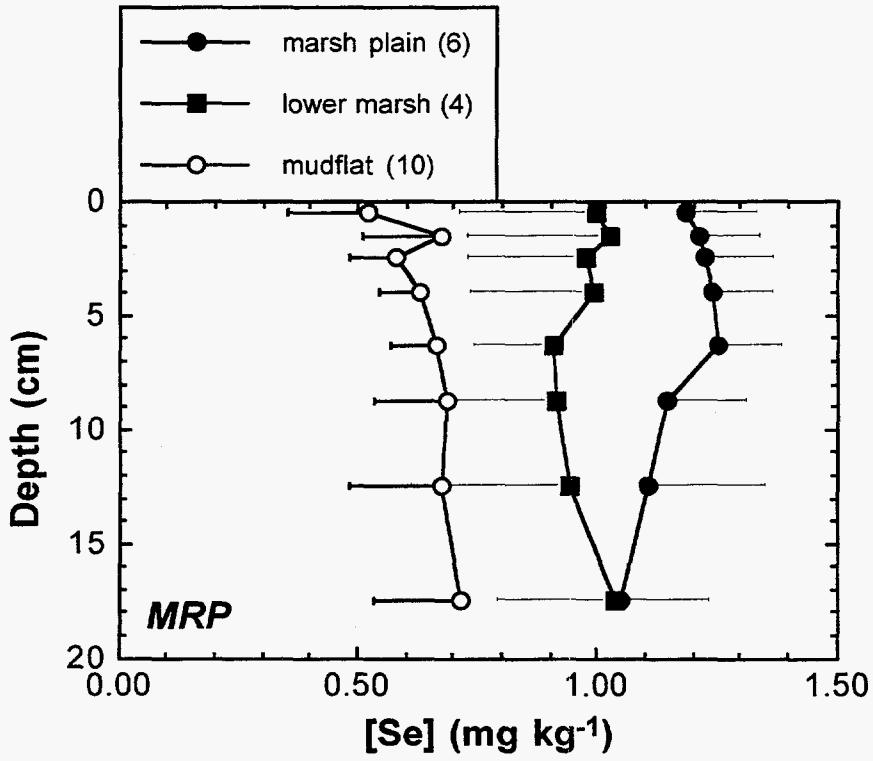

Figure 2.11 Total Se distribution in intertidal sediments from site MRP.

The cores described herein have not been age-dated, but very rough ages can be assigned based on dating done by others in similar environments. Cores collected by Luoma et al. (1996) in Richardson Bay, Grizzly Bay, and San Pablo Bay show mean depositional rates of 1 to 2 cm yr^{-1}. These rates would apply to the mudflat environment, suggesting that the 20 cm cores collected at MRP and SHB were deposited over the last 10 to 20 years. On the other hand, data from L. Wells (Vanderbilt U., personal communication) from a number of marshes around the North Bay show depositional rates on the order of 2 to 5 mm yr^{-1}, suggesting that the 20 cm

cores collected in the lower marsh and marsh plain were deposited over the last 40 to 100 years. Therefore, with the exception of surface sediments, Se at a given depth within the mudflats was deposited at a much different time than Se at the same depth in the marsh. Furthermore, marsh sediments are far more reliable in terms of dating of recent sedimentation because they are subject to much less post-depositional re-working. Mudflat sediments are frequently eroded during storm events, displaced, and re-deposited. This is clearly the case at the MRP site, as seen in the sediment dynamics study (Chapter 4). Thus, great care must be taken when assigning ages to Se, or any other trace element within the mudflats. We plan on age-dating (using Pb-210) a number of cores from each of the sites in the near future.

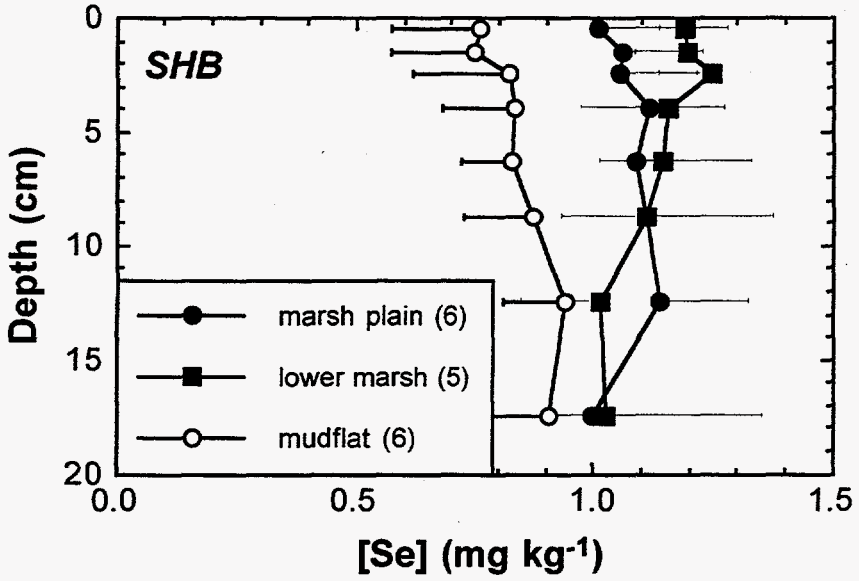

Figure 2.12 Total Se distribution in intertidal sediments from site SHB.

2.4.4 Water-Extractable Se Distribution

Water-extractable Se distribution is shown in Figs. 2.13 and 2.14, for sites MRP and SHB, respectively. This fraction represents Se which is very loosely associated with the sediment and is potentially soluble under ambient conditions. In the marsh, soluble Se is 25-50% Se(IV) and the remainder is (Se(VI) + Se(organic). In the mudflats, Se(IV) is generally less than 25% of soluble Se. Clearly, soluble Se is a minor fraction, generally comprising 0.5 to 1.0 % of the total Se inventory, with the exception of the very near-surface sediments at SHB, where soluble Se was as high as

2% in the lower marsh. No consistent trends emerge, although concentrations are slightly higher in the top 1 to 2 cm.

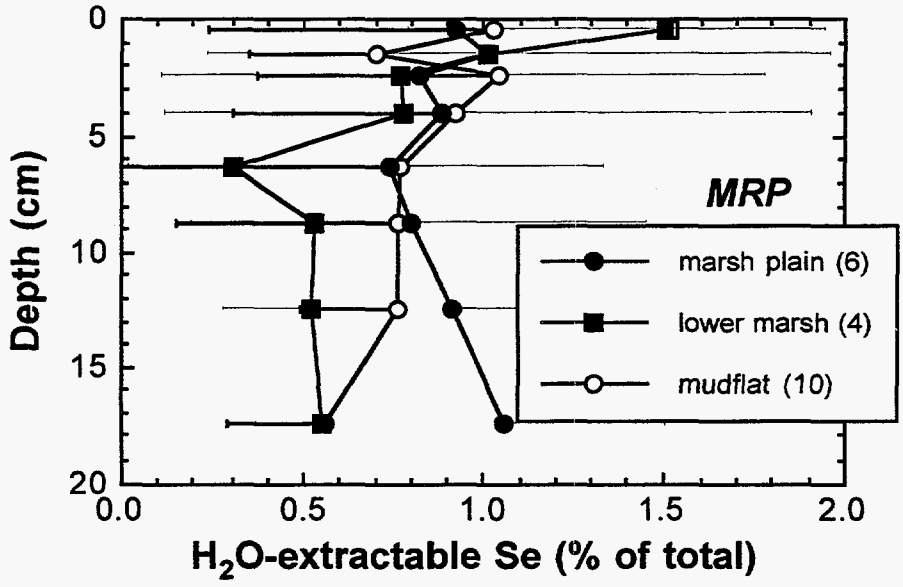

Figure 2.13 Water-soluble Se distribution in intertidal sediments from site MRP.

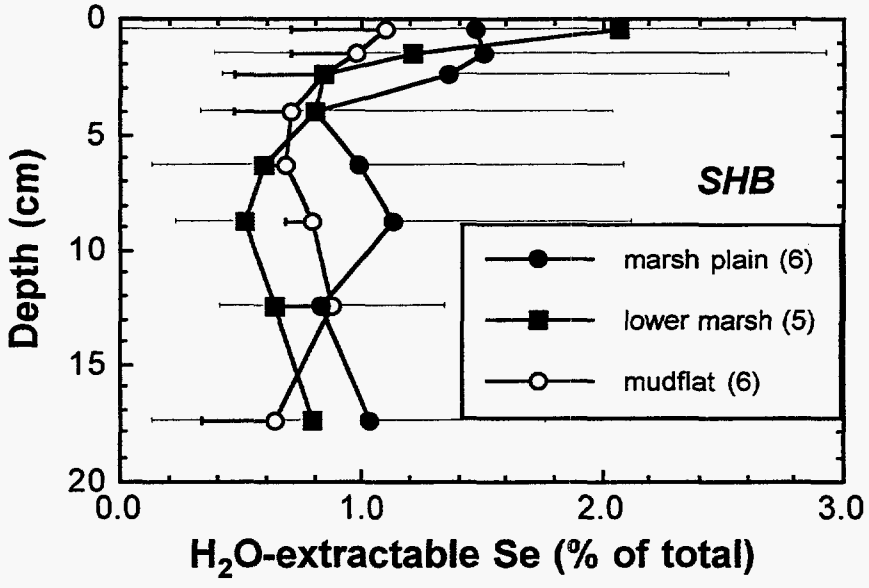

Figure 2.14 Water-soluble Se distribution in intertidal sediments from site SHB.

2.4.5 Phosphate-Extractable Se Distribution

Phosphate (Na_2PO_4)-extractable Se represents primarily adsorbed Se (Tokunaga et al., 1994a). However, the concomitant extraction of precipitated species is quite likely (Gruebel et al., 1988) and cannot be quantified. Furthermore, there is more than one mechanism for Se adsorption onto surfaces, with both strong, inner-sphere complexes and weak outer-sphere complexes observed using X-ray absorption spectroscopy (Hayes et al., 1987, Brown et al., 1989). Therefore, care must be taken in the interpretation of this data and the term "adsorbed Se" will be used to loosely describe this operationally-defined Se fraction.

The phosphate-extractable Se distribution is shown in Figs. 2.15 and 2.16, for sites MRP and SHB, respectively. Adsorbed Se accounts for 2 to 12% of the total inventory, though with the exception of mudflat sediments at the MRP site, it is generally less than 5% of total. It is not clear why the relative percentage of adsorbed Se is highest in the MRP mudflats. Adsorbed Se concentrations follow no consistent trends in depth.

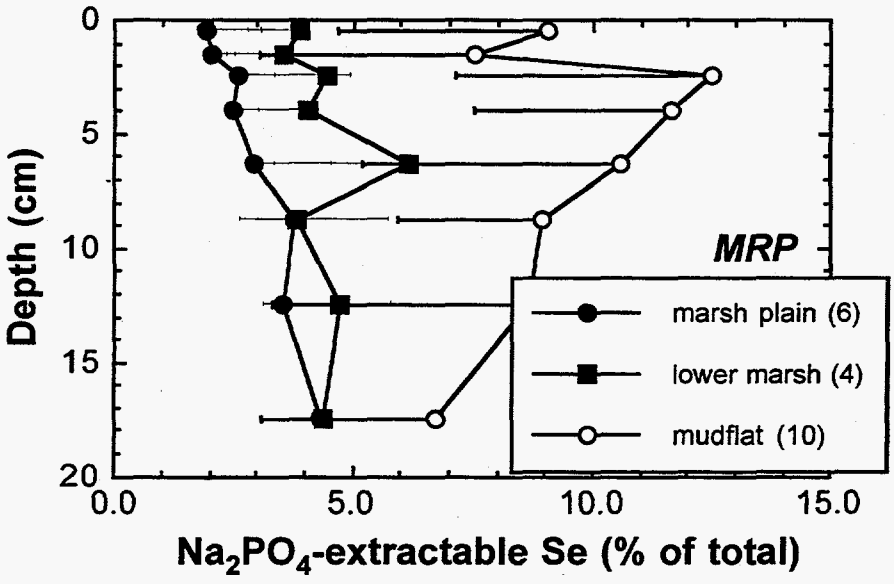

Figure 2.15 Phosphate-extractable ("adsorbed") Se distribution in intertidal sediments from site MRP.

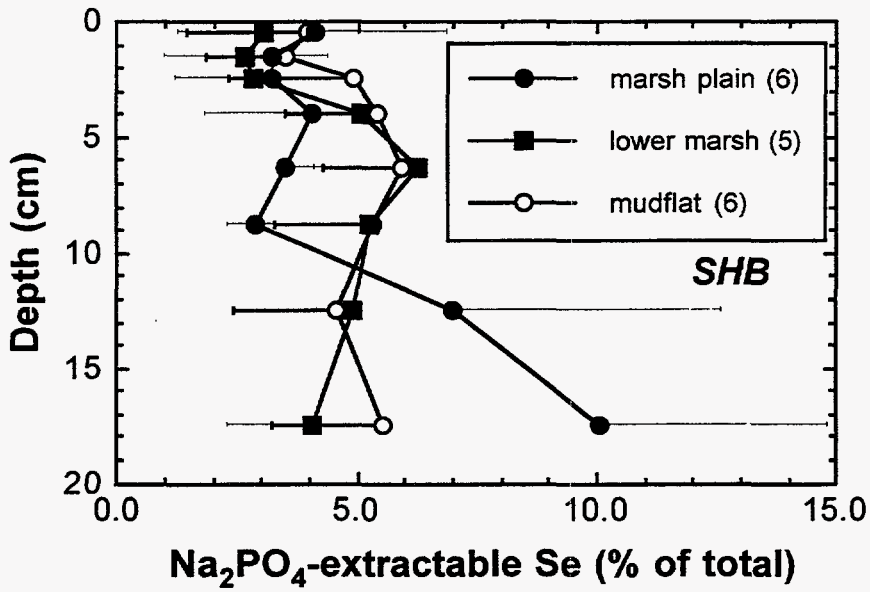

Figure 2.16 Phosphate-extractable ("adsorbed") Se distribution in intertidal sediments from site SHB.

2.4.6 Hydroxide-Extractable Se Distribution

Hydroxide (NaOH)-extractable Se represents a somewhat ambiguous pool of Se associated with organic matter within the sediment. This does not mean that the Se itself is in an organic form, such as selenomethionine. In fact, it has been shown that even in an organic-rich soil, most of the so-called "organically-associated Se" was actually in the Se(IV) form (Zawislanski and Zavarin, 1996). Nevertheless, the NaOH extract serves to break down soil organic matter (Schnitzer, 1982) and liberate any forms of Se which may be associated with it, even if they are merely adsorbed or occluded. From a more practical perspective, it may be said that this Se fraction is less available than the adsorbed or soluble fraction and its release may depend largely on the mineralization of organic matter.

The vertical and spatial distribution of hydroxide-extractable Se is shown in Figs. 2.17 and 2.18, for sites MRP and SHB, respectively. This is a very significant fraction, comprising between 18 and 36% of the total Se inventory. At both sites, th e hydroxide-extractable Se fraction is highest in the mudflat sediments. This is difficult to explain, given that the marsh is far more organic rich than the mudflats (Figs. 2.8, 2.9). No consistent depth-trends are apparent.

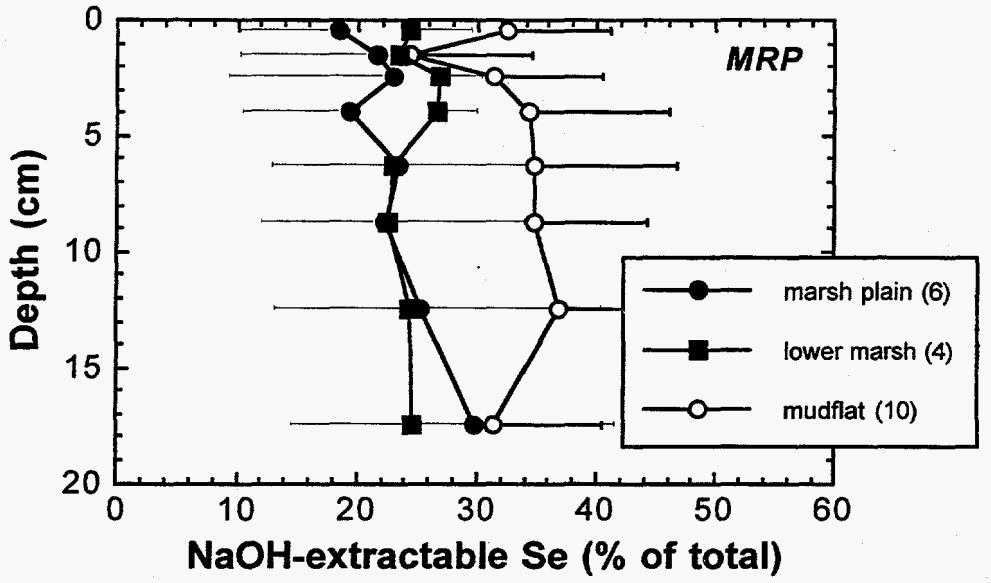

Figure 2.17 Hydroxide-extractable ("organically-associated") Se distribution in intertidal sediments from site MRP.

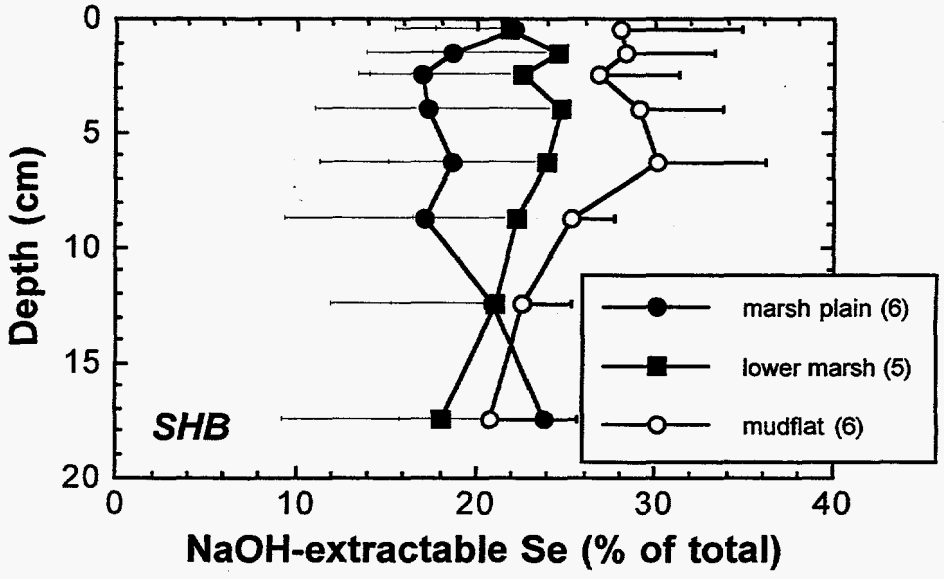

Figure 2.18 Hydroxide-extractable ("organically-associated") Se distribution in intertidal sediments from site SHB.

2.4.7 Sulfite-Extractable Se Distribution

Sulfite (Na_2SO_3)-extractable Se represents primarily zero-valent, or elemental Se (Velinsky and Cutter, 1990). Although this extraction procedure has been shown to be quite effective in removing elemental Se (Zawislanski et al., 1995), it should still be considered operationally-defined until more objective methods, such as x-ray absorption spectroscopy, are applied.

The results of sulfite extraction are shown in Figs. 2.19 and 2.20, for sites MRP and SHB, respectively. This, by far, is the most dominant fraction of Se in the sediments, generally comprising around 50% of the total inventory. Data from all three environments at site MRP fall within a fairly narrow range of values and show no depth trends. At site SHB the elemental Se fraction is lowest in the mudflats and highest in the marsh plain. Also, there is an increase with depth in the marsh plain, suggesting that Se is being mineralized from organic forms into the inorganic zero-valent form. In general, however, the vertical and spatial distribution of the elemental form is apparently at odds with the Eh data (Figs. 2.9, 2.10), in that although Eh generally decreases with depth, elemental Se concentrations do not vary much. This can be explained by the fact that Se reduction is rapid (Tokunaga et al., 1996), while Se oxidation is sluggish (Zawislanski and Zavarin, 1996). Furthermore, reducing conditions and reduced Se forms can be present in anaerobic microsites, even when the bulk sediment or soil is well aerated (Tokunaga et al., 1994b). Finally, the redox state of Se as it enters the sediment system may already be at (0) or lower (see Chapter 3).

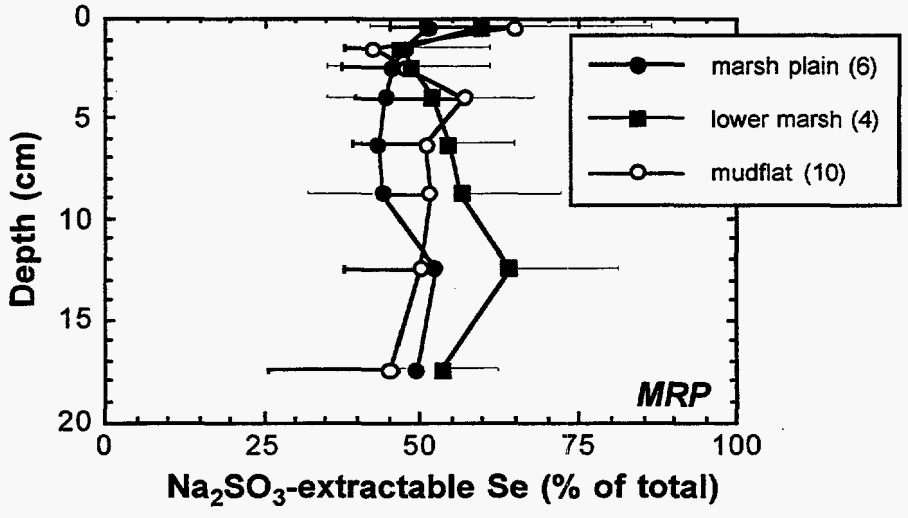

Figure 2.19 Sulfite-extractable ("elemental") Se distribution in intertidal sediments from site MRP.

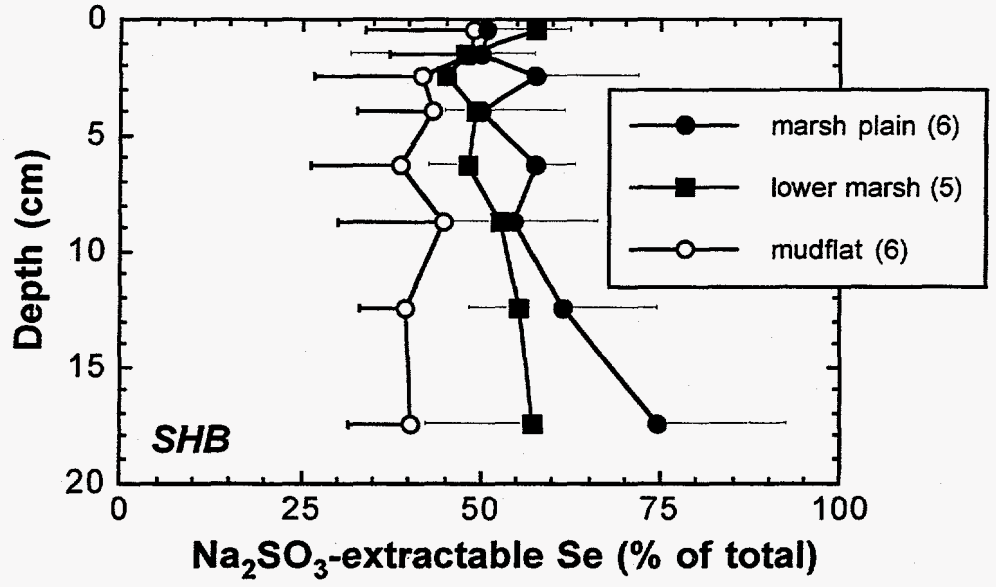

Figure 2.20 Sulfite-extractable ("elemental") Se distribution in intertidal sediments from site SHB.

2.4.8 Summary of Se Fractionation

The relative contributions of each Se fraction in the sediment are shown in Figs. 2.21 through 2.26. The operationally-defined fraction names are used in these graphs

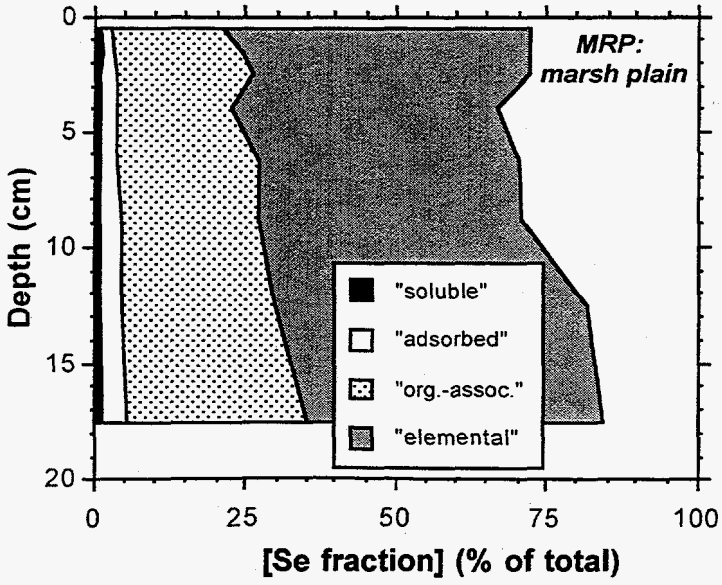

Figure 2.21 Se fractionation in marsh plain sediments from site MRP. The difference between total Se and the 4 fractions shown is "residual Se."

and are shown by site and environment. The most important observation to be made is the relative similarity of the fractionation, both inter- and intra-site. With the exception of increasing elemental and decreasing residual fraction in the marsh plain of site SHB (Fig. 2.24), there are no consistent depth-trends, and elemental Se dominates in all environments.

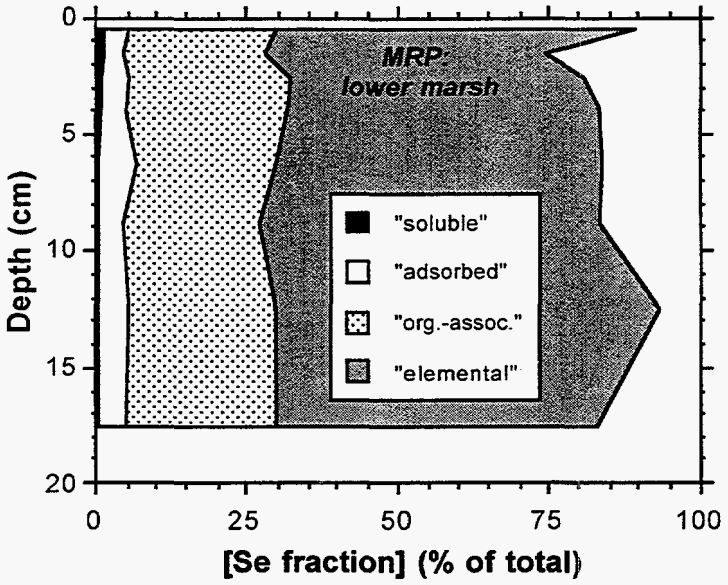

Figure 2.22 Se fractionation in lower marsh sediments from site MRP. The difference between total Se and the 4 fractions shown is "residual Se."

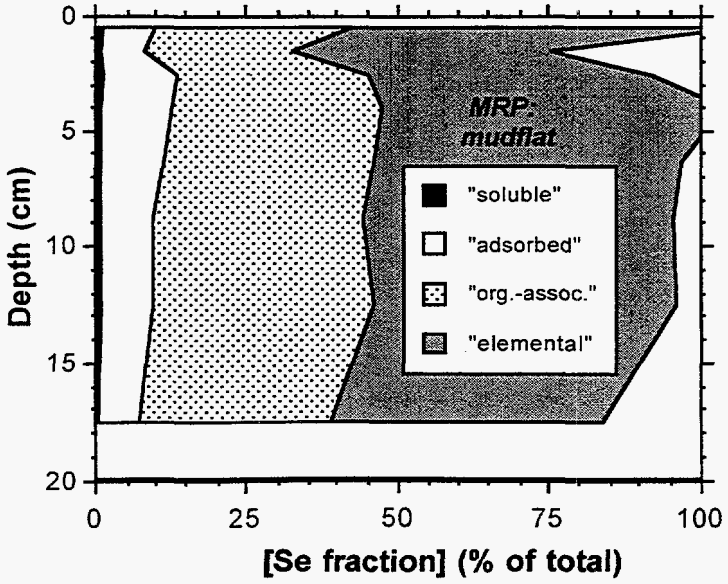

Figure 2.23 Se fractionation in mudflat sediments from site MRP. The difference between total Se and the 4 fractions shown is "residual Se."

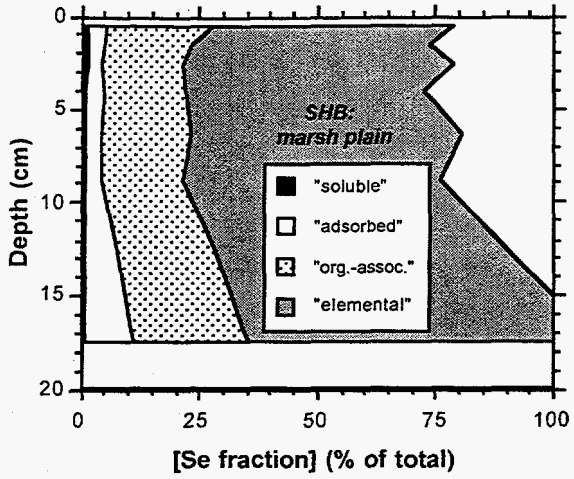

Figure 2.24 Se fractionation in marsh plain sediments from site SHB. The difference between total Se and the 4 fractions shown is "residual Se."

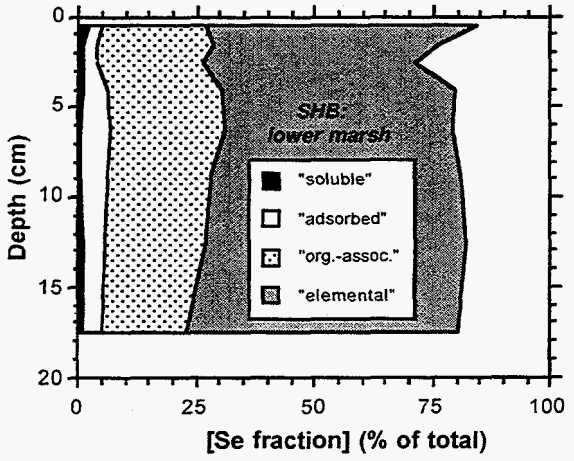

Figure 2.25 Se fractionation in lower marsh sediments from site SHB. The difference between total Se and the 4 fractions shown is "residual Se."

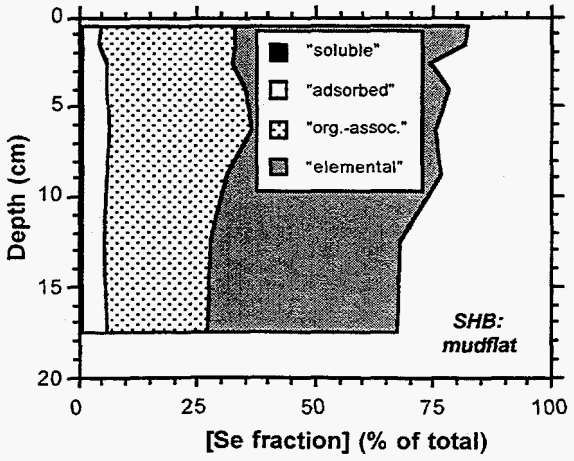

Figure 2.26 Se fractionation in mudflat sediments from site SHB. The difference between total Se and the 4 fractions shown is "residual Se."

2.4.9 Interstitial Se Distribution

Pore waters were removed from the wetland sediments via centrifugation. The distributions of pore water, or interstitial Se concentrations are shown in Figs. 2.27 and 2.28, for sites MRP and SHB, respectively.

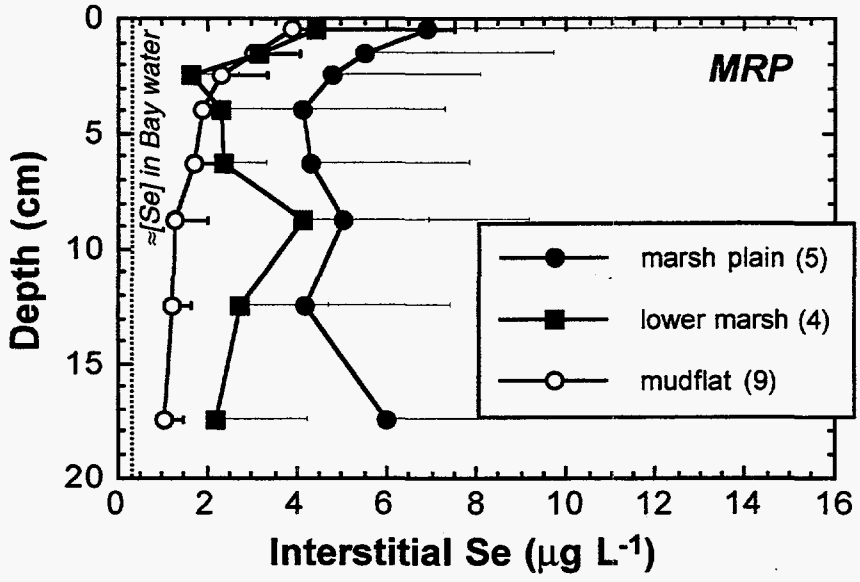

Figure 2.27 Pore-water Se distribution in intertidal sediments from site MRP.

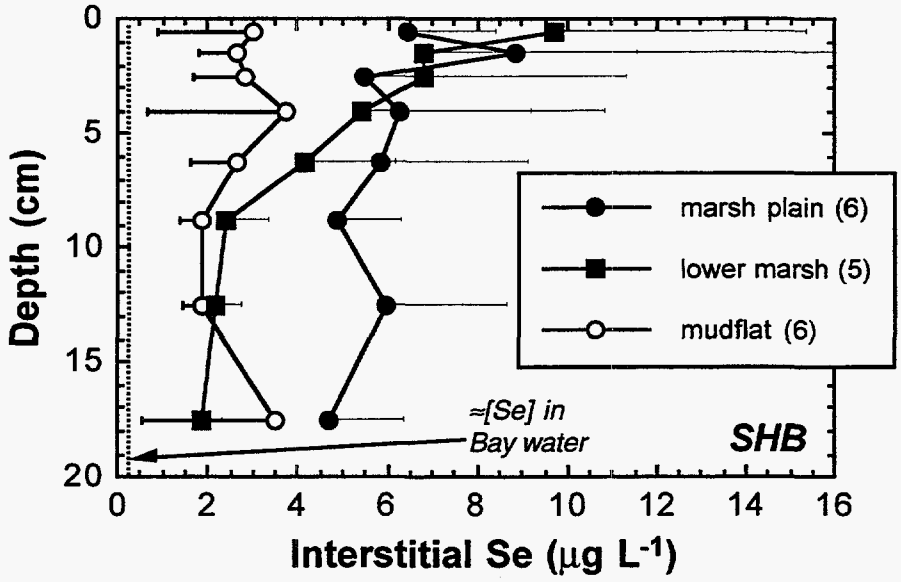

Figure 2.28 Pore-water Se distribution in intertidal sediments from site SHB.

The interstitial Se concentrations generally fall between 1 and 10 μg L^{-1}, in contrast with the Bay water concentrations, generally at or below 0.25 μg L^{-1}. It is therefore apparent that there is an upward diffusive gradient of Se out of the sediments and into the overlying water. Although the profiles in Figs. 2.27 and 2.28 are not entirely consistent, there is a general increase in interstitial Se concentrations toward the sediment surface, suggesting that more oxidized conditions may be responsible for Se solubilization. However, the presence of pore-water Se concentrations in excess of those observed in Carquinez Strait water, suggests that Se solubilization may be taking place even under suboxic conditions. Unfortunately, due to the high dissolved organic carbon content of the pore waters and the very small sample volumes, Se speciation was not feasible. Collection of larger samples and the development of a better-suited variation of the analytical method may make speciation possible in the future.

One possible explanation for elevated soluble Se concentrations in pore water may be the solubilization of elemental Se in the presence of polysulfides (Weres et al., 1989). This possibility needs to be further investigated, including measurements of polysulfide species in field samples, as well as laboratory microcosm experiments under controlled conditions.

Given the observed Se concentration gradients and assuming the very simple model of Fickian diffusion across the sediment-water interface, diffusive fluxes can be calculated, and are expressed in the following equation,

$$J = t_{inun} f^m D_0 \partial C/\partial x, \text{ where}$$

t_{inun} = fraction of time area is under water; marsh = 0.15, mudflat = 0.5
f = porosity (assume 0.8)
m = 3 in surficial sediments (to account for tortuosity; Ullman and Aller, 1982)
D_0 = diffusion coefficient (5×10^{-6} cm^2 s^{-1} at 4.5°C, Li and Gregory, 1974)
∂C = (5 μg L^{-1} - 0.2 μg L^{-1}) (marsh), (2 μg L^{-1} - 0.2 μg L^{-1}) (mudflat)
∂x = 2 cm (depth in sediments over which gradient is calculated).
The resultant fluxes are,

$$J_{marsh} = 0.29 \text{ mg Se } m^{-2} yr^{-1}$$

$$J_{mudflat} = 0.37 \text{ mg Se } m^{-2} yr^{-1}$$

Although several assumptions needed to be made in order to arrive at the above fluxes, they provide us with at least an order of magnitude for this process.

3 Selenium in Surface Water and Suspended Particulates

Suspended sediments were sampled and analyzed for comparison with intertidal sediments and to determine their effect on clam Se concentrations. Since it was found that suspended sediments are critical as a source of Se in the marshes and mudflats, research has focused on determining the processes responsible for Se accumulation in suspended sediments.

Selenium concentrations in two marshes of the Carquinez Strait increase from the mudflats to the marsh plain, and marsh plain concentrations are in the same range as suspended sediment concentrations. In addition, selenium concentrations in interstitial waters are nearly an order of magnitude higher than those in surface waters, which means that there is a concentration gradient that generates a flux directed out of the sediment surface. Combined with measured sedimentation rates and Se concentrations in the deposited sediments, this data points to the fact that Se accumulation in marsh and mudflat sediments is controlled by suspended sediment deposition. What is not clear is which processes are responsible for Se accumulation on suspended sediments and which species of Se are present. The current study has the following experimental objectives to address:

- Determine the seasonal fluctuations in suspended sediment and surface water Se concentrations;
- Speciate Se in suspended sediments and develop correlations between sediment and water properties and suspended particulate matter (SPM)-Se concentrations;
- Evaluate the role of sorption, phytoplankton metabolism, and chemical/microbial reduction of Se from water onto suspended sediments, and characterize the clay mineralogy of representative samples.

3.1 Methods

3.1.1 Sequential Extractions

A sequential extraction procedure was developed from previous techniques used for Se fractionation and speciation (Weres et al., 1989; Velinsky and Cutter, 1990; Tokunaga et al., 1991; Lipton, 1991). Table 3.1 contains the sequence of extractions

and the target species each extraction is designed to remove. Testing of these methods has demonstrated that selenite/selenate spikes are extracted with a 93% efficiency by the first three extractants. Selenomethionine is extracted with a 65-70% efficiency and elemental Se (black and red) with a 78% efficiency. Samples were extracted without drying after removal of interstitial water and determination of water content. Sulfite and HCl-Cr^{2+} extracts were done after NaOH extraction, drying, and grinding. Residual Se is defined as the difference between Se from a total acid digest (TAD) of the sample and the sum of sequentially extracted Se.

Extracts and waters were analyzed by hydride generation flow injected atomic adsorption spectrometry (HG-AAS). Samples with solution concentrations below 1 μg Kg^{-1} were analyzed using either a cold vapor method adapted by Cutter (1978) or a fiage method developed by Tao and Hansen (1994). Total carbon (C) was measured on a Carlo Erba NA 1500 C and N analyzer (Milan, Italy).

Table 3.1 Bay sediments/soils sequential extraction procedure.

Extract Name	Symbol	Solution	Target Se Species
Distilled Water	Dx	Distilled Water	Soluble
Phosphate	Px	0.001 M Na_2HPO_4	Adsorbed
Sodium Hydroxide	OHx	0.02 M NaOH	Organically assoc.
†Sulfite	Sx	1.0 M Na_2SO_3 (pH = 7.0)	Elemental
†HCl-Cr^{2+}	Crx	1.0 M HCl, 1.0 M Cr^{2+}	Pyrite

† Method developed by Velinsky and Cutter, 1990.

3.1.2 Pyrite Se Extraction

Selenium has chemical properties similar to sulfur, and as a result it often is incorporated into sulfur compounds such as sulfur-containing amino acids, polysulfides, and metal sulfur compounds. The dominant metal selenides found in sediments and soils are ferroselite ($FeSe_2$) and mixed Se-S pyrite phases (e.g. FeSSe). Velinsky and Cutter (1990) adapted a method developed by Zhabina and Volkov (1980) combining the method with procedures developed by Cutter and Oats (1987) to analyze for what they termed "pyrite-Se" (ferroselite and FeSSe). The procedure uses Cr^{2+} to reduce Se^{-} to Se^{2-} in an acidic solution from which H_2Se gas is then stripped and trapped using a liquid nitrogen trap (Fig. 3.1). The pyrite method requires extraction of elemental Se, whereas organically-associated Se, SeO_3^{2-}, and SeO_4^{2-} do not interfere

significantly with the analysis. Extraction of elemental Se by the pyrite method was reported by Velinsky and Cutter (1990) to be inefficient and variable (27% for n=19), therefore an efficient extraction procedure for removal of elemental Se was required for preparation of sediments for pyrite extraction. Velinsky and Cutter (1990) developed a method for extraction of elemental Se using a pH 7 buffered 1M Na_2SO_3 solution which does not remove a significant portion of organically-associated Se or SeO_3^{2-}/ SeO_4^{2-}.

The efficiency of the pyrite extraction is approximately 81 ± 12%, as reported by Velinsky and Cutter (1990), but in combination with the error in the elemental Se extraction (91 ± 8.6%), the uncertainty can be as high as 20% with a standard deviation of 16%. The limit of quantification is 2.0 ng Se, for a maximum sample size of 80 mg, which corresponds to a sediment concentration of 0.025 μg Se g^{-1}. Larger sample sizes (>80 mg) result in a larger H_2S peak which elutes earlier than H_2Se and interferes with quantification of pyrite Se.

Due to errors in the Velinsky and Cutter (1990) paper and differences between the optical cell design described by Velinsky and Cutter (1990) and that used on the LBNL atomic absorption spectrometer (AAS), the chromatographic column dimensions, flow parameters, and stripping/trapping apparatus design needed to be altered. The column dimensions specified by Velinsky and Cutter (1990) required a 6.35 mm diameter Teflon tubing of approximately 40 cm in length packed with 50/80 mesh Poropak PS resin. Cutter (personal communication) has confirmed that 3.18 mm diameter tubing results in less dispersion mixing of the H_2Se and H_2S gas plumes and better chromatographic resolution. Differences in the optical cells between the two systems led to baseline fluctuations in LBNL measurements resulting from fluctuations in the flow rate and changes in gas density upon removal of the u-trap from the liquid N_2. To suppress this effect, higher flow rates were required. Higher flow rates are desirable in chromatographic systems because flow times are shorter and dispersion has less time to broaden peaks, but it also has the undesired effect of making peaks that are well resolved at low flow rates elute more closely together. This is a current problem with the LBNL system. To minimize this problem, longer column lengths were tried along with different resins that have different affinities for the two gases. The proximity of the two peaks (approximately 20 seconds apart), has resulted in greater overlap and problems with detection of H_2Se.

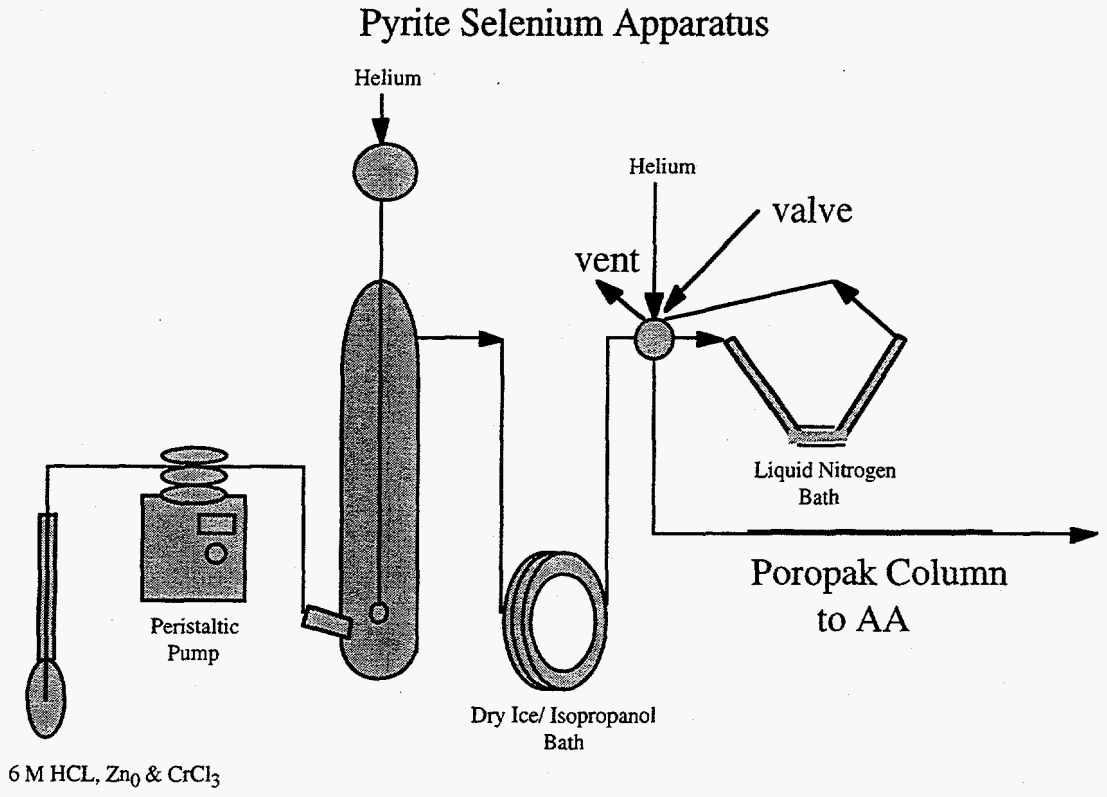

Figure 3.1 Pyrite Se analysis apparatus. Sediment samples are placed in the stripping vessel, degassed for 3 min., reacted with Cr (II) in HCl, and the Se is concentrated onto silanized glass wool in a liquid nitrogen trap. After the reaction is complete, the valve is turned and the glass wool trap is removed from the LN_2 in order that the H_2Se will pass through the Poropak column and onto the AAS for integration.

3.1.3 Water and Suspended Sediment Sampling

Water and SPM within the Carquinez Strait were sampled bi-weekly at the MRP site in the mudflats and from the dock. 21 liter volumes were taken from the field to the laboratory where they were centrifuged (12,000 rpm) and filtered using a 0.45 µm Millipore nitrocellulose filter. Water was double filtered and acidified (4 mL of concentrated HCl per liter of solution) for analysis, while sediments were freeze-dried and stored for TAD and sequential extraction.

3.1.4 Sorption Studies

The effect of salinity on suspended sediment sorption of selenite was measured using batch techniques with 24 hr equilibration times. Synthetic seawater was prepared from a typical concentration recipe found in Stumm and Morgan (1981). The seawater was diluted to produce solutions with salinities of 10, 15, 20, 25, and 30 g kg^{-1}.

Selenite concentrations ranged from 0.1, 0.5, 1.0, 5.0, to 10.0 ppb. Due to interferences from carbonate and other salts found in the synthetic seawater, only the 5.0 and 10.0 ppb Se solutions have been analyzed.

3.1.5 Characterization of Suspended Sediment Mineralogy

Representative samples of suspended sediments were chosen for x-ray diffraction spectrometry, and prepared for analysis of whole samples and clay mineralogy. Analysis was done at 0.01°/sec over the range of 5 to 70° 2θ on a Shimatsu with a slit width of 5 nm.

Clays were isolated from the suspended sediment using a method presented by Dixon and Weed (1989). Suspended sediments were treated with 5-6% hypochlorite solution in a hot (100°C) sonicating bath until all organic matter was extracted. Clay solutions were then rinsed with 2% Na_2CO_3 to remove the residual hypochlorite, and then suspended in distilled water for 24 hr. The supernatant solution was removed and the residual solids resuspended to remove residual clays. The clay solutions were centrifuged and saturated with K or Mg. K-saturated slides were smeared moist onto slides and scanned at room temperature, and after heating to 350 and 550 °C. Mg-saturated slides were prepared air-dry, treated with ethylene-glycol or glycerol and scanned. All samples were scanned with Cu-K alpha radiation.

3.2 Results and Discussion

3.2.1 Water and Suspended Sediment Se Concentrations

Due to the high degree of resuspension in the mudflats, SPM concentrations were high in near-shore samples, while dock samples contained sediment concentrations that correlated well with deep channel surface samples. Average Se concentrations in SPM are higher than sediment concentrations in the mudflat but similar to those in the MRP marsh. SPM-Se concentrations agree with measurements by Cutter (1989) for surface water measurements taken in the Carquinez Strait. Total Se in SPM increased with decreasing SPM concentration (Fig. 3.2). SPM concentrations increase with increasing wind/wave action and storm drainage, and these forces govern the particle size of suspended sediments.

Dissolved concentrations of total Se and Se(IV) (Table 3.2) are in the same range as those previously reported for the Carquinez Strait (Cutter, 1989; Cutter and San Diego-McGlone, 1990). Variations in dissolved total Se appear to shadow the variations in SPM-Se, but data are too preliminary for a comprehensive assessment (Fig. 3.2). The

proximity of the MRP site to the Shell Refinery influences dissolved Se concentrations due to insufficient mixing which may account for the high variability in Se concentrations at the dock and in the mudflats.

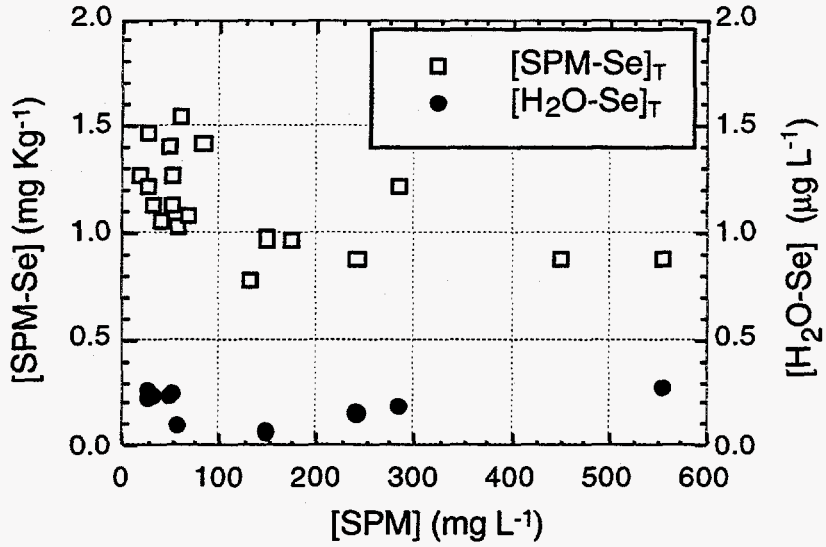

Figure 3.2 Suspended sediment concentrations in water at the MRP site sampled off the MRP dock pier. SPM-Se and dissolved-Se concentrations are plotted versus SPM concentrations in water.

Table 3.2. Se speciation in MRP surface waters.

Date Sampled	Se (IV)† ng L^{-1}	Se_T† ng L^{-1}
12/12/95	49	73
1/3/96	15	102
3/20/96	62	233
3/22/96	22	160
4/8/96	44	274
5/1/96	162	241
6/19/96	77	224
9/19/96	40	219
10/16/96	59	218

† = reading error of 3%.

3.2.2 Pyrite Se Extraction

Analysis of MRP initial screening samples (sampled 5/17/95) from the upper and lower horizons of the marsh and mudflats revealed low concentrations of pyrite Se that were below detection. Chromatographic resins were changed in an attempt to improve separation. Poropak QS (50/80 mesh) improved separation, but resulted in poorer peak shape. With better separation, detection limits of the current system could be as low as the system used by Velinsky and Cutter (1990). The limit of quantification for the LBNL system is approximately 0.075 μg Se g^{-1} depending on the concentration of sulfur in the sediments. Velinsky and Cutter (1990) report high concentrations of pyrite Se for subsurface sediments (15-18 cm, 18-21 cm, and 33-36 cm depths with concentrations of 0.037, 0.190, 0.044 μg Se g^{-1}, respectively) from the Great Marsh (Lewes, DE) where total Se concentrations are comparable to values found at MRP and SHB.

Comparison of the Velinsky and Cutter (1990) data with that from MRP suggests that perhaps a more sensitive system is necessary to quantify pyrite Se, and that higher pyrite Se concentrations would be expected in MRP and SHB sediments. Further improvements on the pyrite Se system are planned to lower the detection limit including improvements to the chromatographic column. This alteration will allow for greater peak separation, and lower limits of quantification.

3.2.3 Speciation of Se in Suspended Sediments

In order to understand the mechanisms which control Se accumulation in SPM, it is necessary to speciate SPM-Se as well as correlate concentrations with other properties. Total C correlates weakly with SPM-Se ($r = 0.661$, Fig. 3.3), but NaOH-extractable Se comprised only 12-16% of TAD extractable Se. Sulfite-extractable (or elemental) Se was very low, comprising approximately 4% of the total Se. Cutter (1985), analyzing biogenic particles and suspended sediments using a method developed by Tessier et al. (1979), found that the Se in suspended sediments was predominantly in the residual fraction (90 to 93.3 %, in TAD of residual) after exchangeable (1.7 to 2.0 %, 1 M $MgCl_2$ pH 7.0), carbonate (1.8 to 2.0 %, 1M NaOAc, pH 5.0), and Fe-Mn bound (and 3.1 to 6.0 %, dithionite-citrate-bicarbonate) were sequentially removed. Speciation studies to date therefore, appear to fail to determine what form Se takes in suspended sediments, but data suggest an association with organic carbon.

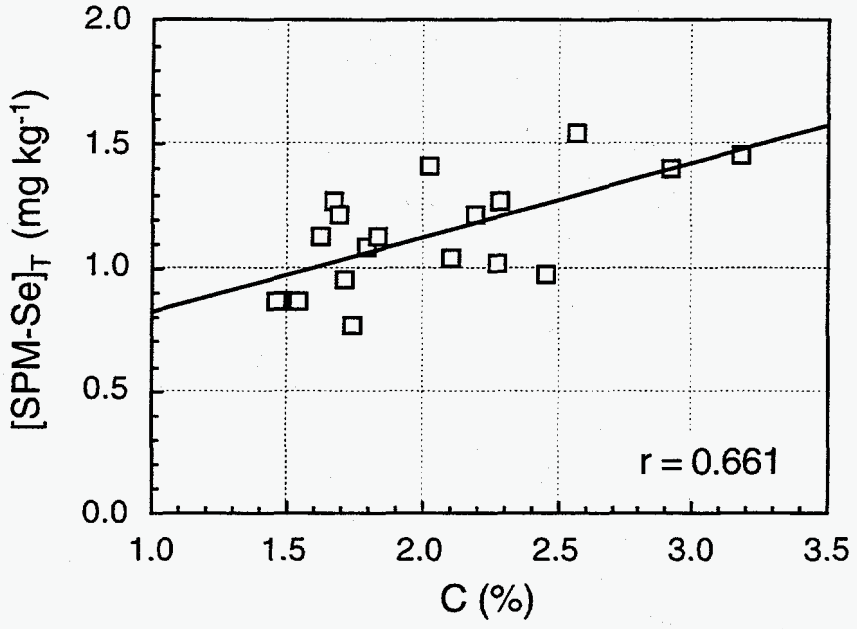

Figure 3.3 SPM-Se versus SPM-C in MRP suspended sediment samples taken from the MRP dock pier from 12/5/95 to 12/31/96.

Preliminary results show that SPM-Se is inefficiently extracted by the sequence developed for soils (Fig. 3.4; 78% residual). Marsh soils high in organic matter also had low extraction efficiencies, but C concentrations for those soils were nearly an order of magnitude higher than in suspended sediments (10 % vs. 1 to 3 % C), and yet efficiencies were considerably higher (30-40% residual). Cutter (1985) resorted to using a TAD extraction after finding that the efficiency of the peroxide treatment used by Tessier et al. (1979) did not result in 100% recoveries. The results of the Cutter extractions appear to agree with preliminary measurements for suspended sediment speciation. A complete comparison is limited by the fact that Cutter did not report recoveries for NaOH extractions on these samples (that treatment was used on biogenic particles only). Cutter assumed that all the Se found in the residual fraction was in the form of "organic" Se. Given the low concentration of carbon in suspended sediments from the MRP site, if organic associations are responsible for the non-extractable Se, then Se concentrations in these organic fractions are quite high.

Luoma et al. (1992) attribute high particulate-Se concentrations to phytoplankton bioconcentration of selenite through metabolic transformation into selenocysteine or selenomethionine, and blame this bioconcentration for increased Se levels in clams. Several studies have shown that selenite can be bioconcentrated in phytoplankton by factors as high as 10^4 and 10^5 (Zhang et al., 1990). Assuming a selenite concentration

in the Carquinez Strait of 100 ng L^{-1}, the expected Se concentration in phytoplankton would fall in the range of 1.8 to 26.3 mg kg^{-1} (Zhang et al., 1990; Zawislanski et al., 1996). Thus the phytoplankton contribution to suspended sediment Se in the Carquinez Strait would fall between 0.18 and 0.789 mg kg^{-1} assuming 70% of the organic carbon in suspended sediments comes from phytoplankton.

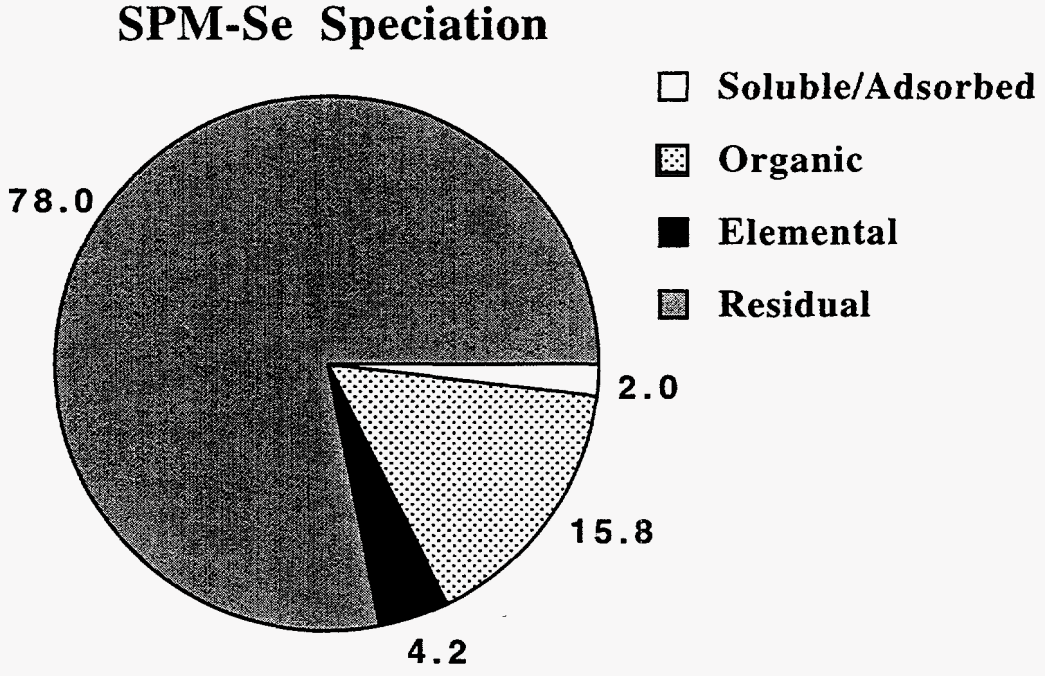

Figure 3.4 Speciation of Se on representative suspended sediment collected off the Martinez pier.

If phytoplankton does bioconcentrate Se from Carquinez Strait waters, there are more forms than just selenite present, and their efficiencies are not completely understood. Also, one would assume that total Se concentrations in suspended sediments would correlate with chlorophyll concentrations extracted from the sediments. But measurements of chlorophyll-a, -b, and -c in SPM do not correlate with SPM-Se in this study. Data presented by Cutter (1989) for solution concentrations of SPM versus chlorophyll-a showed a weak correlation ($r = 0.607$). Attempts to manipulate the Cutter (1989) data by multiplying the chlorophyll values by a concentration factor and the dissolved Se concentration did not improve the fit. One reason such a correlation may not work is due to the difference in the two studies. Cutter (1989) tabulated data for a salinity gradient that began at the Golden Gate Bridge

and ended in the San Joaquin/Sacramento rivers over a period of 3 days, while the LBNL data is taken solely from the Carquinez Strait MRP site over 12 months (i.e. in an area where salinity fluctuations are much less severe). Zhang et al. (1990) attributed the rapid disappearance of selenite from solution to phytoplankton-surface adsorption, and not metabolism. As is shown in the next section, salinity has a strong influence on selenium sorption in suspended sediments, and therefore may significantly affect Se uptake by phytoplankton.

3.2.4 Sorption Study

Sorption of selenite decreases with increasing salinity (Fig. 3.5). This result agrees qualitatively with the idea of ligand exchange with HCO_3^- and other anions (Balistrieri and Chao, 1987). However, the decrease is greater than would be predicted, given the absence of anions which are known to strongly compete with selenite, such as phosphate (Neal et al., 1987) or silicate (Balistrieri and Chao, 1987). It is unclear therefore, why sorption onto the MRP suspended sediment is strongly influenced by ionic strength, but it may be that surface sites are dominated by organic matter or cell tissue from phytoplankton that were filtered out of Bay water and freeze-dried onto the colloids. Also, complexation of Se(IV) at higher ionic strengths could be a factor. Further experiments will be run with fresh suspended sediments to determine what impact desiccation and size fractionation might have on the adsorption process.

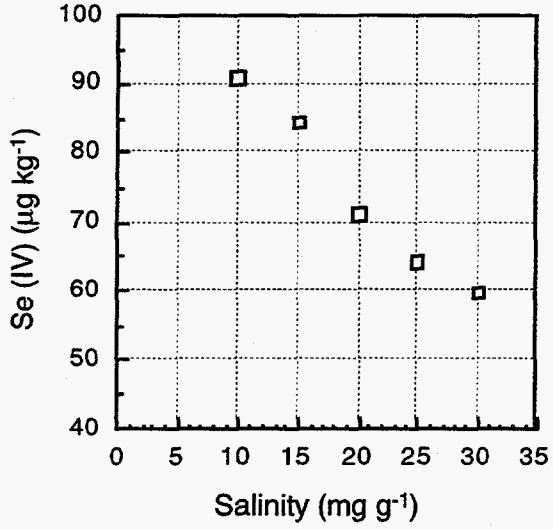

Figure 3.5 Adsorption of a 10 µg Se (IV) kg^{-1} spike in synthetic seawater of different salinity and onto resuspended, freeze-dried suspended sediments from the MRP site.

3.2.5 Suspended Sediment Characterization

XRD analysis of the whole suspended sediment samples revealed that they are dominated by quartz with small phyllosilicate peaks, and little other identifiable mineralogy. Fig. 3.6 contains three typical spectra for samples obtained in May, July, and October of 1996. There are discernable differences between spectra, therefore samples were sedimented to isolate the less than 2 μm fraction for further characterization.

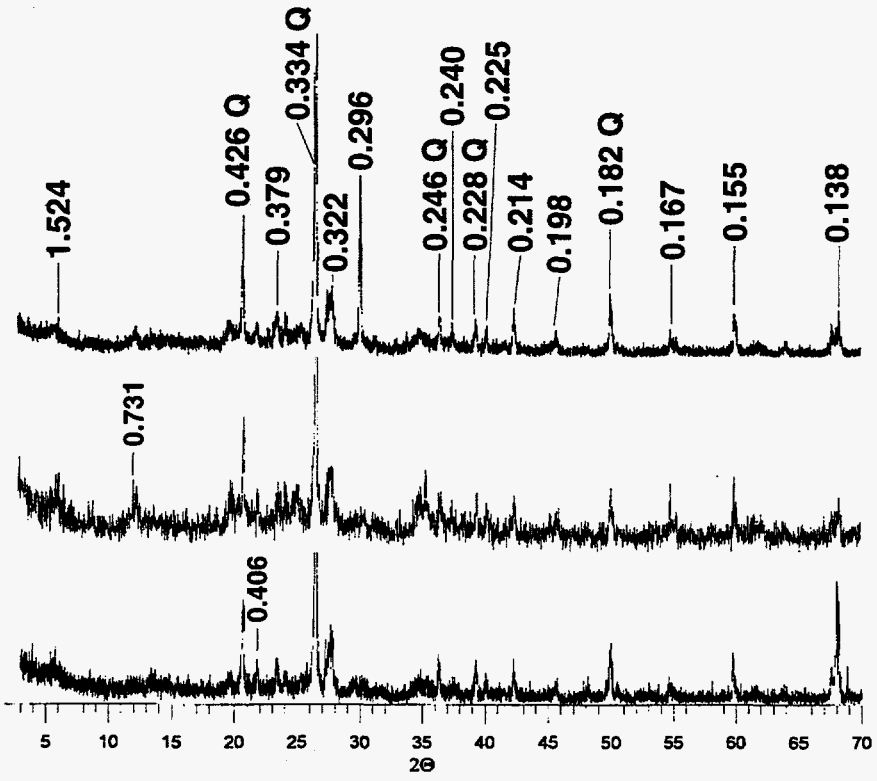

Figure 3.6 XRD spectra of suspended particulate matter from May, July, and October (from top to bottom) of 1996 from the Carquinez Strait.

Fig. 3.7 clearly shows the spectra for a TSM sample taken on 8-29-96, and glycolation revealed that the peak which shifted from 1.5 to 1.45 nm is a montmorillonite clay. A weak illite shoulder appears downfield of montmorillonite. The other basal peaks are from muscovite and kaolinite, in that order, with weaker

peaks that are potentially from muscovite and montmorillonite downfield of the kaolinite peak. Examination of three samples from May, July, and October revealed very little variation in mineralogy. No crystalline metal oxide peaks were discernable in any of the samples analyzed. The dominant mineralogy of the fines appears to be montmorillonite, muscovite, and kaolinite. Illite is present in a very small concentration.

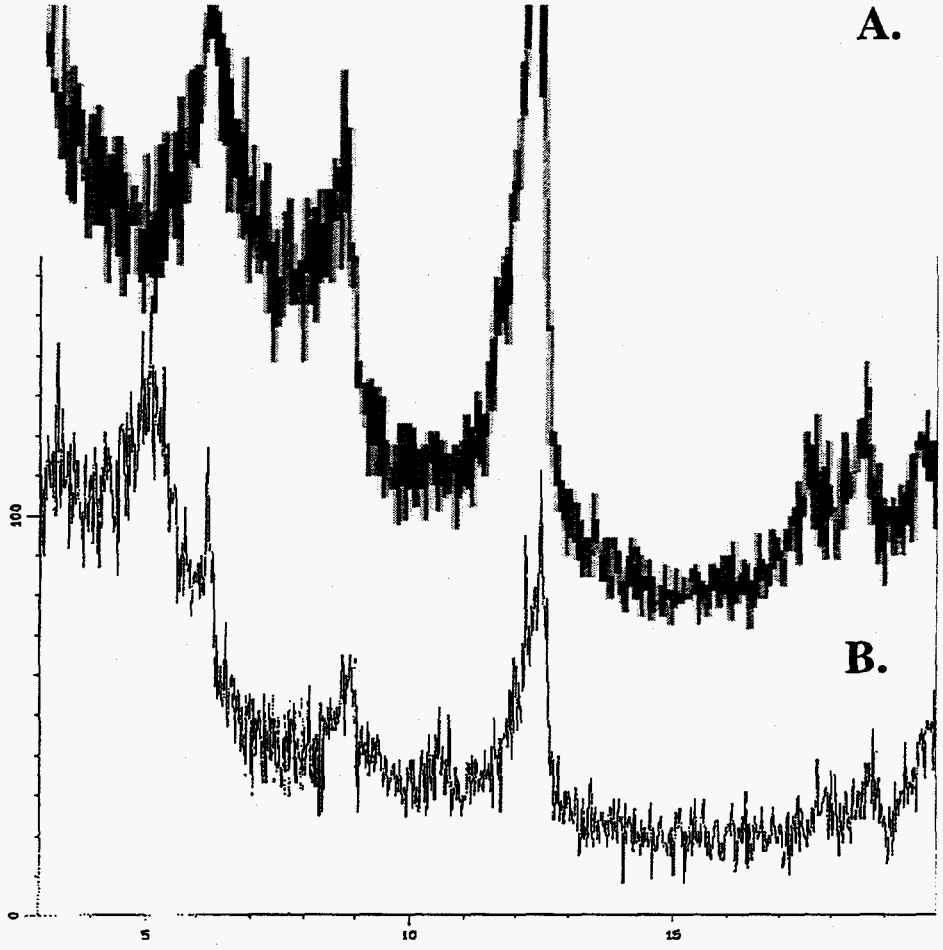

Figure 3.7 XRD spectra of fines from TSM sample collected on 8-29-96, glycolated (A) and untreated (B).

4 Sediment Dynamics: Influence on Se Accumulation

Data presented in previous chapters suggests that Se accumulation in the mudflats and marshes may be strongly influenced by sedimentation dynamics. Specifically, the deposition of sediment in these areas may be the primary means by which Se enters the wetland system. A sediment budget is being developed for two sites along the Carquinez Strait and associated rates of Se accumulation are being measured.

While there have been many studies that have measured rates of accretion and erosion in wetlands (e.g. Harrison and Bloom, 1977; Pethick, 1981; Stumpf, 1983; Stoddart et al., 1989; Orson et al., 1990; and Childers, et al., 1993), these have generally been concerned with long-term rates over broad areas. There have been very few attempts to document marsh sediment dynamics at a higher resolution, both spatially and temporally. One study by Pethick (1992), shows an interesting correlation between changes in elevation of a mudflat and similar but opposite elevation changes in the adjacent marsh plain. This suggests a coupling of the processes that create and maintain both mudflats and marsh plains.

Research into the sediment dynamics of Martinez Regional Park and Southampton Bay wetlands was initiated in February 1996. The goal of this project is to develop a high-resolution record of the erosion and accretion of sediment along a transect from the mudflat to the high marsh and to measure the effect on Se accumulation. Data from the MRP site have been more thoroughly analyzed and are presented herein.

4.1 Methods

Twelve erosion/sedimentation pins and sediment traps were installed at Martinez Marsh in March of 1996. The pins are 60-cm lengths of stainless steel rod. The sediment traps consist of 10 x 10 cm squares of plastic with long bolts at each corner to serve as anchors. The smooth plastic surfaces were roughened by gluing fine sediment on them and then painted orange to facilitate their recovery.

The pins and traps were installed along a 95 m transect that is perpendicular to the shoreline and spans from the high marsh to the mudflat (Fig. 4.1). The pins were inserted into the mudflat and marsh plain so that only the top 30 cm of each pin

remained unburied. The traps were installed adjacent to the pins and flush with the ground surface.

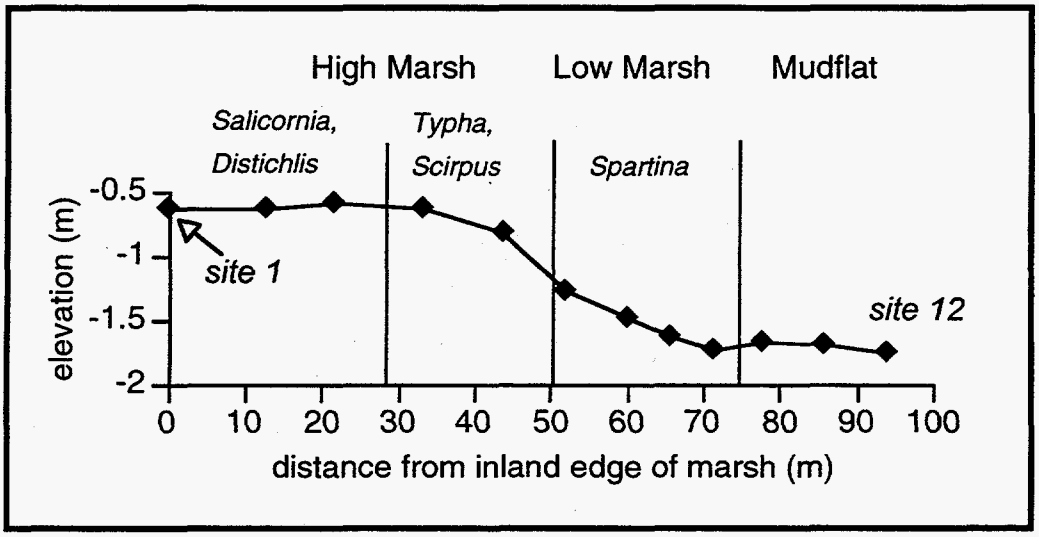

Figure 4.1 Transect through the Martinez wetlands with a 10× vertical exaggeration. Each symbol indicates the location of an erosion/sedimentation pin and sediment trap. The pins and traps are numbered in increasing order from marsh plain to the mudflat.

The pins and traps are monitored monthly. The exposed portion of the pins is measured to the nearest millimeter. Sediment from each trap is collected, freeze-dried, and weighed. The sediment is ground to a powder, digested (TAD) and subsequently analyzed for total Se using HGAAS (see Appendix A for details on extraction and analysis procedures). In addition, a subsample is analyzed for C and N, using a Carlo Erba NA 1500 C and N analyzer (Milan, Italy). The carbon/nitrogen ratios are helpful in estimating the relative contribution of organic material.

4.2 Sedimentation Dynamics

4.2.1 Results

A plot of monthly changes of the marsh surface at each pin (Fig. 4.2) shows seasonal and spatial trends. The most obvious is the rapid accretion of sediment at the border between the high marsh and the low marsh (Pin 6). Pin 5 also indicated rapid accretion, however much of it was caused by the accumulation of cattail litter which is subject to decomposition.

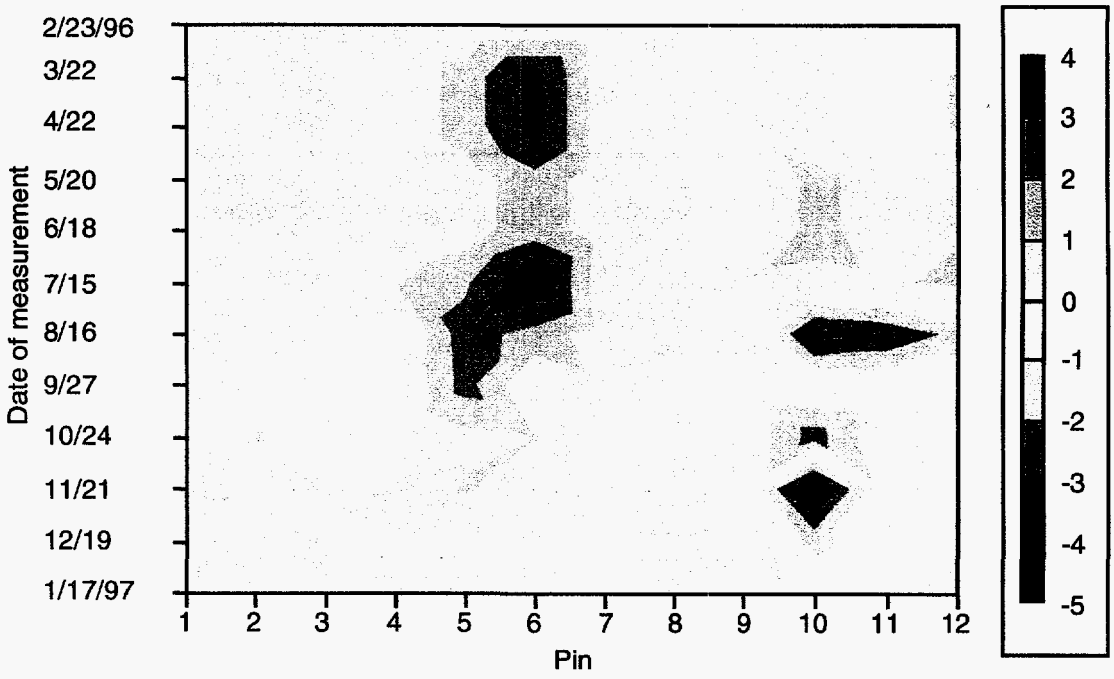

Figure 4.2 Monthly changes in the elevation (in cm's) of the surface at each pin. Red indicates accretion, while blue indicates erosion, both relative to the elevation on 2/23/96.

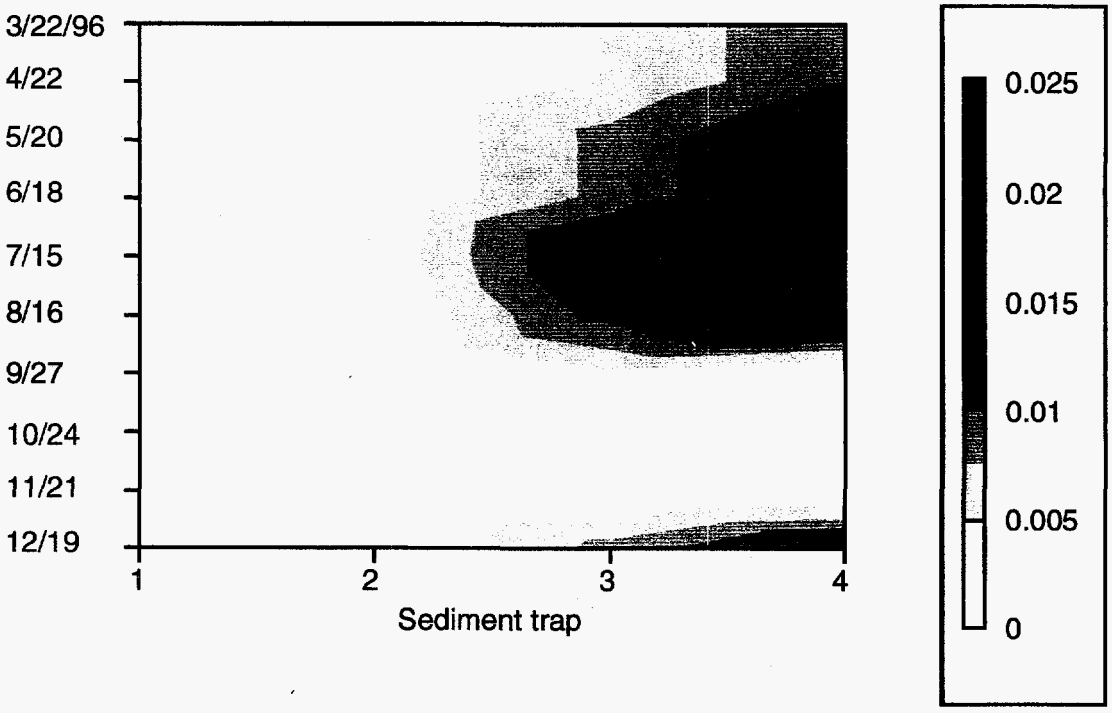

Figure 4.3 Rates of accretion (kg m^{-2} day^{-1}) on the marsh plain only (traps 1-4).

The instability of the mudflat surface is apparent. The mudflat acts as a temporary storage area for sediment during the spring and fall and as a source of eroding sediment during the summer and winter. Furthermore, erosion of the mudflat coincides with the periods of highest deposition at Pin 6.

Unlike the pins, the sediment traps can only measure deposition, though much smaller changes in mass can be detected. Fig. 4.3 clearly shows the effect of the subtle topography of the marsh plain. Although the rates are low, there is a distinct decrease in sedimentation from the bayward side to the landward side of the marsh plain.

4.2.2 Discussion

Sedimentation dynamics throughout the wetland system (marsh plain, low marsh, and mudflat) are controlled by three factors. The first is the transport of water and sediment down into the San Francisco estuary from the Sacramento and San Joaquin Rivers. The stage of these rivers will affect the water surface level of the estuary and, therefore, the frequency and magnitude of marsh flooding. Higher inundation frequencies and magnitudes will increase the amount of sediment brought into the marsh.

The amount of sediment brought into the estuary is a function of time as well as river discharges. The first high flows of the rainy season will flush out most of the fine sediment that had accumulated in the watershed during the summer. In fact, the peak sediment discharge usually occurs before the peak flows.

The second important variable is the tidal regime. Schoellhamer (1996) observes that, although spring tides are not strong enough to produce bottom shear stresses sufficient to resuspend significant amounts of sediment, they are effective in the lateral advection of suspended sediment. He concludes that suspended sediment concentrations (SSC) increase as a spring tide is approached and decrease as a neap tide is approached. The decrease in SSC is due to the slower currents and the longer periods of slack water.

The final critical factor is the wind. The direction of the wind may strongly influence the net flow of suspended sediment while the magnitude of the wind determines whether resuspension of sediment will occur. Schoellhamer (1996) concludes that, in the South San Francisco Bay, wind shear may be the most important factor in the transport of sediment throughout the estuary.

Unfortunately, most of the data necessary to investigate the relationship between the aforementioned processes and Martinez site are not yet available. However, some inferences can be made. The Delta is subjected to strong westerly winds nearly every

day during the summer. These winds produce wind waves that can resuspend sediment. This meteorological condition, coupled with reduced discharges of water and sediment from the rivers caused by the summer drought, may explain some of the patterns seen in Fig. 4.2.

During the spring and early summer the winds are light (with the exception of the occasional storm) and the mudflat is able to store sediment that settles onto it. This sediment is very fine and does not have time to become well consolidated. With the arrival of the thermal winds in the summer, this sediment is scoured out and the input of sediment from upstream is insufficient to replace it. It also appears that some of this resuspended sediment is re-deposited at the border between the high marsh and the low marsh (Pin 6, Fig. 4.2). The presence of *Scirpus* and *Typha* undoubtedly plays an important role in this re-deposition by absorbing the wave energy and enhancing sedimentation. In the early fall, the winds diminish and the erosion of the mudflat ceases until the storm season begins in late fall.

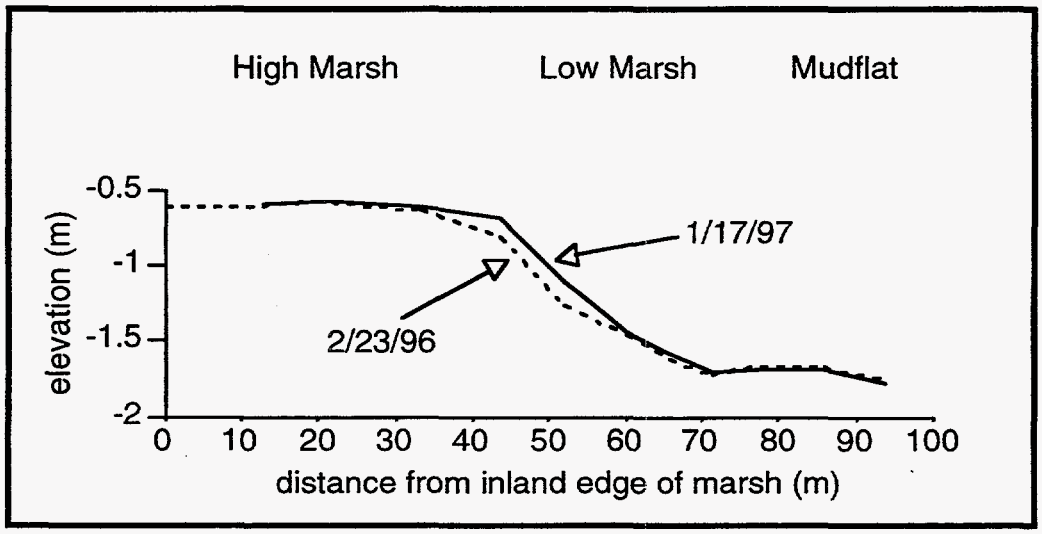

Figure 4.4 Changes in the surface elevation of the Martinez Marsh from Feb. 1996 to Jan. 1997, with a 20× vertical exaggeration

Fig. 4.4 clearly shows that, along this transect, the marsh is growing out towards the bay. This lateral growth simply indicates that the influx of sediment to the area exceeds it removal. This is surprising since many of the Bay Area's wetlands visited by the author are actively eroding along their borders with the bay. In fact, there are signs of erosion along much of the Martinez Marsh shoreline. It has been suggested (L.E.

Wells, personal communication) that the widespread erosion of marshes throughout the Bay Area may be linked to the large influx of sediment washed down from the Sierra Nevada during the period of hydraulic mining. When this pulse of sediment passed through the estuary, many wetlands experienced rapid growth (Gilbert, 1917). It has recently been hypothesized that the wave of sediment has finally passed through the system, thereby altering the sediment balance in the estuary. The marshes can no longer be maintained in their present configuration and are eroding back to a different equilibrium state.

4.3 Selenium, Carbon, and Nitrogen

4.3.1 Results

Total Se concentrations in trapped particulates are shown in Fig. 4.5. Se concentrations increase from the traps placed in the mudflats to the traps on the marsh plain, from approximately 0.5 $\mu g\ g^{-1}$ to 1.0 $\mu g\ g^{-1}$. The increase in Se concentrations occurs at trap 6, at the interface between the *Spartina* zone and the *Typha/Scirpus* zone. During the period of July through August, by far the highest Se concentrations were observed at trap 5, up to 2.4 $\mu g\ g^{-1}$. A very similar pattern is observed in the total carbon (C) data (Figure 4.6). Because of the need to reanalyze certain samples, C data from the March-April set is not shown here, nor in subsequent figures. This data, as well as additional Se and C data will soon be available for the period from September 1996 and December 1996. Carbon levels in the mudflats are between 0.5% and 3%, increase near the *Spartina-Typha/Scirpus* transition zone (trap 5), and are as high as 10% in the marsh plain. The two high C values measured at trap 5 in July-August and again in August-September correspond to high Se values, as seen in Fig. 4.5.

A direct comparison of Se and C is shown in Fig. 4.7. Although there is clearly a positive correlation between sediment Se and C, it is not a linear one. Se concentrations appear to plateau at C > 5%, but then increase again at C > 10%. More samples with high C concentrations are needed to increase the confidence in this trend. In Fig. 4.8, Se concentrations are plotted against percent N in the trapped particulates. Once more, there is a relative paucity of data in the high-N range. However, a positive, possibly linear relationship is apparent. Finally, a positive correlation between Se and the C/N ratio is shown in Fig. 4.9.

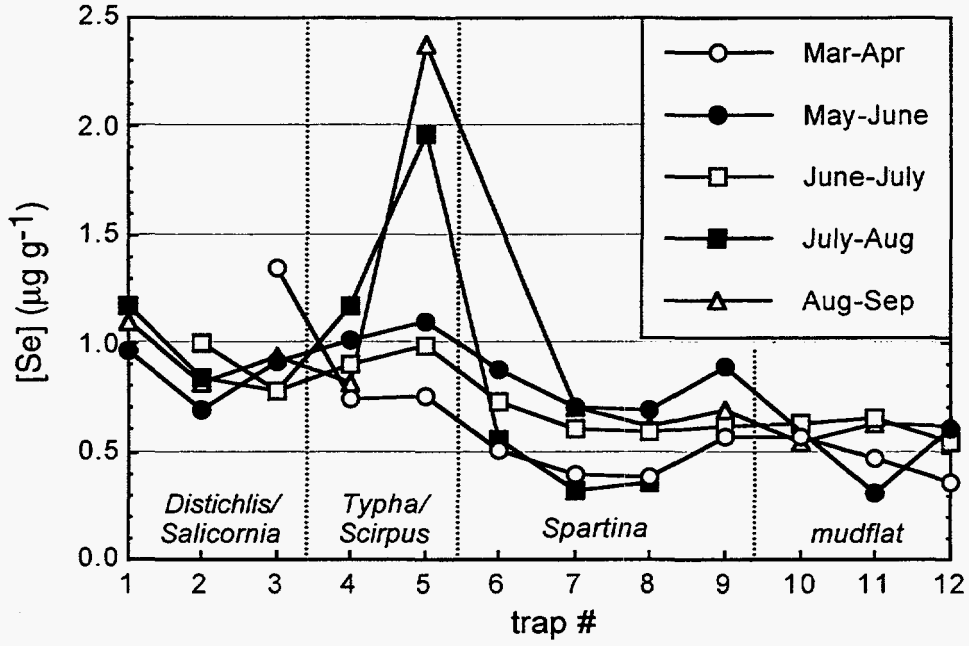

Figure 4.5 Total selenium on sediments trapped in the Martinez wetlands.

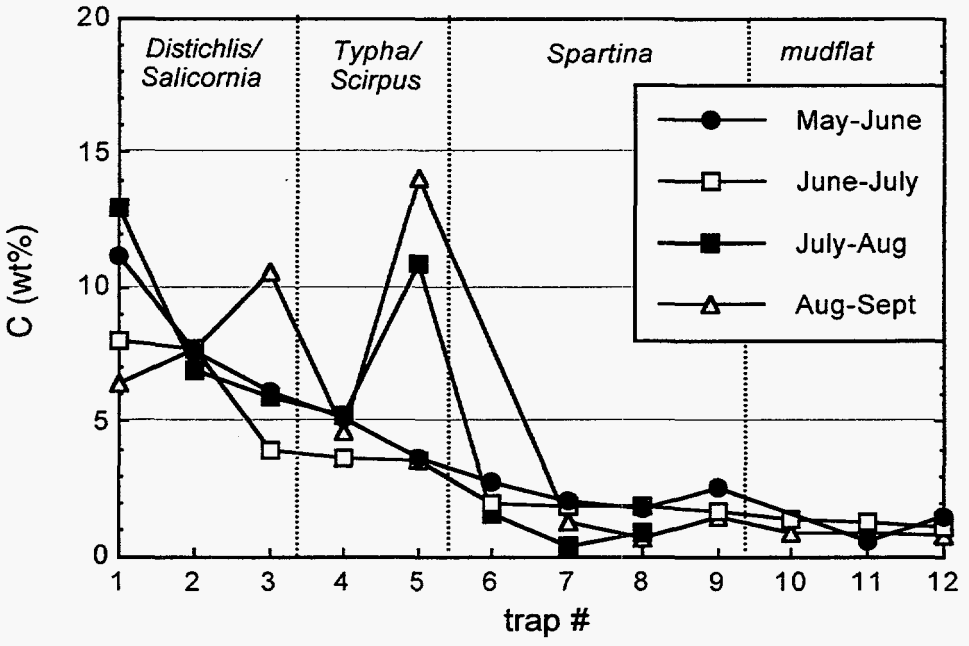

Figure 4.6 Total carbon on sediments trapped in the Martinez wetlands.

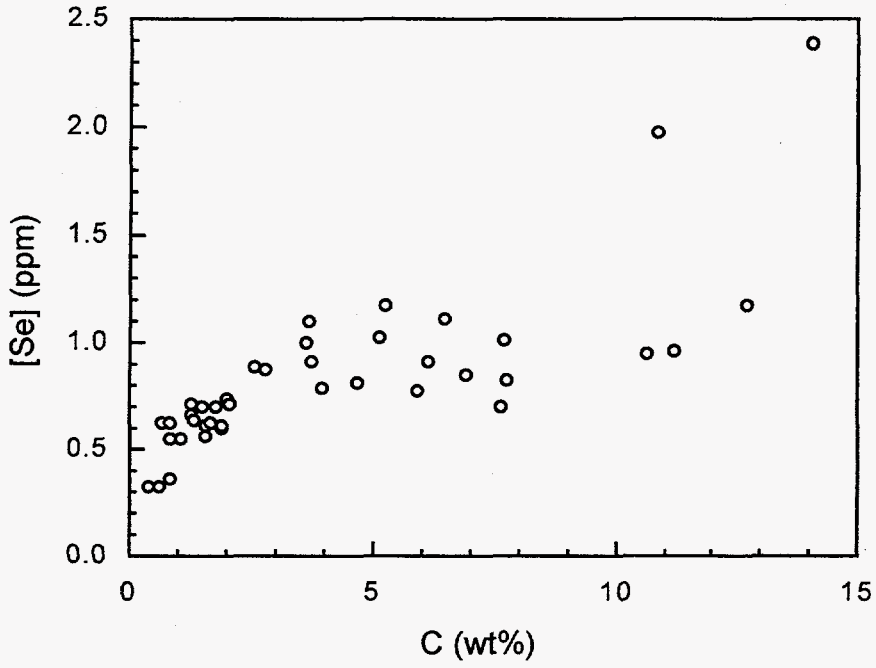

Figure 4.7 The relationship between Se and C on sediments trapped in the Martinez wetlands.

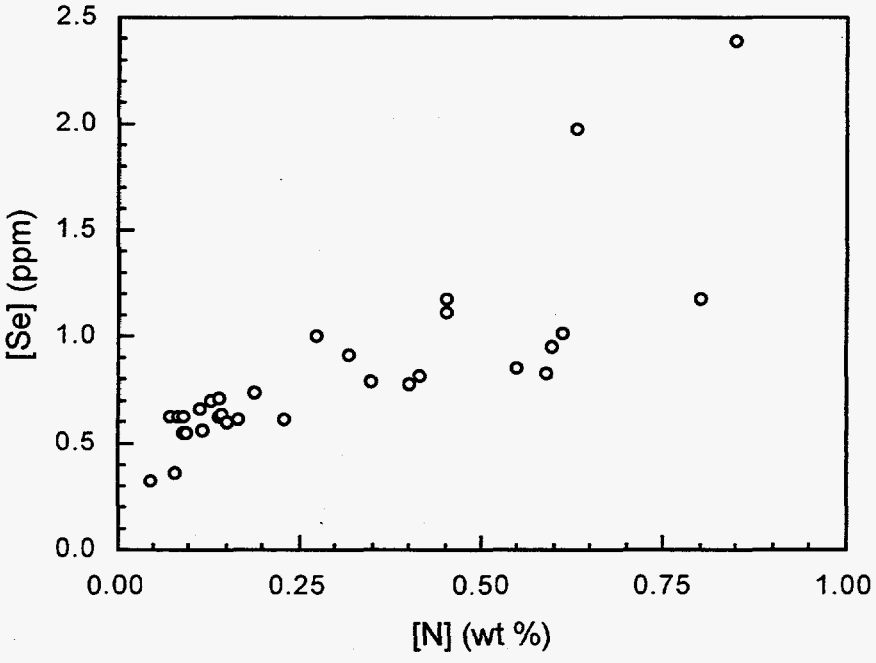

Figure 4.8 The relationship between Se and N on sediments trapped in the Martinez wetlands.

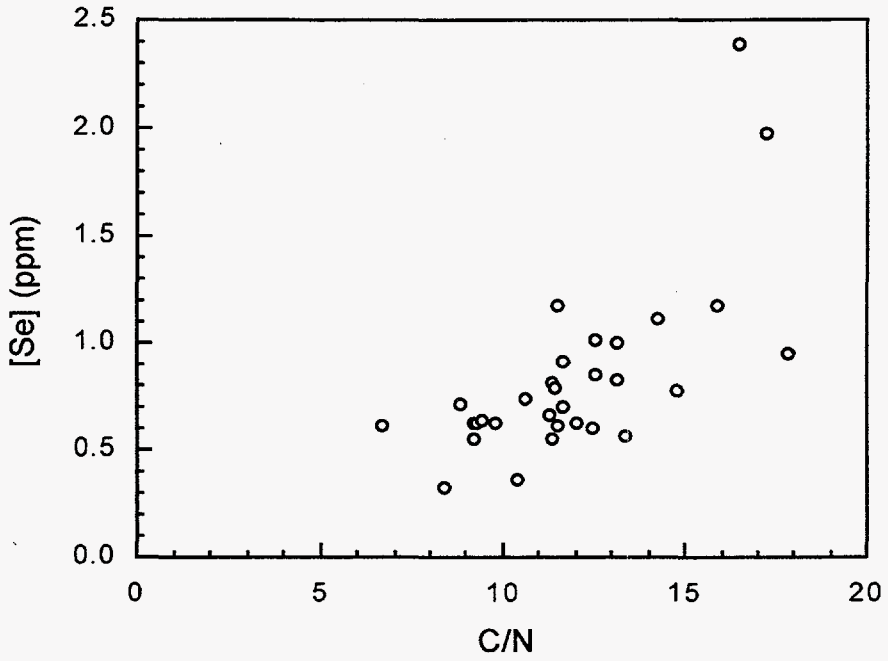

Figure 4.9 The relationship between Se and the C/N ratio on sediments trapped in the Martinez wetlands.

4.3.2 Discussion

The landward increase in Se concentration on trapped sediments may be indicative of a size-separation of particulates in the wetlands system. As seen from the sedimentation/erosion patterns presented in Fig. 4.2, the mudflats are a high-energy regime in which tidal action and wind gusts can produce resuspension and also maintain coarser particles in suspension. Ongoing work on the size-composition of particulates trapped in different regimes will shed further light on this issue. On the other hand, the low marsh and marsh plain environments are lower and lowest energy environments in the wetlands, respectively. This is also borne out by the net sedimentation data, shown in Fig. 4.4, where it is quite apparent that the bulk of the suspended particulates settle out at within the low marsh and the resultant sedimentation rates in the marsh plain are very low (Fig. 4.3).

A comparison between Se in trapped sediments, averaged over the 7 month period from March through September 1996, and Se concentrations in the top 1 cm of sediment, sampled in December 1995, is shown in Fig. 4.10. The surface sediments were not sampled at the exact location of the sediment traps but are within a few meters of the transect and include more than one data point per location. The *Spartina* zone,

which was not fully developed at the time, was not sampled as intensively. Qualitatively, there is very good agreement between the trapped sediment-Se and Se on surface sediments. However, surface sediment concentrations in the marsh plain are generally higher than on the trapped sediments, while those in the mudflats are often lower. The marked peak in trapped sediment Se within the *Typha/Scirpus* zone is the most notable discrepancy between these two data sets. It is possible that this is a seasonal effect which may not be resolvable until 12 months of data are available. If this is the case, it may be that high-Se sediments deposited in the low marsh are subsequently displaced to the marsh plain, which would explain the higher surface sediment Se in the *Distichlis/Salicornia* zone. On the other hand, reducing conditions on the marsh plain may result in additional Se sequestration on surface sediments.

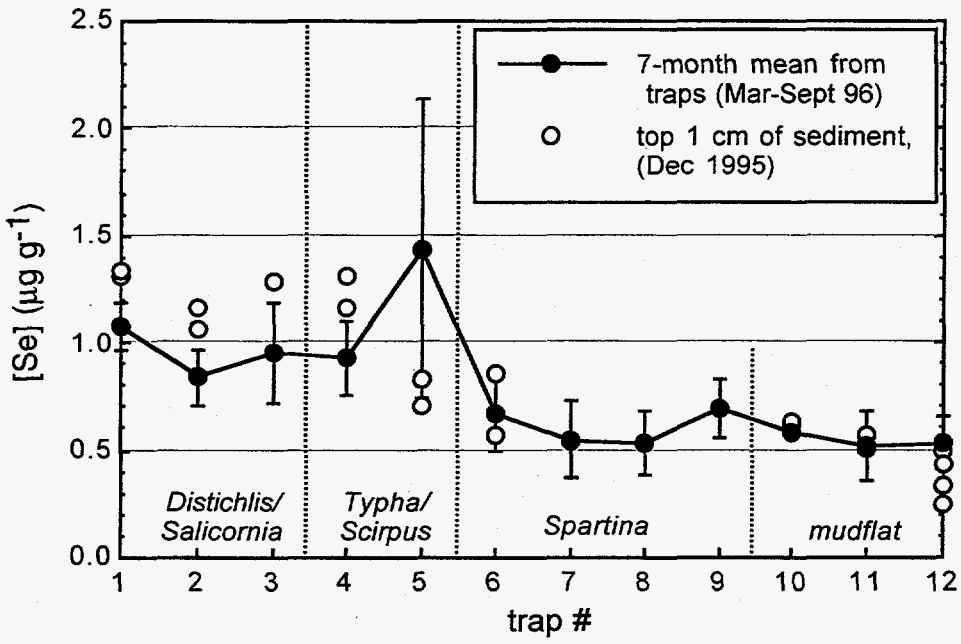

Figure 4.10 Total selenium on trapped sediments and surface sediments sampled in the Martinez wetlands.

The C trends observed in Fig. 4.6 suggest that particulates which are being deposited in the marsh plain contain much more organic matter than those settling on the mudflat. This agrees with the idea that there is a size separation of particulates normal to the shoreline. The C-rich particulates being deposited on the marsh plain may have a high biogenic component, such as plankton, which would also explain the high

Se levels. It should be noted that based on the sampling of water from the Carquinez Strait (see Section 3.2), the bulk suspended particulates generally carry between 1 and 1.5 $\mu g\ g^{-1}$ Se and contain between 1.5 and 3% C. As discussed in Section 3.2, the inability to effectively extract and identify Se species associated with suspended particulates may be indicative of a large biogenic component. The low Se and C concentrations observed on both the surface and trapped sediments in the mudflat may be a result of a size separation and the settling out of coarse, largely inorganic particles. The relatively lower Se in the surface sediments shown at trap 12 in Fig. 4.10 suggests the existence of some mechanism, such as diffusion, in removing Se from the sediments.

The fact that the tidal wetlands are hydrologically and hydromechanically dynamic cannot be ignored. It is clear that sediments in the mudflats are being actively deposited and resuspended. Therefore it is possible that the source for the trapped sediments is local resuspension and that the data are not indicative of long-term trends. Although this is plausible in the mudflats, it is less so in the marsh, and especially in the marsh plain, where the shallow water depth and the presence of thick stands of plants greatly reduces the energy of the system. Since the net effect on the wetland was one of accretion, it can be concluded that new sediment is being brought into the system.

Finally, the presence of plant litter needs to be considered. As pointed out earlier, traps within the low marsh often collected plant litter, which, although it certainly contributes to the chemical composition of the sediment, does not have a major net effect on marsh accretion. As seen in Fig. 4.6, high C values at trap 5 are probably related to the plant litter. Se concentrations (Fig. 4.5, trap 5) are also elevated at that time. However, it needs to be noted that Se concentrations in plant tissue within the marsh are generally significantly lower than in the sediments. Therefore, it is possible that the litter acts as a reducing surface for Se immobilization. Further data on plants and plant litter is presented in Chapter 5.

4.4 Summary

The preliminary analysis presented herein will be augmented as data from a complete year of monitoring becomes available. C and N data from surface sediments is now being reanalyzed and will help resolve questions regarding the degree of resuspension in the system. Eventually, discharge and SSC from the Sacramento and San Joaquin Rivers as well as wind data from the field site will be compared with the pin and trap data to explore any correlation.

Some conclusions, however, can be made from this preliminary analysis. The first is that the mudflat serves as a temporary storage area for sediment and that the state of the mudflat depends primarily on the wind conditions and the influx of sediment from upstream. Secondly, along this transect, the marsh is laterally accreting. This is surprising given the general trend of eroding marsh shorelines throughout the Bay Area. This may be related to the local geography of the shoreline, dominated to the east by engineered structures. An analysis of historical aerial photos of Martinez Marsh may shed light on this bayward expansion. Thirdly, Se concentrations on trapped sediments are indicative of a size-separation of suspended particulates between the high-energy mudflats and the low-energy marsh plain. The assumed inverse relationship between particle size and Se concentration needs to be further tested, the proportion of organic particulates needs to be measured, and the influence of plant litter on Se immobilization needs to be considered.

Finally, a preliminary estimate of the sediment-Se flux into the tidal wetlands can be made, though only for the marsh, since a complete year of data is needed to characterize the dynamic mudflat. Based on the range of sedimentation rates observed in the marsh (Fig. 4.3), and the concentration of Se on the settling particulates (Fig. 4.5), sediment-Se deposition in the marsh ranges from less than 1 mg m^{-2} yr^{-1} in the most upland parts of the marsh plain, to 7 mg m^{-2} yr^{-1} in the lower marsh, although most values fall at or below 3 mg m^{-2} yr^{-1}. Even though the marsh is much less dynamic than the mudflats, there is clearly the possibility of sediment redistribution at different times of year, and this analysis will not be complete until 12 months of data are collected. Furthermore, it is not known as to how representative this 12 month period is compared with other years and the range of Se accumulation rates presented herein needs to be considered in this light.

5 Plant Selenium, Biomass, and Decomposition Rates

Uptake of pore water by plants is an important flux which controls the vertical re-distribution of solutes, including Se. Although it may be a small fraction of the total Se inventory in the sediment system, soluble Se is the only form which can be physically displaced in the subsurface. Root extraction of pore water, advection, and diffusion are the primary mechanisms for such displacement. Furthermore, once incorporated into plant tissue, Se is generally converted to an organic form and upon the plant's death becomes part of the sediment system. Measurements of plant tissue-Se and the rates of plant litter decomposition are discussed below.

Vertical selenium fluxes in the marsh are largely dependent on plant uptake and assimilation. Assimilation is defined as one of three known fates for Se once it passes from the interstitial water into the root. Se can be:

- assimilated into amino acids such as selenomethionine or selenocysteine,
- (temporarily) accumulated in inorganic form, primarily in the form of selenate, or
- volatilized as dimethyl selenide and thereby eliminated from the system.

Most of the Se is eventually converted into amino acid form (Gissel-Nielsen, 1979) and consequently has the potential of adding organo-Se to the existing pool through the decomposition of plant material. To investigate the role of emergent marsh plants in selenium cycling, the following components are being addressed:

- aboveground biomass of six predominant emergent marsh plant species: *Scirpus robustus, Scirpus californicus, Salicornia sp., Typha latifolia, Distichlis spicata, Spartina foliosa,*
- total Se concentrations in above-ground and below-ground plant components,
- total Se concentrations for root-associated soils, and,
- decomposition rates for plant material in the marsh.

Based on the biomass data, turnover rates of plant material will be estimated. The calculation is based on annual production and mean yearly live biomass. The Se data will help develop a species-specific correlation between root and shoot Se, as well as a correlation between available soil Se and plant Se. It will also help quantify the relative contribution of plant material to the overall Se mass balance. By measuring the turnover rate, the amount of Se returned to the marsh through decomposition will be estimated.

Most of this work is still in progress as a full year of data is necessary. Therefore, a complete analysis with respect to plant turnover rates is not possible. This presentation will be limited to a description of methods, available data, and preliminary analysis of litter decomposition rates.

5.1 Methods

5.1.1 Biomass Sampling

Sampling consists of clipping all of the aboveground material falling within a 0.25 m^2 area at 5 randomly selected sites for each species. All vegetation is clipped to ground level and placed in a plastic bag for transport. Site selection, for quadrat placement, is based on the level of disturbance and species homogeneity and is otherwise random. "Standing live" and "standing dead" plants within each species are separated in the laboratory. "Standing dead" refers to an intact, free-standing dead plant. These are further defined by color and general appearance; plants which are dead and uprooted are not included. Samples are then rinsed, dried at 70°C for 72 hours, and weighed. All reported weights are for dry tissue.

The first sample set was collected between 1/15/96 and 1/23/96. The second sample set was collected between 6/28/96 and 7/3/96. Both of these sets have been processed and data is available. A third sample set, collected between 1/21/97 and 2/3/97, is currently being analyzed.

5.1.2 Total Selenium Determination in Plant Tissues

Total selenium values in both above- and below-ground tissues are determined through a wet ashing procedure modified from Ganje and Page (1974). This method, which is described in detail in Appendix A, involves grinding of the dried plant tissue to a fine powder, and subsequent acid and peroxide digestion, followed by analysis using hydride-generation atomic absorption spectroscopy.

5.1.3 Total Selenium Determination in Root-Associated Soil

Soil-root composites for each quadrat were sampled from the marsh in January 1996 and frozen until the time of extraction. Two subsamples of soil were removed from the composite as determined by their affiliation with the roots. Only soil from within 1 cm of the roots was used. The total selenium concentration in the soils is determined by an acid digestion procedure (see Appendix A).

5.1.4 Litter Bag Study

The litter bag procedure is adapted from White et. al. (1978). Above-ground plant material was collected from random locations in the marsh at the Martinez Regional Park Site in June of 1996. In the laboratory, samples were rinsed, then dried at 70°C for 72 hours. Approximately 20 g of dry plant shoots and leaves were placed in 20 cm by 20 cm nylon mesh bags with 2 mm diameter holes. Seventy-two bags were constructed: 24 *Spartina* bags, and 12 bags each of *Typha, Scirpus, Salicornia*, and *Distichlis*. These bags were sewed closed. Bags of each of the plant species were connected in sets of two with paper clips and nylon string. Using 30-cm-long threaded rods, these bags were secured on the surface of the marsh along a transect within the study site on 7/4/96. The bags were placed in their respective environments as to mimic as closely as possible their natural habitat (Fig. 5.1).

Spartina plants were collected in monthly intervals whereas the bags of the other four species were collected every two months. This sampling strategy was based on the high decomposition rates of *Spartina* found in other studies (e.g., White and Trapani, 1982). A set of two bags was sampled for each plant species. The collection dates for *Spartina* bags were 8/2, 9/13, 10/13, 11/18, and 12/19 1996 and 1/18/97. Other bags were collected on 9/13, 11/18, and 1/18/97. The same sampling scheme will continue until June 1997.

Litter bags were transported to the laboratory after collection. Plant material was placed in plastic bags which were put into an ultrasonic bath for 5 minutes. The plant material in the bags was subsequently rinsed through a 2 mm sieve for 20 to 30 seconds. An assumption was made that anything passing through the sieve would be material that would have been washed by the tides through the mesh bags and was therefore discarded. Samples were dried for 72 hours at 105°C. Biomass was measured after the samples had been dried. Samples were later ground in a coffee grinder. Total selenium values were determined through a wet ashing procedure modified from Ganje and Page (1974).

Figure 5.1 Distichlis spicata litter bags in the Martinez marsh.

5.2 Results

5.2.1 Biomass

The biomass of each species is shown in Figs. 5.2-5.6, with the data from the MRP site on the left and SHB on the right of each plot. The tall plants, both *Scirpus* species and *Typha*, have greater biomass than the short species, *Distichlis* and *Salicornia*. The biomass of *Spartina* varies significantly from the first to the second sampling period. As mentioned in Section 2.1, the density of *Spartina* plants increased significantly during the spring of 1996.

Spartina sp. was the only species which had both standing live and dead plants in January 1996 (Fig. 5.2). Both *Scirpus* species and *Typha* had both live and dead plants in June/July 1996, while *Salicornia* and *Distichlis* did not have dead plants during either sampling. When taking both live and dead plants into account, no significant changes in the biomass of *S. californicus* were observed (Fig. 5.3). The biomass of *S. robustus* decreased at both sites, with the dead plants contributing significantly to the total biomass in the summer of 1996 (Fig. 5.4). The total biomass of *Typha* did not change significantly, although approximately 25% and 35% of the plants were dead in

June/July at MRP and SHB, respectively (Fig. 5.5). Only minor changes were observed in the biomass of *Distichlis* and *Salicornia* (Fig. 5.6). Overall, *Typha* had the largest biomass, followed by *S. californicus*, *S. robustus*, and then the marsh plain plants, *Distichlis* and *Salicornia*. Overall, most of the biomass was represented by live plants, during both sampling events.

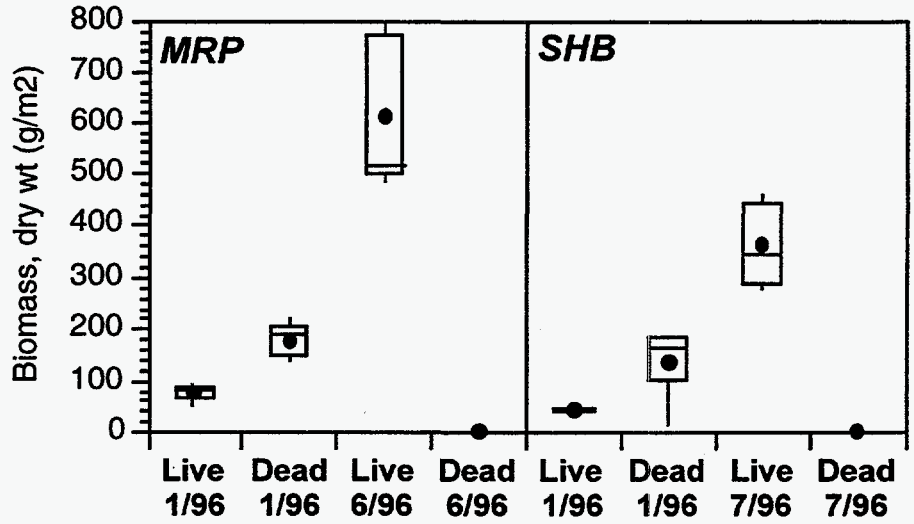

Figure 5.2 Biomass of Spartina *at sites MRP and SHB. For this and the following 14 figures, filled circles represent the arithmetic mean of three to five values; box denotes one standard deviation; whiskers show range of values; line inside box is median value.*

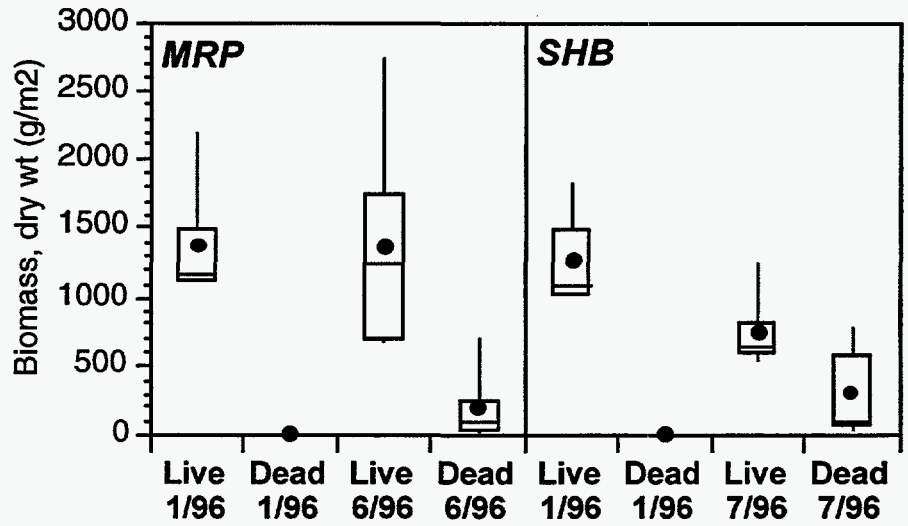

Figure 5.3 Biomass of Scirpus *californicus at sites MRP and SHB.*

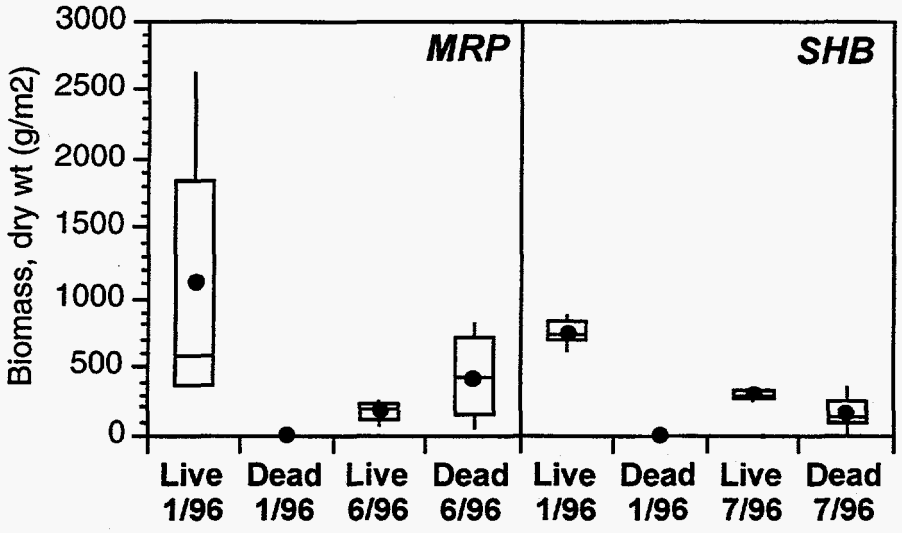

Figure 5.4 Biomass of Scirpus *robustus at sites MRP and SHB.*

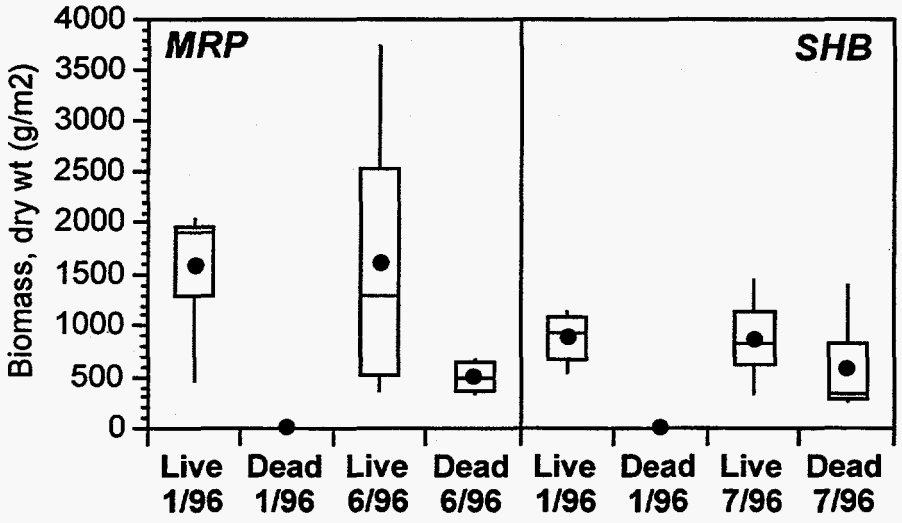

Figure 5.5 Biomass of Typha latifolia *at sites MRP and SHB.*

5.2.2 Total Selenium Determination in Plant Tissues

Total Se in plant tissues is presented in two ways: normalized to plant tissue mass ($\mu g\ g^{-1}$) and as the mass of Se projected over an area ($\mu g\ m^{-2}$). The former expression is helpful in evaluating Se accumulation in plant tissue, while the latter approach permits comparison of Se accumulation with other fluxes. Above-ground plant tissue Se data is shown in Figs. 5.7-5.16, with the data from the MRP site on the left and SHB on the right of each plot.

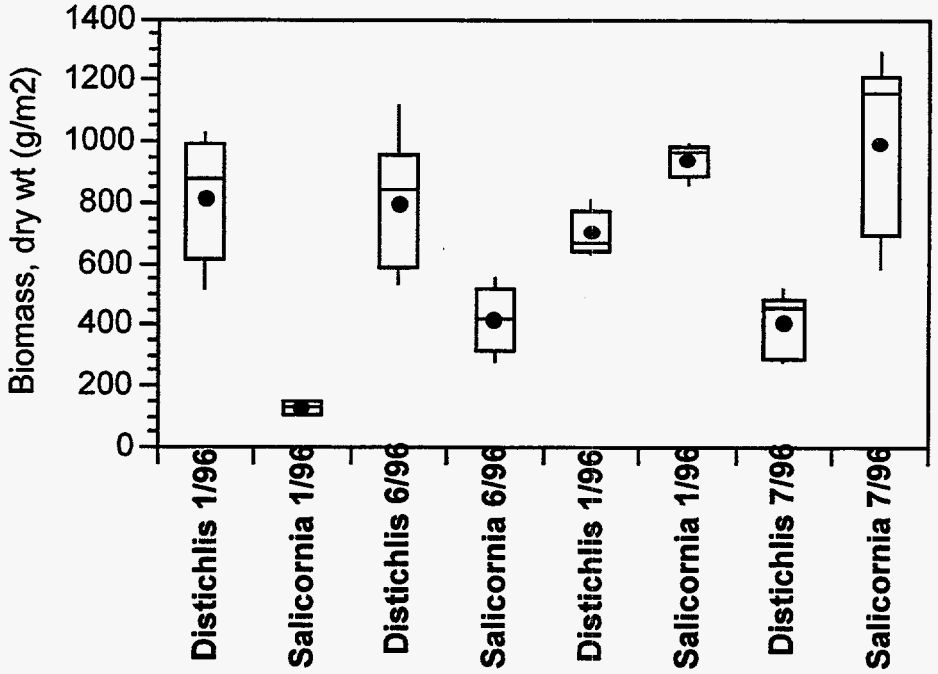

Figure 5.6 Biomass of marsh plain plants at sites MRP and SHB.

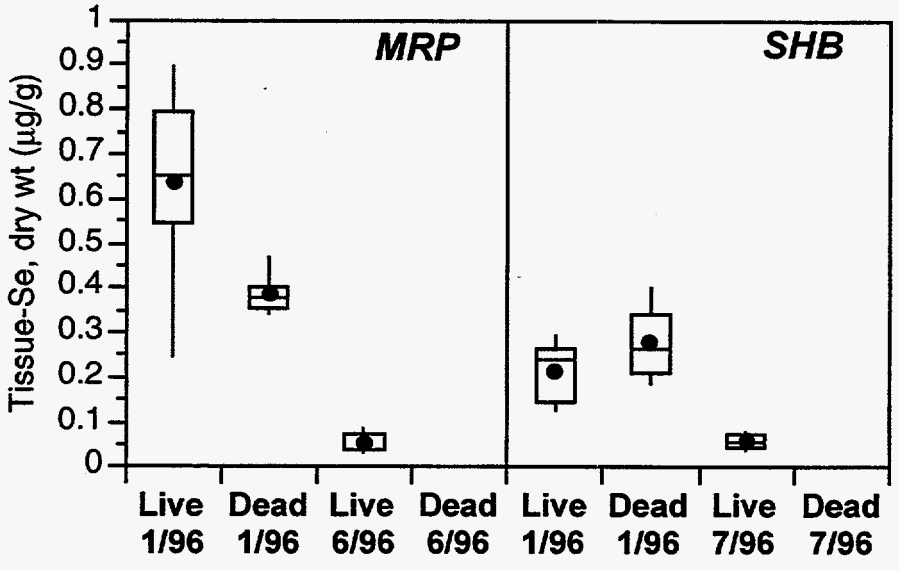

Figure 5.7 Tissue-Se concentrations in Spartina *at sites MRP and SHB.*

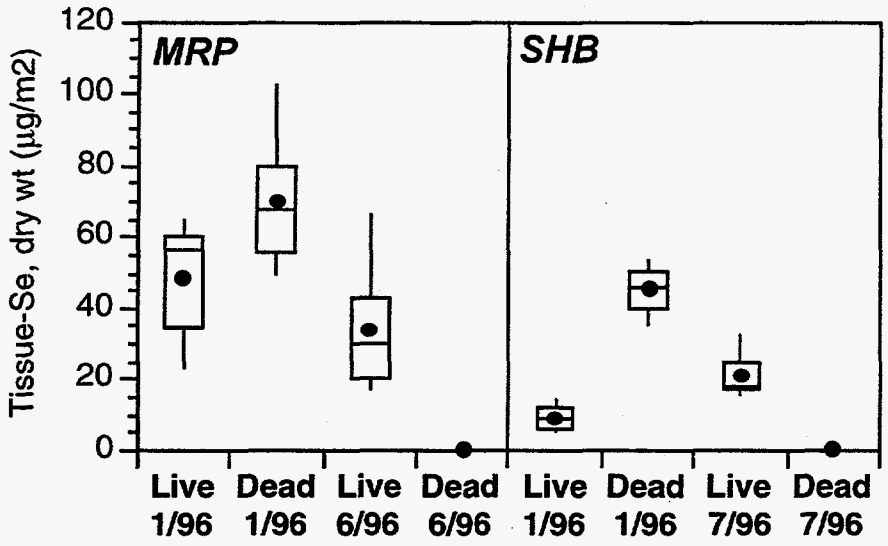

Figure 5.8 Tissue-Se mass in Spartina *at sites MRP and SHB, normalized to marsh area.*

Inversely to its biomass (Fig. 5.2), tissue-Se concentrations in *Spartina* decreased by approximately 90% between winter and summer (Fig. 5.7), while the total mass of Se accumulated by *Spartina* decreased by 75% and 50% at MRP and SHB, respectively (Fig. 5.8). Such trends suggest that the accumulation of Se in *Spartina* tissues is time-dependent and only a comparison at the same time of year should be used to define annual trends. Nonetheless, it is clear that Se levels in older *Spartina* plants, as seen in the difference between the live and dead populations in 1/96, are higher than in younger plants.

Se concentrations in both *Scirpus* species decreased from winter to summer, most markedly when comparing live tissue concentrations (Fig. 5.9 and 5.11) and in general at site SHB. Se concentrations in dead tissue in the summer were not much lower than live tissues in the winter, suggesting that some fraction of the live plants consisted of a new generation. The total mass of Se in *S. californicus* decreased by 30% at the MRP site and by 40% at the SHB site (Fig. 5.10, while the total mass of Se in *S. robustus* decreased by 50% and 70% at sites MRP and SHB, respectively (Fig. 5.12).

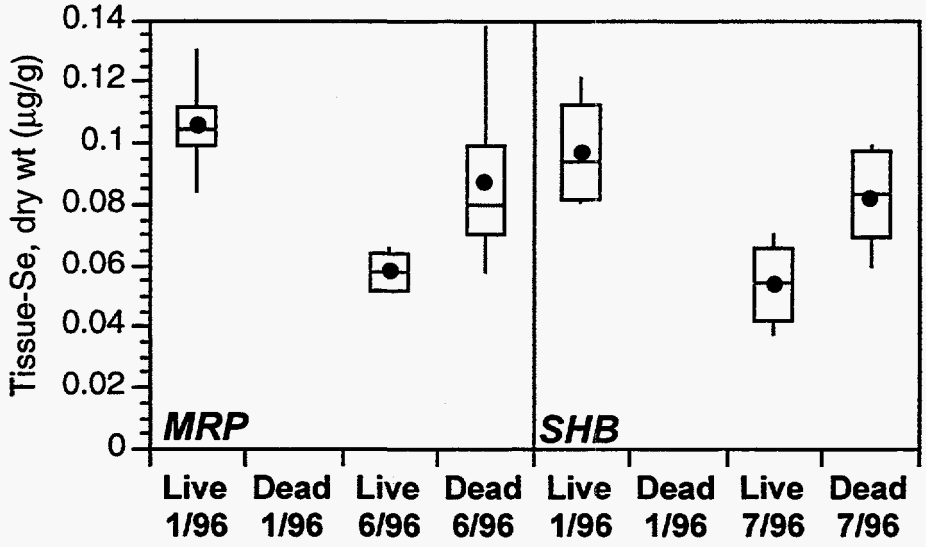

Figure 5.9 Tissue-Se concentrations in Scirpus californicus *at sites MRP and SHB.*

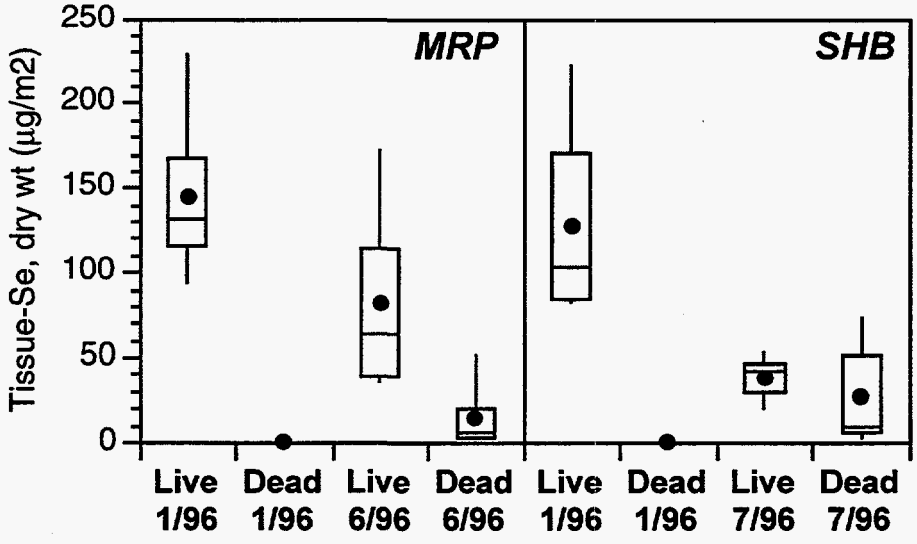

Figure 5.10 Tissue-Se mass in Scirpus californicus *at sites MRP and SHB, normalized to marsh area.*

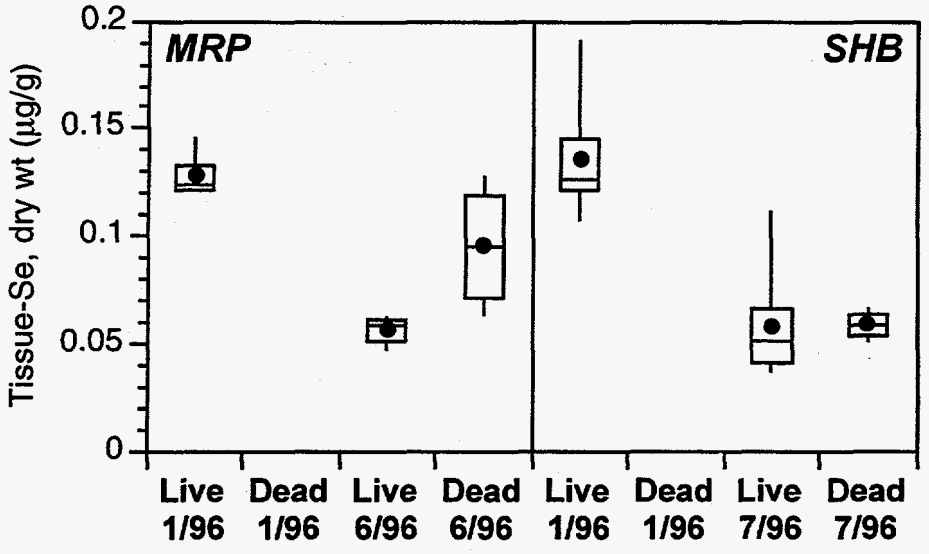

Figure 5.11 Tissue-Se concentrations in Scirpus robustus *at sites MRP and SHB.*

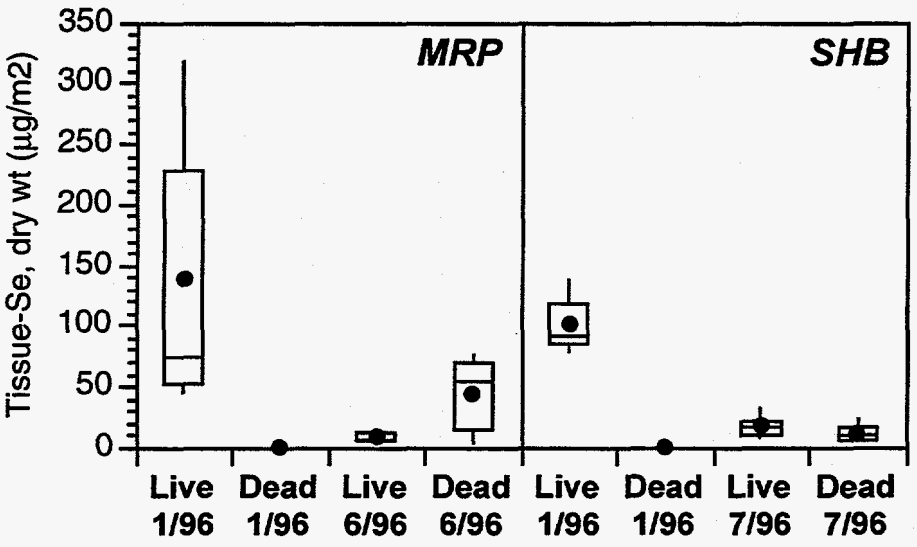

Figure 5.12 Tissue-Se mass in Scirpus robustus *at sites MRP and SHB, normalized to marsh area.*

Tissue-Se concentrations in *Typha* did not change significantly over the 6-month period (Fig. 5.13). Although the mean concentration in live tissue sampled at SHB in 1/96 was very high, this was due to some outliers which heavily skewed the distribution. Overall, approximately one-third of the total Se mass in the summer of 1996 was in dead tissue (Fig. 5.14).

Tissue-Se concentrations in marsh plain plants decreased at both sites (Fig. 5.15), by as much as 50%. Consequently, the total Se mass also decreased, except in the case of Salicornia at MRP, where an increase in biomass resulted in a slight net increase in Se mass (Fig. 5.16).

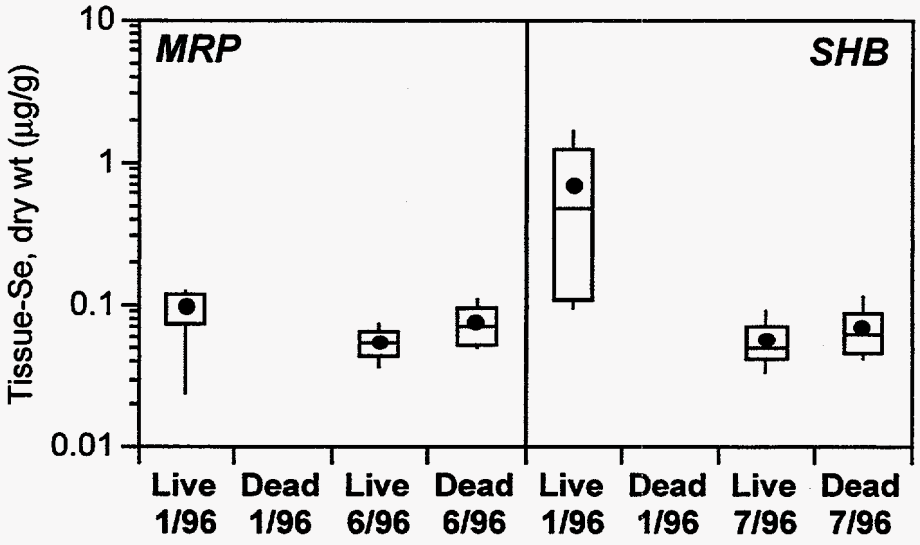

Figure 5.13 Tissue-Se concentrations in Typha latifolia *at sites MRP and SHB.*

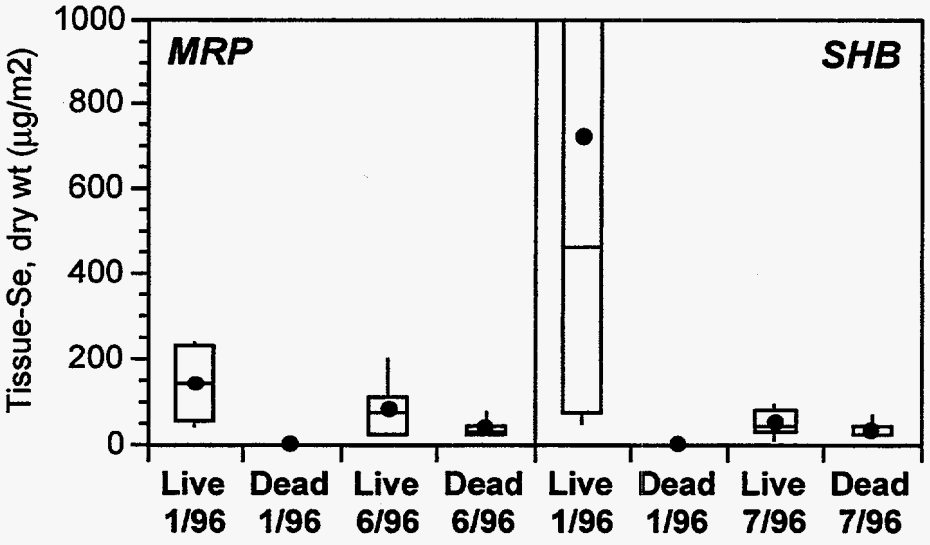

Figure 5.14 Tissue-Se mass in Typha latifolia *at sites MRP and SHB, normalized to marsh area.*

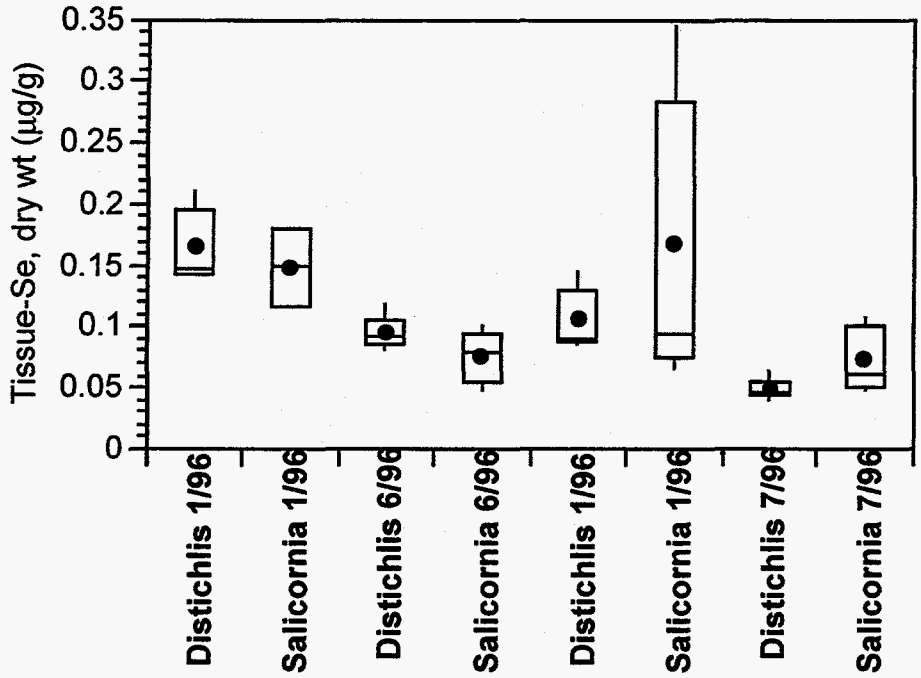

Figure 5.15 Tissue-Se concentrations in Distichlis spicata *and* Salicornia sp. *at sites MRP and SHB.*

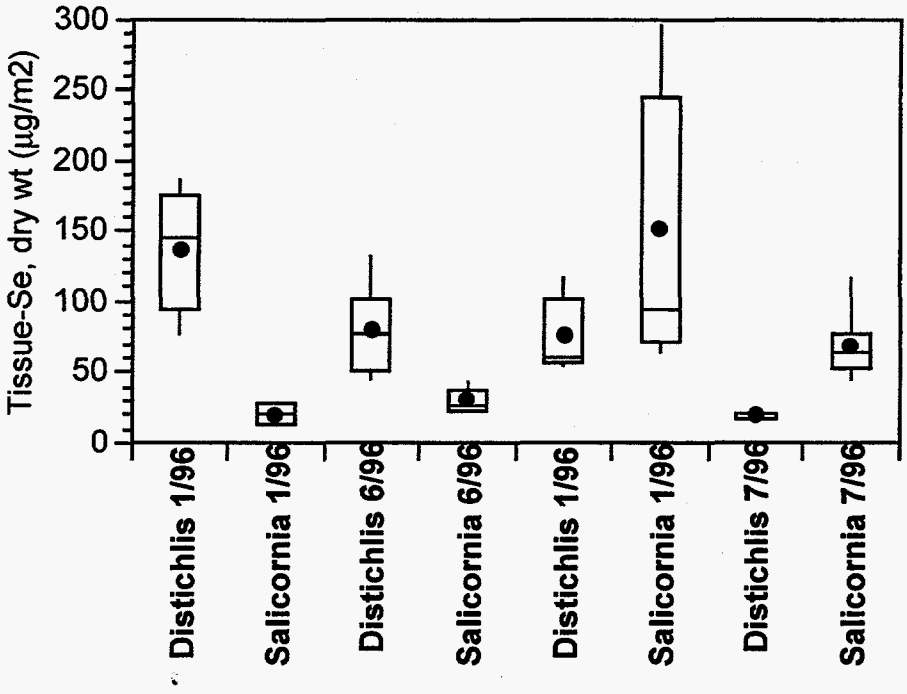

Figure 5.16 Tissue-Se mass in Distichlis spicata *and* Salicornia sp. *at sites MRP and SHB, normalized to marsh area.*

5.2.3 Total Selenium Determination in Roots and Root-Associated Soil

The measurement of root biomass is an extremely time-consuming procedure, especially in the marsh plain, where it is nearly impossible to separate intertwined pickleweed and saltgrass roots. Therefore, plant roots where sampled for the purpose of measurement of tissue-Se concentrations to ascertain whether roots are accumulating Se to levels similar to the above-ground tissue. Soil which was in direct contact with the root was sampled to see whether root extraction of pore-water results in an enrichment of the surrounding soil with respect to Se. The results of these measurements are shown in Fig. 5.17 and 5.18 for sites MRP and SHB, respectively.

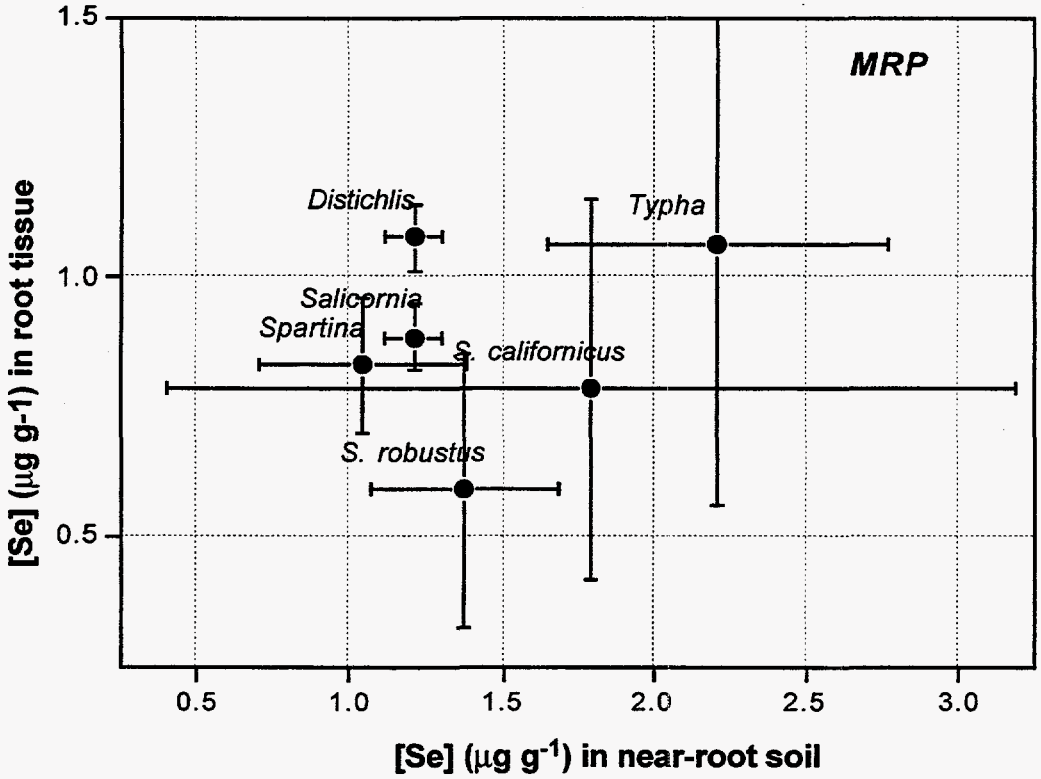

Figure 5.17 Se concentrations in roots of marsh plants at site MRP, vs. Se concentrations in near-root soil.

Near-root soil contains higher concentrations of Se than the bulk soil (see Chapter 2), especially in the lower marsh. This suggests that either the extraction of pore waters by plant roots leads to the enrichment of sediments with respect to Se, or that reducing conditions around plant roots cause Se reduction and immobilization, or both (Tokunaga, 1994b). The overall effect of this process on Se cycling in the marsh needs

to be considered. No correlation was found between soil-Se and root-Se concentrations, neither intra- nor inter-species. This is not surprising, since Se concentrations in the root are influenced by the levels of dissolved Se, the degree to which Se is excluded during root uptake, and the age of the plant. Se concentrations are consistently higher in roots than shoots. With the exception of *Spartina*, for which the root-Se concentrations were only 2-3 times higher than the shoots, the roots of other species contained 4 to 10 times greater Se concentrations than their respective shoots. This agrees qualitatively with very limited data found in the literature. In two reports (Schuler et al., 1990; Smith et al., 1988), Se concentrations in *Typha* sp. rhizomes were found to be 3 to 4 times greater than in the shoots.

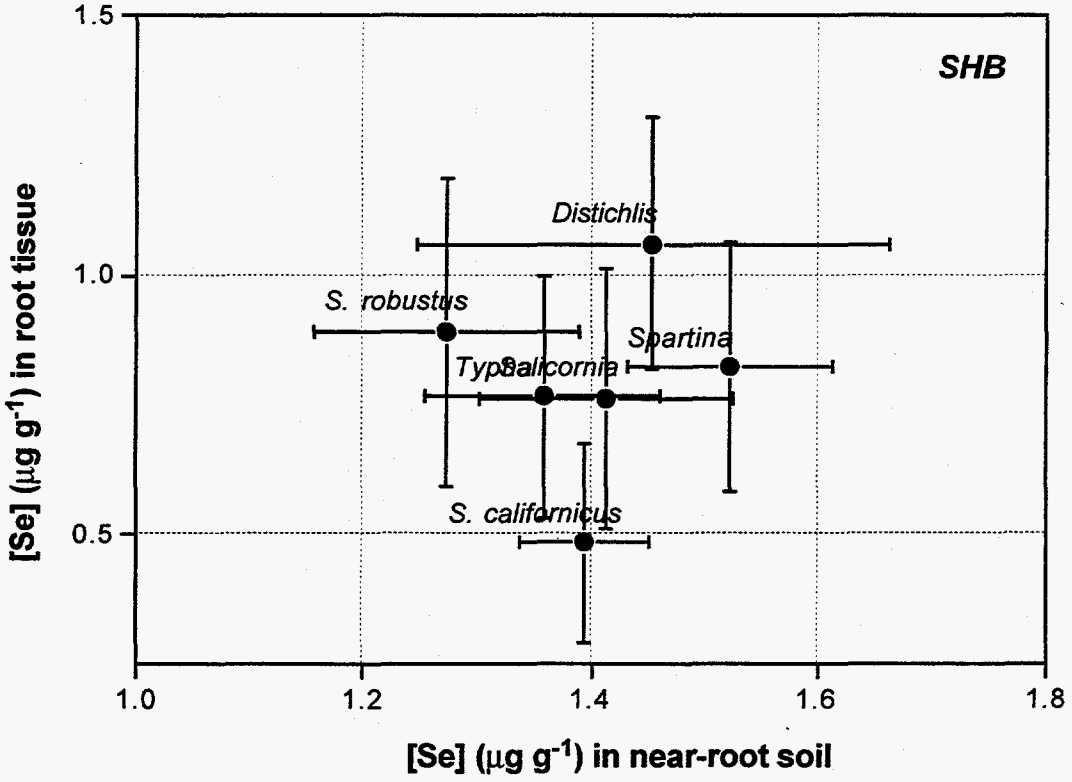

Figure 5.18 Se concentrations in roots of marsh plants at site SHB, vs. Se concentrations in near-root soil.

Because of the relative difficulty in measuring belowground biomass, there is a relative paucity of such data compared with aboveground biomass. Nevertheless, based on data from the literature, belowground biomass of emergent marsh species can be

comparatively large. The range of relative proportion of belowground to aboveground biomass for plants of interest is shown in Table 5.1.

Table 5.1 Ranges of belowground to aboveground biomass ratios for emergent marsh species.

Plant species	BLG/ABG	Reference
Spartina alterniflora	0.17	White et al., 1978
Spartina cynosuroides	4.9 - 9.5	Bellis and Gaither, 1985; Schubauer and Hopkinson, 1984
Typha latifolia	0.41 - 2.27	McNaughton, 1966; Whigham and Simpson, 1978
Scirpus sp.	2.3 - 3.7	Toivonen and Lappalainen, 1980; Whigham and Simpson, 1978
Distichlis spicata	14.6	Bellis and Gaither, 1985
Salicornia sp.	N/A	

It is clear from this table that belowground biomass generally exceeds aboveground biomass, sometimes by an order of magnitude. Combined with the high Se concentrations in plant roots, the belowground biomass may be an important storage term in the Se cycle. For instance, assuming that the belowground biomass of *Distichlis spicata* at MRP is 10 times greater than the aboveground biomass (8000 vs. 800 g m^{-2}) and the average root-Se concentration is 1.1 $\mu g\ g^{-1}$, then the total mass of Se stored in the *Distichlis* root mass is 8.8 mg m^{-2}. This is significant compared to the annual input of Se with suspended sediment deposited in the marsh plain, which is between 1.5 and 5 mg m^{-2} (see Chapter 4, Fig. 4.3), but rather small compared to the total inventory of Se in the top 1 m of sediment, which is on the order of 1,500 mg m^{-2}.

5.2.4 Litter Bag Study

Plant litter decomposition rates for each of the major emergent plant species are being measured at the MRP site. In addition, Se concentrations and C/N ratios are determined for each collected litter bag. Results from the first six months of this study are shown in Figs. 5.19-22. Decomposition rates (Fig. 5.19) follow, in a qualitative sense, first-order reaction trends. Contrary to findings from the literature (White and Trapani, 1982), *Spartina* litter did not decompose much faster than the other species.

Scirpus californicus decayed fastest (half-life ≈ 40 days), followed by *Typha* and *Spartina* (75 days), *Salicornia* (≈ 175 days), and *Distichlis* (≈ 200 days). The intra-species noise observed in Fig. 5.19 gives an idea of the spatial variability of the decomposition process. The lower decay rates in the marsh plain plants was expected because of the infrequent flooding of this area. Most of the half-lives described above fall into the ranges found in the literature (Vymazal, 1995).

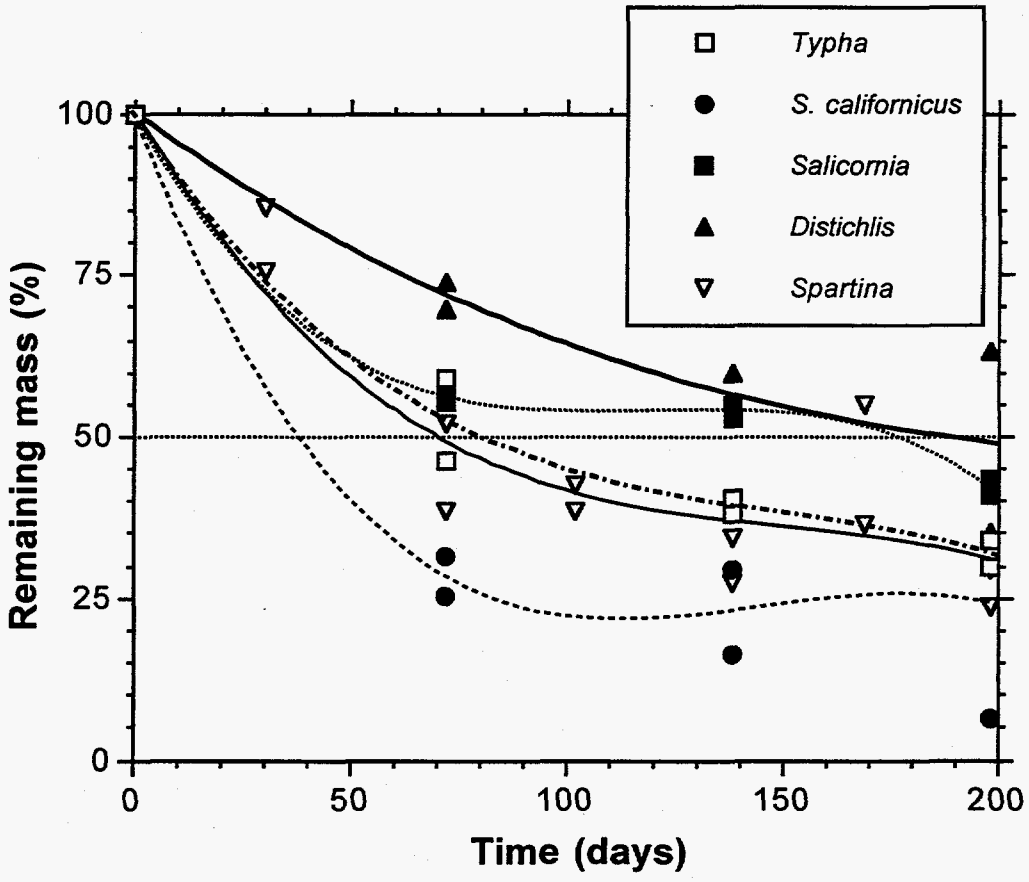

Figure 5.19 Decay of plant litter of five major emergent plants at site MRP. Polynomial fits are shown for clarity and do not imply a specific reaction model.

Trends in tissue-Se concentrations are shown in Fig. 5.20. With the exception of *Salicornia*, all species showed a marked increase in Se concentrations. In *Spartina* litter, Se concentrations were highest after only 30 days of exposure in the field, going from 0.05 ppm to around 0.7 ppm. The largest increase was observed in the *S. californicus* litter bags, although the increase was much more gradual. There are at least two possible reasons for increases in Se concentrations: 1) decay of plant components with low Se, with the remaining, more resistant parts containing higher Se concentrations,

or, 2) influx of Se from Bay water. In order to test these possibilities, the total mass of Se in each litter bag was calculated. The results are shown in Figs. 5.21 and 5.22. It is clear from these data that Se mass is being added to these systems, with the exception of *Salicornia,* which loses some Se. *Spartina* initially gains over 10 times the original mass of Se but subsequently gradually loses it. *S. californicus* also gains several times its original Se mass, but then starts losing some after day 150. Clearly, more data is needed to resolve these trends, but this preliminary analysis suggests that plant litter is providing an active surface for the sequestration of Se from the water column. This may be an important route for Se immobilization in the marsh.

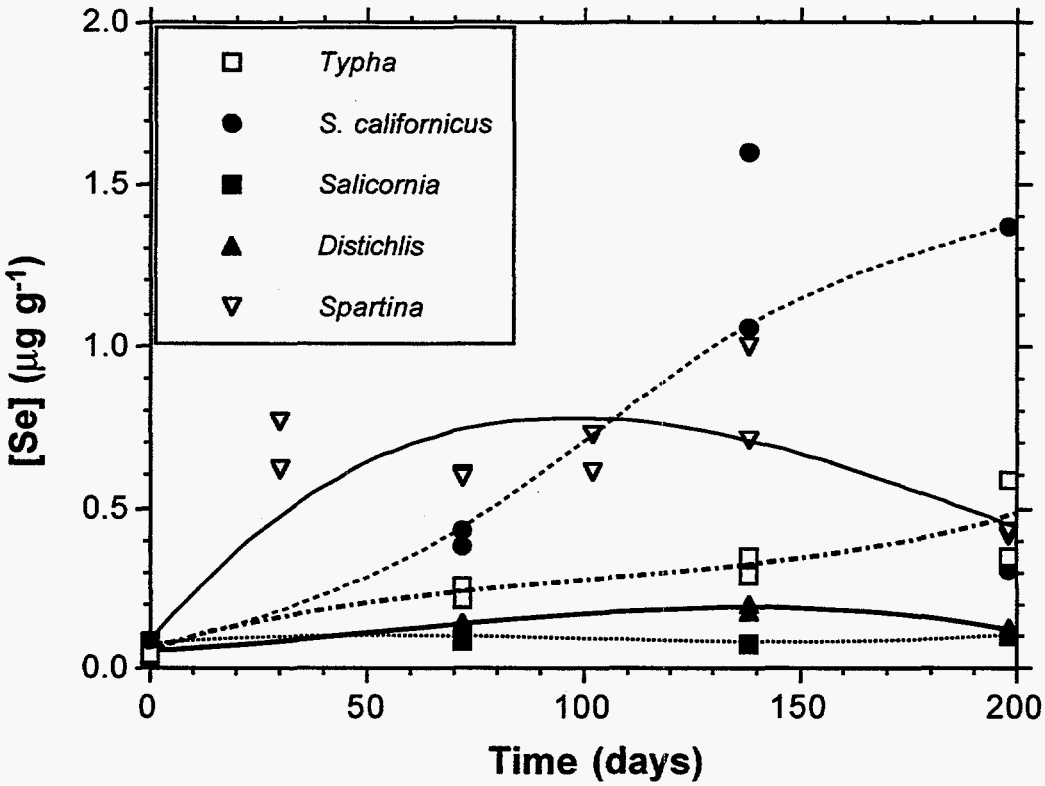

Figure 5.20 Changes in Se concentrations in plant litter of five major emergent plants at site MRP. Polynomial fits are shown for clarity and do not imply a specific reaction model.

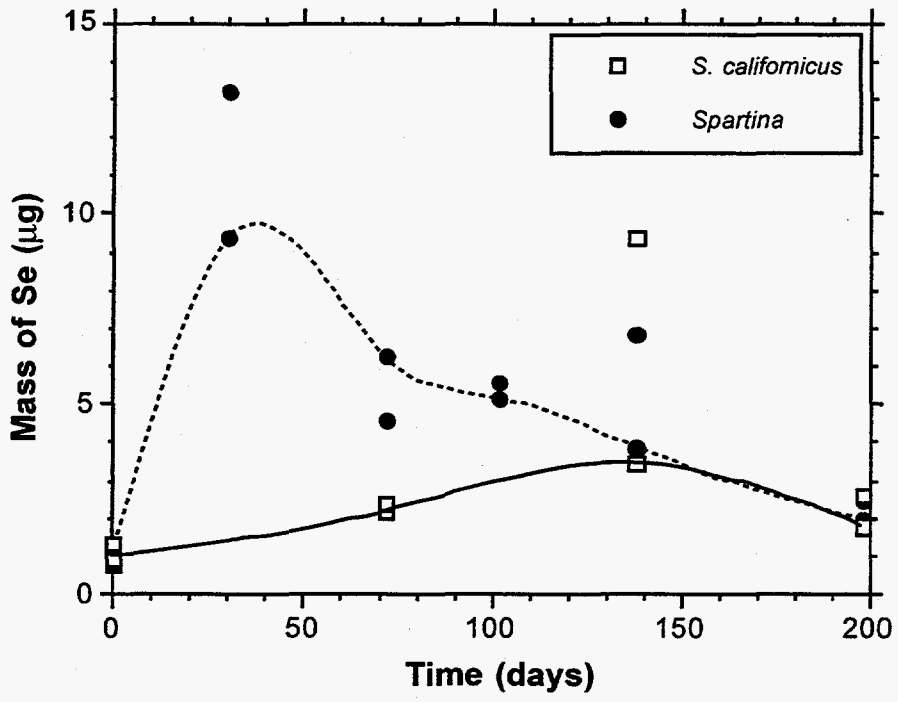

Figure 5.21 Changes in Se mass in plant litter of Spartina and S. californicus at site MRP. Polynomial fits are shown for clarity and do not imply a specific reaction model.

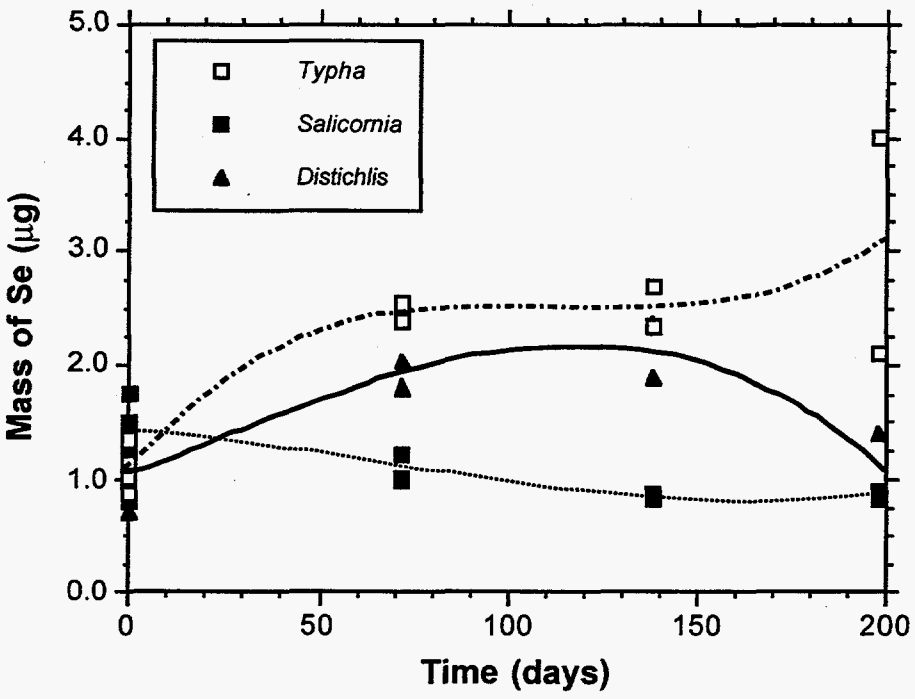

Figure 5.22 Changes in Se mass in plant litter of Typha, Salicornia, and Distichlis at site MRP. Polynomial fits are shown for clarity and do not imply a specific reaction model.

5.3 Summary

Although the results of both plant and litter bag sampling are not complete, several preliminary conclusions may be drawn. Aboveground plant tissue generally contains low Se concentrations, approximately 0.1 $\mu g\ g^{-1}$, while belowground concentrations are up to an order of magnitude higher. Combined with the fact that the belowground biomass is likely much greater than the aboveground biomass, especially in the marsh plain, roots and rhizomes may be important links in the Se cycle, especially in the redistribution of dissolved Se in the root zone and incorporation of selenate and selenite into plant tissue. Such incorporation undoubtedly leads to the formation of organo-Se compounds, thereby affecting the overall speciation and bio-availability of Se in the marsh sediment. The ongoing study will define ranges of aboveground plant turnover rates. The turnover rates for belowground parts will need to be estimated based on limited information from the literature.

The litter bag study has identified decaying plant litter as a surface for Se immobilization, probably due to adsorption. Further work is needed to quantify this process, its kinetics, and its long-term effects on Se accumulation in the marsh. It may be difficult to estimate the degree to which the decomposed plant material is incorporated into the underlying sediment.

6 Selenium Reduction Under Ponded Conditions

Rates of Se accumulation with settling particulates and Se release from the sediment via diffusion from pore water to overlying water have been estimated based on field measurements and presented in previous chapters. The possibility of a third important flux, that of Se reduction and immobilization in the sediments, was investigated and is presented below.

A comparison of Se concentrations in settling particulates with Se levels in the near-surface sediments in the marsh plain (Fig. 4.10) was suggestive of another source of Se to the marsh sediments. Given their high organic content, it is possible that under ponded conditions marsh sediments become reducing enough to cause a conversion of Se(IV) and Se(VI) to reduced forms, such as Se(0), or possibly even Se(-II) at greater depths (Tokunaga et al., 1996), especially if the process is microbially mediated. Redox potential measurements on cores from throughout the intertidal wetlands (Figs. 2.9 and 2.10) indicated that conditions were not anoxic near the sediment surface, and in most cases Eh was in the range of +100 to +400 mV. When compared with limited batch laboratory measurements of Se species stability in the presence of sediments (Masscheleyn et al., 1990), this range of Eh values would fall primarily in the Se(IV) and Se(VI) fields, with only minor reduction to Se(0) expected above 0 mV. On the other hand, in a pure Se-H_2O system, Se(0) is predicted to be stable below an Eh of 150 mV at pH 7.5 to 8 (McNeal and Balistrieri, 1989; at [Se] = 1 μM). Given the complexity of both chemical and biochemical processes in soils, it is not possible to unequivocally assign Se stability fields. Nonetheless, it is clear that the conversion of Se(IV) to Se(0) is not favored above Eh of 150 mV. In order to assess the relative significance of Se reduction from the water column in Se accumulation on marsh and mudflat sediments, a laboratory microcosm experiment was conducted to measure rates of Se reduction under ponded conditions.

6.1 Experiment Design

6.1.1 Sampling and Preparation

A $10 \times 20 \times 10$ cm monolith of sediment was sampled at low tide from the mudflats and another from the marsh plain in the MRP wetlands. At first, larger samples were removed using a shovel and subsequently were cut to size using a sharp blade. The marsh sample contained intact plants (primarily *Distichlis spicata*) and a plant litter layer of approximately 5 mm thickness, while the mudflat sample contained no vegetation or plant fragments. These samples were placed in Lucite containers, which were specifically manufactured for this purpose (Fig. 6.1). These boxes had pre-drilled ports for Eh measurement and water sampling, which were sealed with plugs during the sediment sampling. The Lucite boxes were sealed to prevent leakage of water, and transported immediately to the laboratory. The boxes were kept under a N_2 atmosphere until they were each instrumented with 30 Pt electrodes for Eh measurement, and 30 porous cups for sampling of pore water and ponded water. The electrodes and porous cups penetrated approximately 1.5 cm of the sediment in order to minimize edge effects on the measurement. The boxes were instrumented within 8 hours of sample collection.

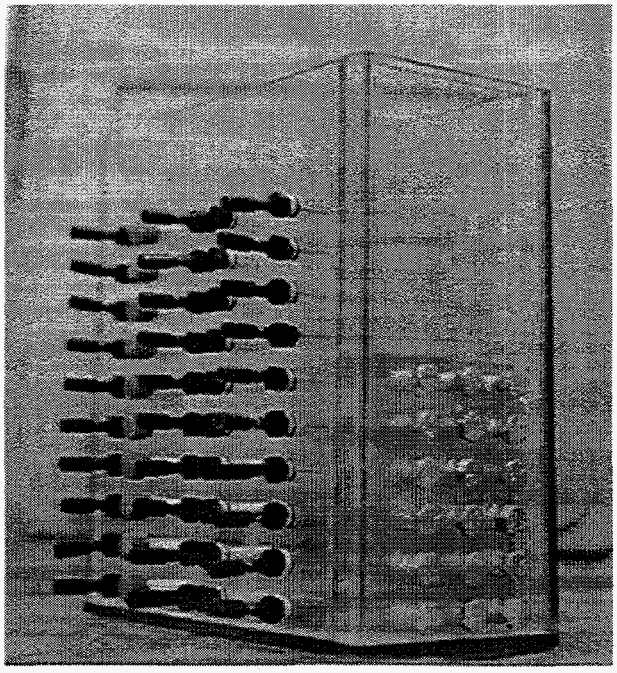

Figure 6.1 Microcosm chamber, with Pt electrodes for Eh measurements and porous ceramic cups for water sampling.

At the same time that sediments were collected, samples of Carquinez Strait water were taken from the subtidal area offshore Martinez. The water samples were filtered through a 0.45 μm filter in order to eliminate suspended particulates. This was done because the experiment was designed to isolate and study Se reduction from Bay water and not from suspended particulates, which would have introduced additional variables. The water samples were kept refrigerated until they were used during the experiment. The Bay water sample was analyzed using both the cold-trap HGAAS and the lanthanum co-precipitation HGAAS methods, which are discussed in Chapter 9. The speciation results were in fairly close agreement, and are shown in Table 6.1, with the total Se concentration from both methods being 0.218 μg/L. The experiment was conducted at room temperature, which did not fluctuate by more than ± 2°C from 22°C.

Table 6.1 Results of Se speciation of Bay water for microcosm experiment, using two analytical methods.

Method	Se (IV) ($\mu g\ L^{-1}$)	Se(VI) ($\mu g\ L^{-1}$)	Se(organic?) ($\mu g\ L^{-1}$)	Total Se ($\mu g\ L^{-1}$)
cold-trap HGAAS	0.059	0.064	0.095	***0.218***
La-coprecip HGAAS	0.063	0.031	0.124	***0.218***

6.1.2 Experiment I: Ponding Over One Tidal Cycle

Initial Eh readings were taken 20 minutes prior to ponding. Water was introduced to the system very slowly (over a 10 min period), in order to prevent disturbing and resuspending the sediments or organic debris. A total of 2,300 mL of water, corresponding to a 10 cm column of water, was ponded on top of the sediment in each microcosm (Fig. 6.2) via ports which were 1 cm above the sediment surface. Eh was measured from 15 locations in the overlying water and 15 locations in the sediment in each microcosm, on an approximately hourly schedule, although since measurements were made by hand, some data gaps exist during early morning periods. Samples of surface and pore waters were collected less frequently because the removal of water from the system caused vertical displacement in the water column, especially since, given the low Se concentrations, at least 30 mL needed to be collected. The pH and electrical conductivity (EC) of each water sample was measured prior to acidification. Samples were stored refrigerated prior to analysis.

Water was drained after 6.5 and 15 hours from the marsh plain and mudflat sample, respectively. These ponding times were chosen to represent the maximum amount of time each environment might be flooded during an extreme high tide. During most high tides, though, these environments would only be ponded for half as long. Water was drained very slowly in order to prevent disturbance to the sediment-water interface and samples of these "drain waters" were collected. After the draining, both microcosms were allowed to partially dry out and re-oxidize. The mudflat sediment never came back to its original redox state, probably because of the inadequate drainage provided by the microcosm container. The near-surface of the marsh plain sample became re-oxidized close to initial values after approximately 6 hours, though the bottom portion of the microcosm did not do so until after 2 days of drying, likely a result of poor drainage in this part of the container.

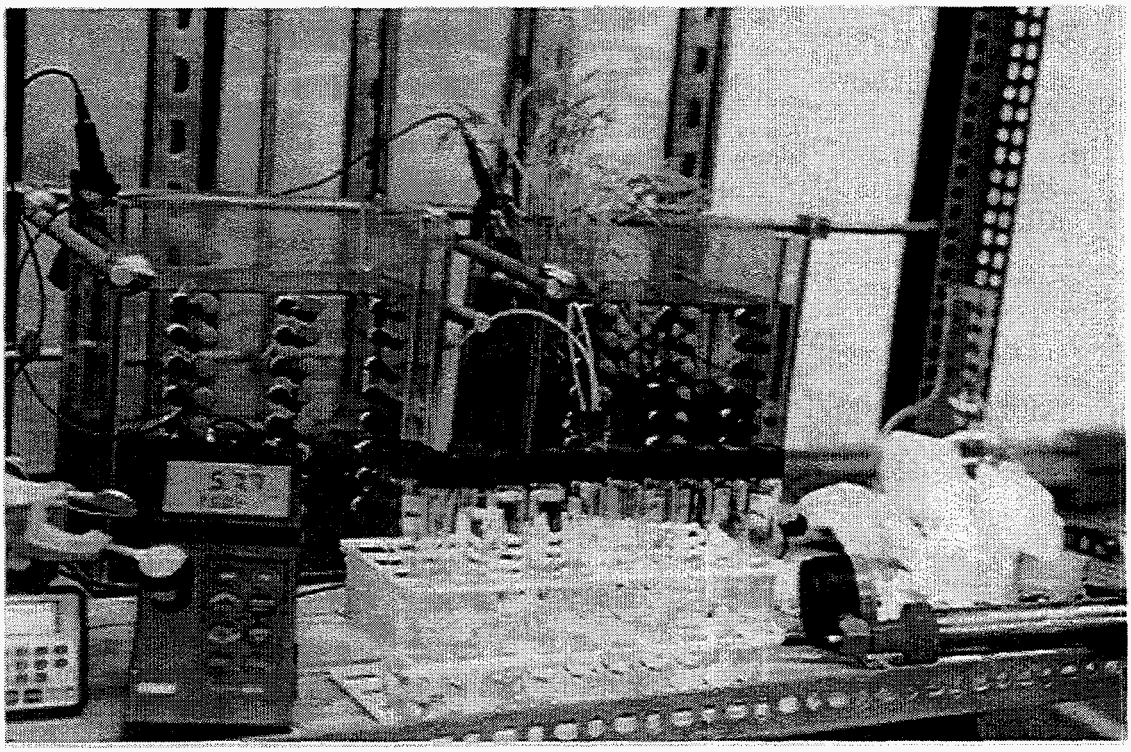

Figure 6.2 Microcosm chambers with mudflat (left) and marsh plain (right) sediment and ponded water, Eh measurement and pore water sampling in progress.

6.1.3 Experiment II: Extended Ponding

After the original Eh conditions were re-established, the marsh plain microcosm was flooded again, this time using the Bay water sample spiked with 2 µg/L of selenite,

and remained flooded for nearly a month. This was done in order to observe redox and Se immobilization trends under long-term ponded conditions, such as would be observed under stagnant ponding due to topographic irregularities. Tokunaga et al. (1996) observed such effects in a similar laboratory microcosm, though one with much higher Se concentrations (2 to 3 orders of magnitude higher). They noted Se reduction after ponding periods of days, not hours. The Se spike was introduced in order to make it possible to collect smaller (5 to 15 mL) samples of water and therefore cause less of a disturbance to the system. Eh was measured on an hourly basis for the first 6 hours, 6 times during the next 24 hours, and daily thereafter. Water samples were collected at 0.4, 4.5, 16, 62, and 400 hours after the initiation of ponding. Water was drained from the microcosm after 25 days of ponding and samples of the "drain water" were collected.

6.2 Results

6.2.1 Eh Trends - Experiment I

Changes in Eh as measured in the mudflat and marsh plain microcosms are shown in Figs. 6.3 through 6.5 and 6.6 through 6.8, respectively. Three depth profiles (A, B, and C) are shown for each microcosm, three vertical columns along which measurements were taken. Profile B was measured in the central part of the microcosm, under the assumption that it was probably least affected by boundary conditions.

As seen from Figs. 6.3 through 6.6, sediment-Eh in the mudflat microcosm generally did not drop below 0 mV during the 15 hours of ponding, with the exception of the (-1 cm) depth in profile A, which started out at -100 mV and declined to -200 mV. The Eh of the overlying water, either at (+1 cm) or (+2 cm), did not decrease at any time during the experiment. After water was drained, it took 1 to 2 days before Eh values came back up to pre-ponding levels, suggesting that the conditions imposed on the system did not adequately mimic the field setting. The drainage from the microcosm chamber was not complete and probably resulted in pockets of stagnant water and slower-than-natural re-oxidation of the system. The rate at which sediment-Eh declined during the 15-hr ponding was slow, but Eh values did drop to a range which may favor some Se reduction to Se(0). However, the overlying water, even at 1 cm above the sediment-water interface, did not become reduced, suggesting that Se losses from the water column should be minor, if any.

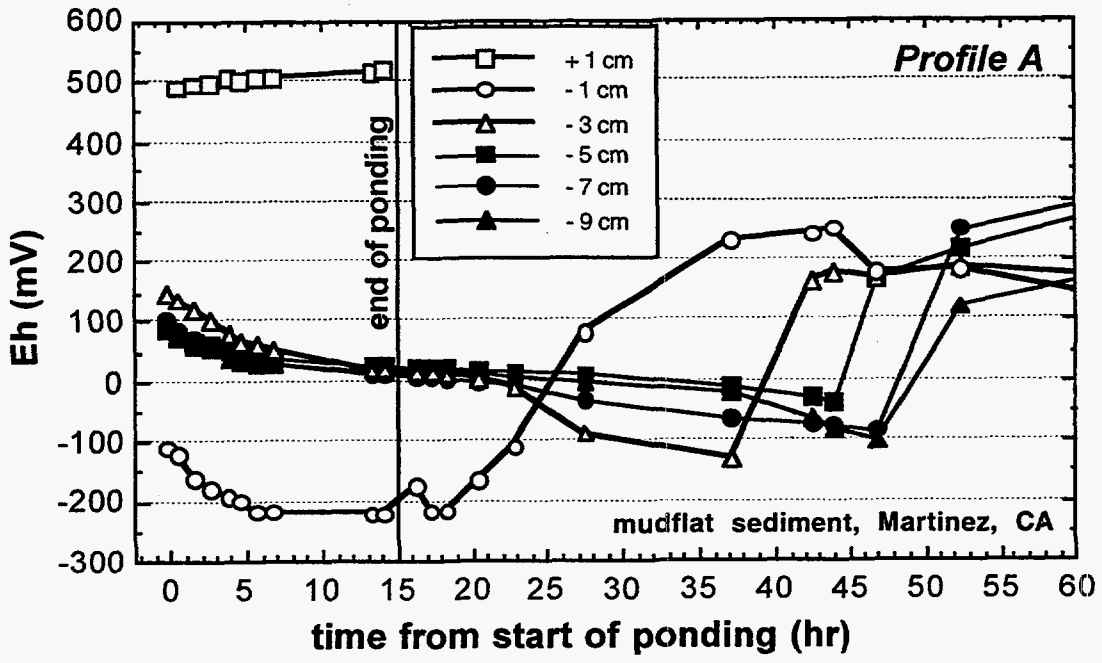

Figure 6.3 Redox potential trends in the sediments (depths < 0) and the overlying water (depths > 0), in the mudflat microcosm ponded for 15 hours, Profile A.

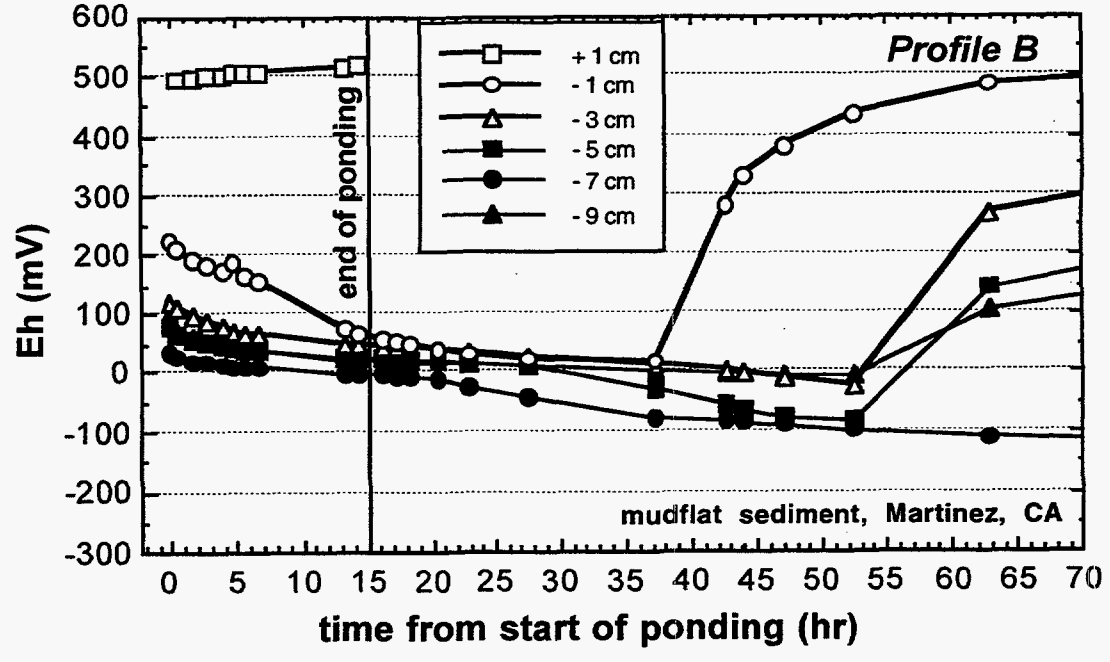

Figure 6.4 Redox potential trends in the sediments (depths < 0) and the overlying water (depths > 0), in the mudflat microcosm ponded for 15 hours, Profile B.

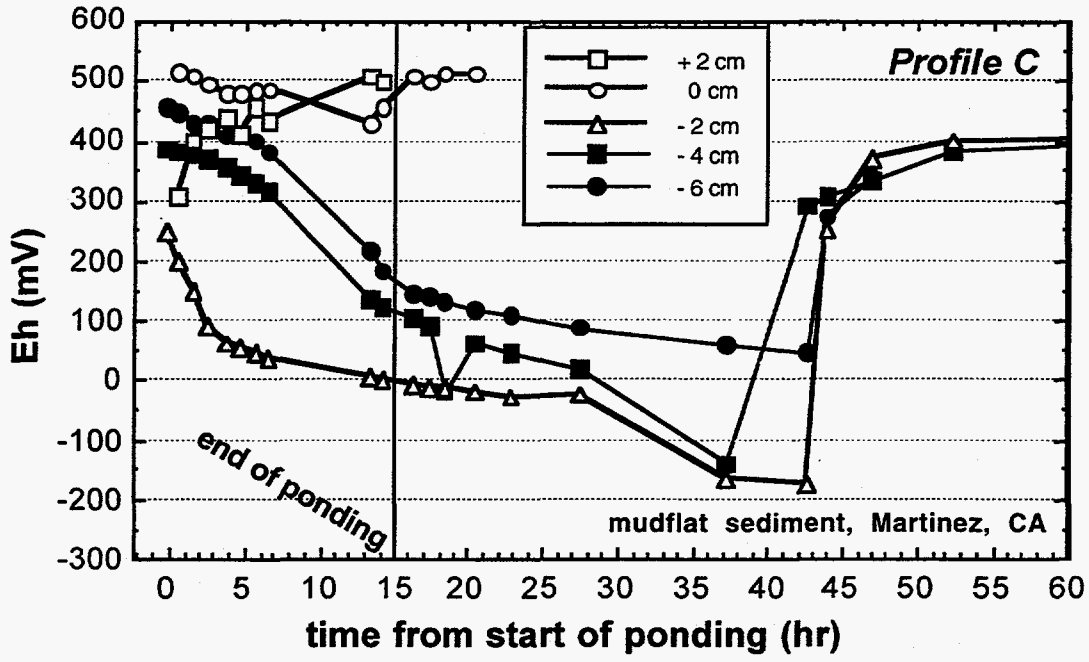

Figure 6.5 Redox potential trends in the sediments (depths < 0) and the overlying water (depths > 0), in the mudflat microcosm ponded for 15 hours, Profile C.

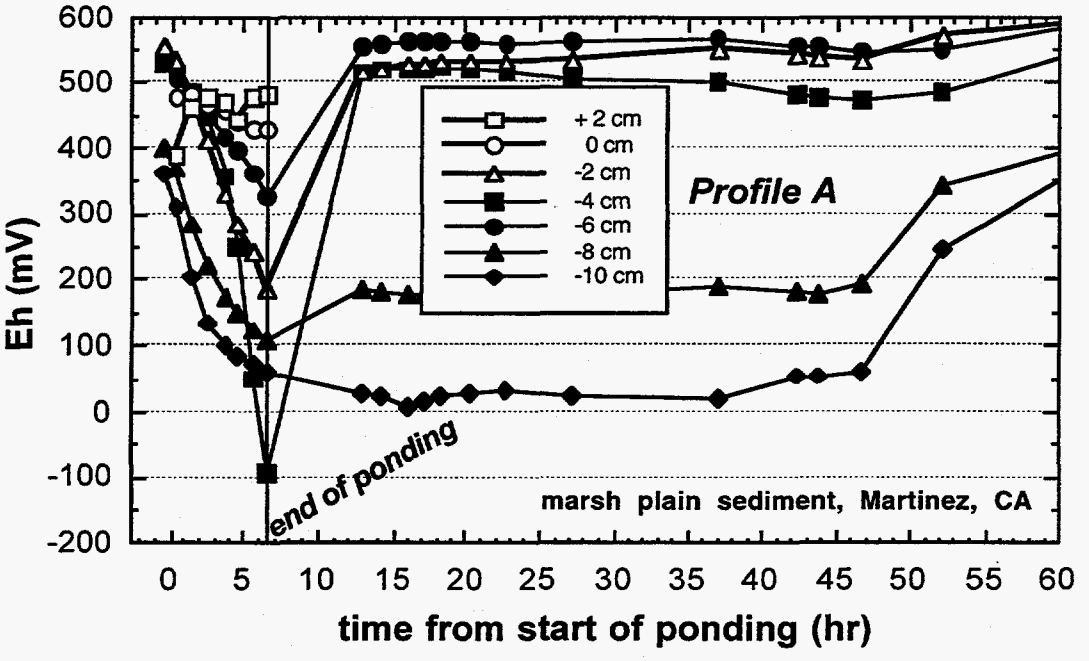

Figure 6.6 Redox potential trends in the sediments (depths < 0) and the overlying water (depths > 0), in the marsh plain microcosm ponded for 6.5 hours, Profile A.

Redox trends in the marsh plain microcosm (Figs. 6.6 through 6.8) were markedly different from those in the mudflats. All sediment depths in all three profiles exhibited similar reduction rates during the ponding period of 6.5 hours, with the average decline being 300 mV, or about 50 mV hr^{-1}. With the exception of some of the deeper sediment measurements, Eh did not drop below 0 mV, and all of the measurements at the sediment-water interface stayed above 150 mV. After water was drained, most of the Eh values increased to pre-ponding levels within approximately 6 to 10 hours, indicating that the microcosm was an adequate model of the natural habitat. However, some of the deeper sediments and sediments below a depth of 4 cm in Profile C, did not return to pre-ponding redox potentials for 50 hours after water was drained, once again showing that drainage was incomplete.

The Eh of the overlying Bay water did not change during the 6.5 hour ponding, and the Eh of the sediment-water interface remained at or above 250 mV in all three profiles, strongly suggesting that the natural tidal cycle in the marsh plain is too short to induce conditions which could result in the immobilization of Se from the water column.

6.2.2 EC and Se Trends, Experiment I

Electrical conductivity did not vary by more than ±7% in either microcosm during the ponding of Experiment I (data are not shown). This behavior is indicative of a lack of significant vertical solute displacement via either advection or diffusion during this short-term ponding. Therefore, any changes in Se concentrations would have to be due to adsorption or reduction. However, the EC of the ponded water and that of the mudflat water were, not surprisingly, very similar, so that advective and diffusive processes would be difficult to distinguish.

As mentioned earlier, few water samples were collected in order not to disturb the solute distribution in the system. Most samples were collected at or just below the sediment-water interface, since that was where Eh changed the most, though in the case of the mudflat microcosm, it did not change much at all (see Fig. 6.3-5). Dissolved Se concentrations measured at selected points are shown in Figs. 6.9 and 6.10, for the mudflat and marsh plain microcosms, respectively. Although the Se concentrations are not stable over the entire period of ponding, the net changes are not indicative of chemical reduction. For instance, in the mudflat microcosm, Se concentrations from two different points 1 cm below the sediment-water interface show opposite trends, one decreasing and one increasing with time, but these differences are probably an indication of small-scale spatial variability and its manifestation due to the removal of a

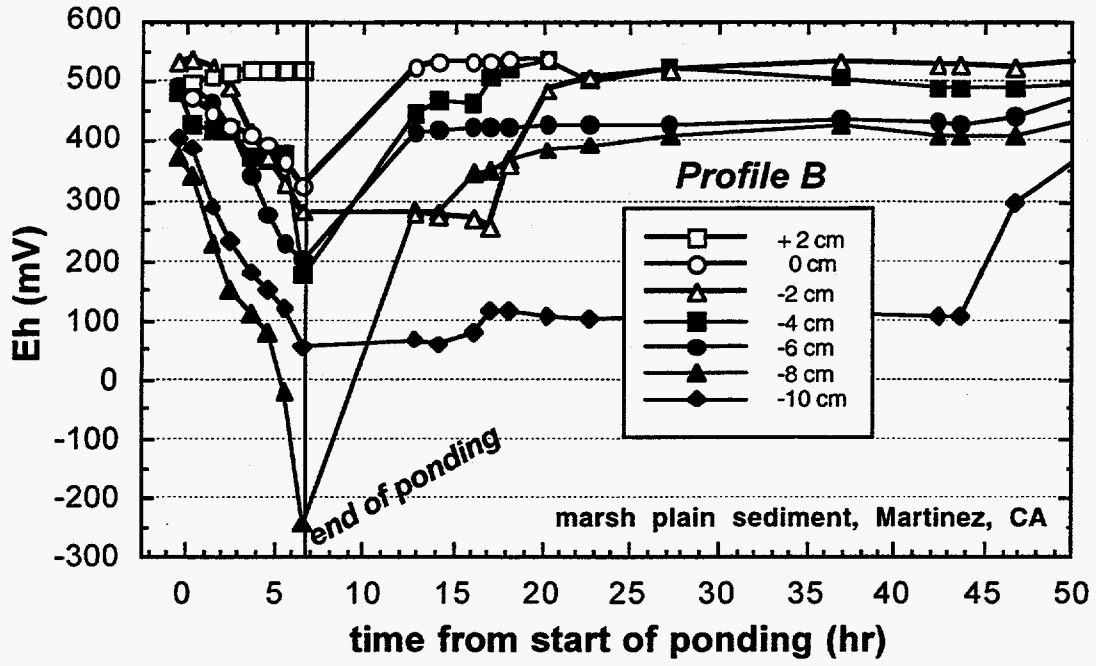

Figure 6.7 Redox potential trends in the sediments (depths < 0) and the overlying water (depths > 0), in the marsh plain microcosm ponded for 6.5 hours, Profile B.

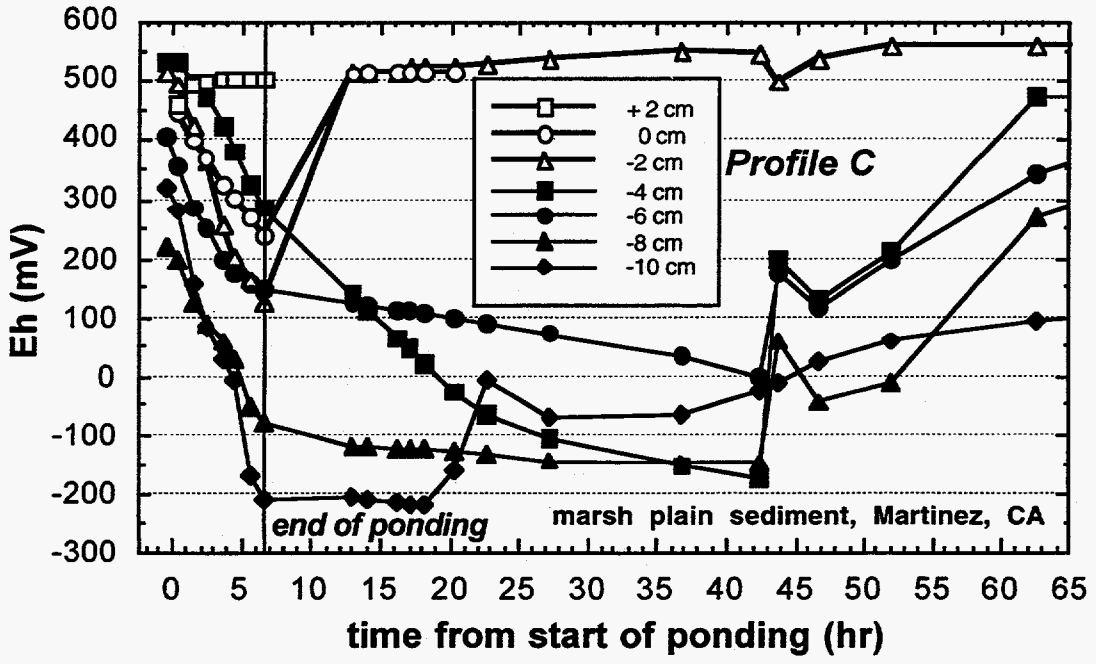

Figure 6.8 Redox potential trends in the sediments (depths < 0) and the overlying water (depths > 0), in the marsh plain microcosm ponded for 6.5 hours, Profile C.

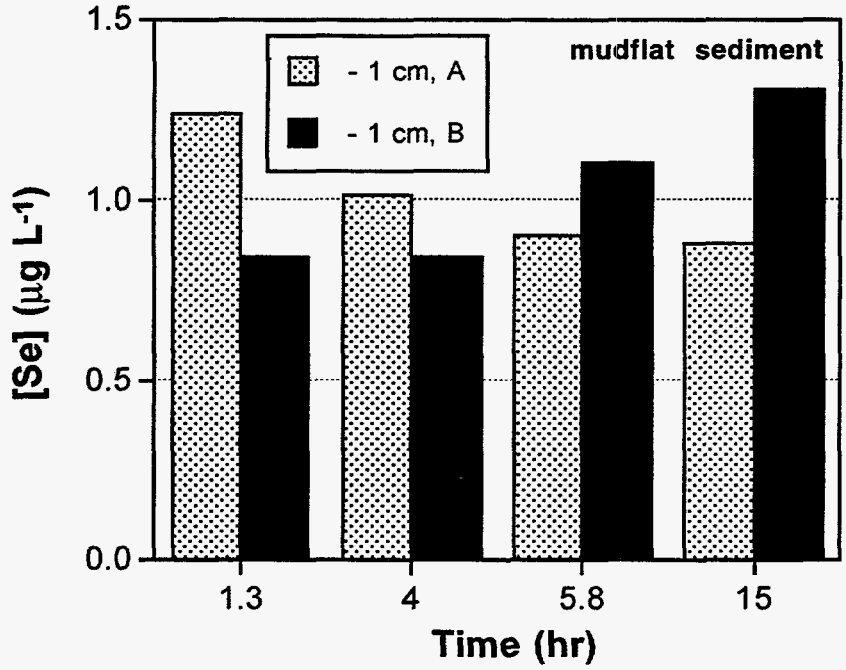

Figure 6.9 Total dissolved Se measured at two points 1 cm below the sediment-water interface of the mudflat microcosm (Profiles A and B), over 15 hours of ponding.

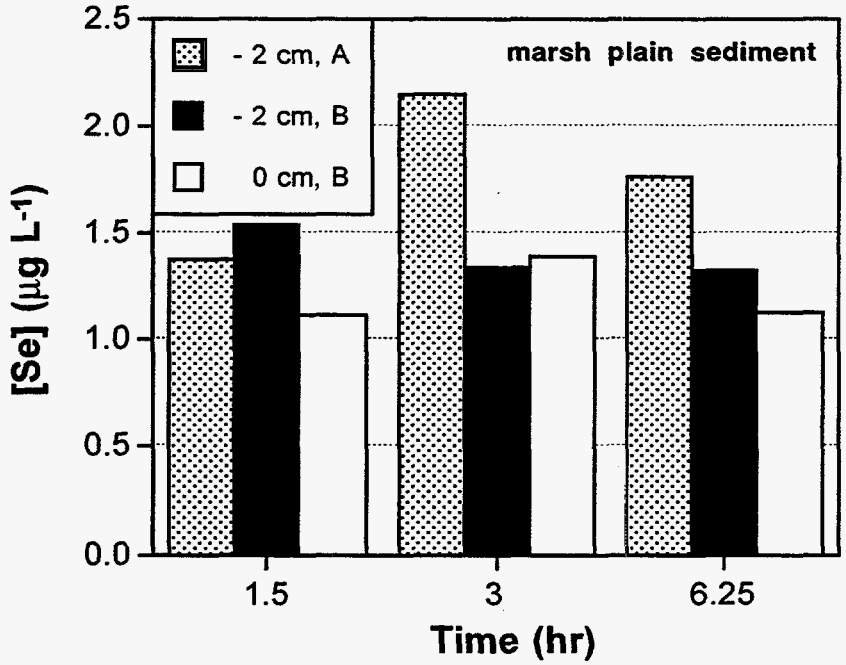

Figure 6.10 Total dissolved Se measured at three points below and at the sediment-water interface of the marsh plain microcosm (Profiles A and B), over 6.5 hours of ponding.

finite quantity of water resulting in a redistribution of pore water around the sample port. On average, a 1 to 2 cm radius of soil is affected during pore water sampling.

6.2.3 Eh trends, Experiment II

Changes in Eh as measured along three vertical profiles in the long-term ponding of the marsh plain microcosm are shown in Figs. 6.11 through 6.14. These profiles correspond to the same locations monitored in Experiment I. Only the first 100 hours of the experiment are shown here because very few changes occurred thereafter. During the first 6 hours of ponding, sediment-Eh follows the same trends as in Experiment I, i.e., decreasing by approximately 50 mV hr^{-1}. Subsequently, the decrease becomes logarithmic, approaching a plateau at around -200 to -300 mV after some 50 to 70 hr. The most rapid decrease in Eh is observed at depth "0", i.e., at the sediment-water interface, likely due to the presence of an organic litter layer at the sediment surface. The surface Eh falls below 0 mV after approximately 15 to 20 hours of ponding. According to laboratory experiments by Masscheleyn et al. (1990), reduction of Se(IV) to Se(0) may be expected below this redox potential.

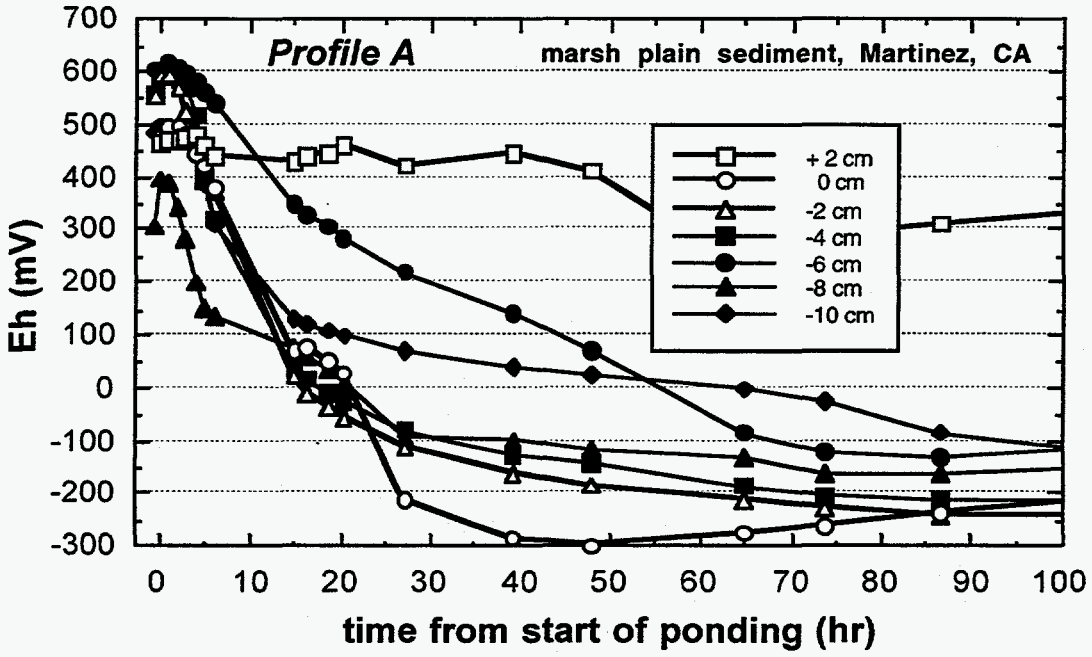

Figure 6.11 Redox potential trends in the sediments (depths < 0) and the overlying water (depths > 0), in the marsh plain microcosm ponded for 400 hours, first 100 hours shown, Profile A.

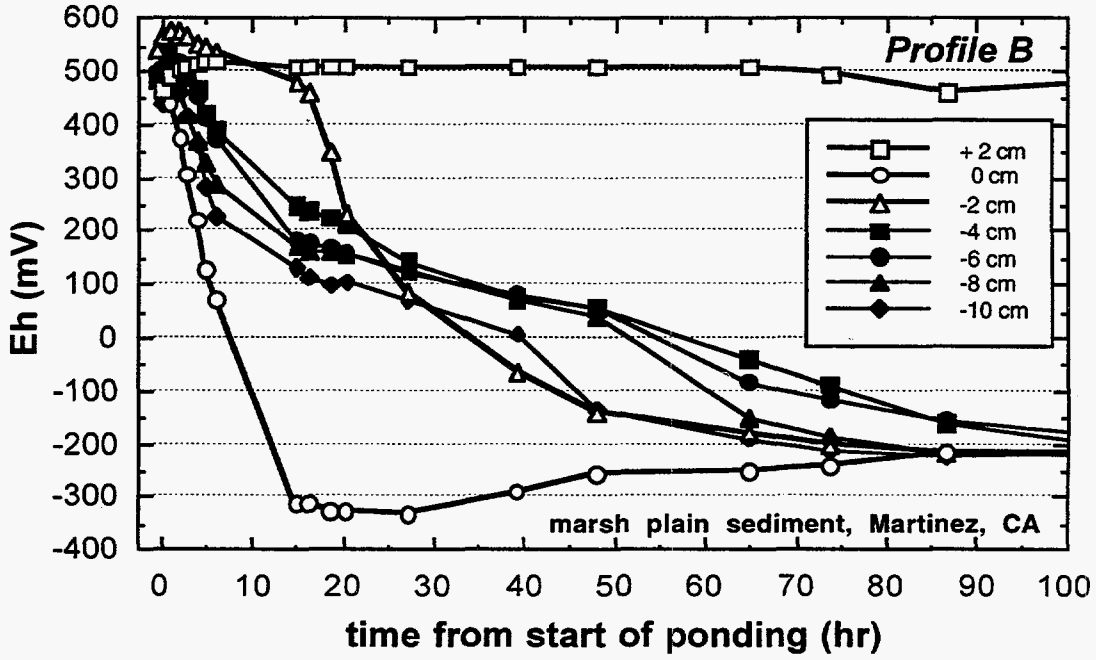

Figure 6.12 Redox potential trends in the sediments (depths < 0) and the overlying water (depths > 0), in the marsh plain microcosm ponded for 400 hours, first 100 hours shown, Profile B.

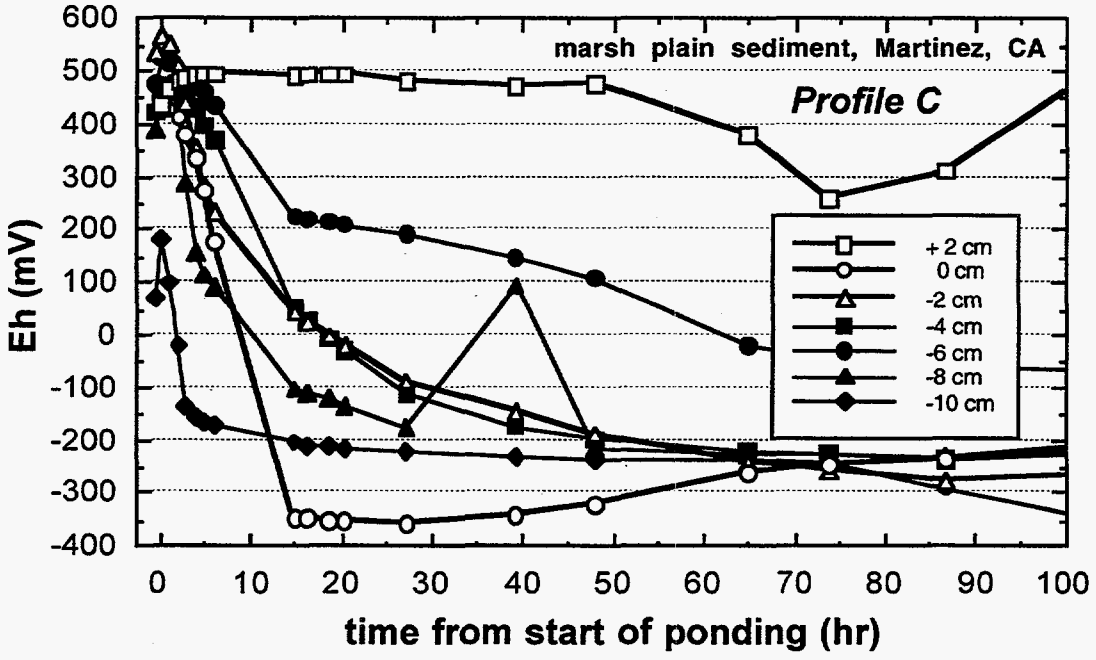

Figure 6.13 Redox potential trends in the sediments (depths < 0) and the overlying water (depths > 0), in the marsh plain microcosm ponded for 400 hours, first 100 hours shown, Profile C.

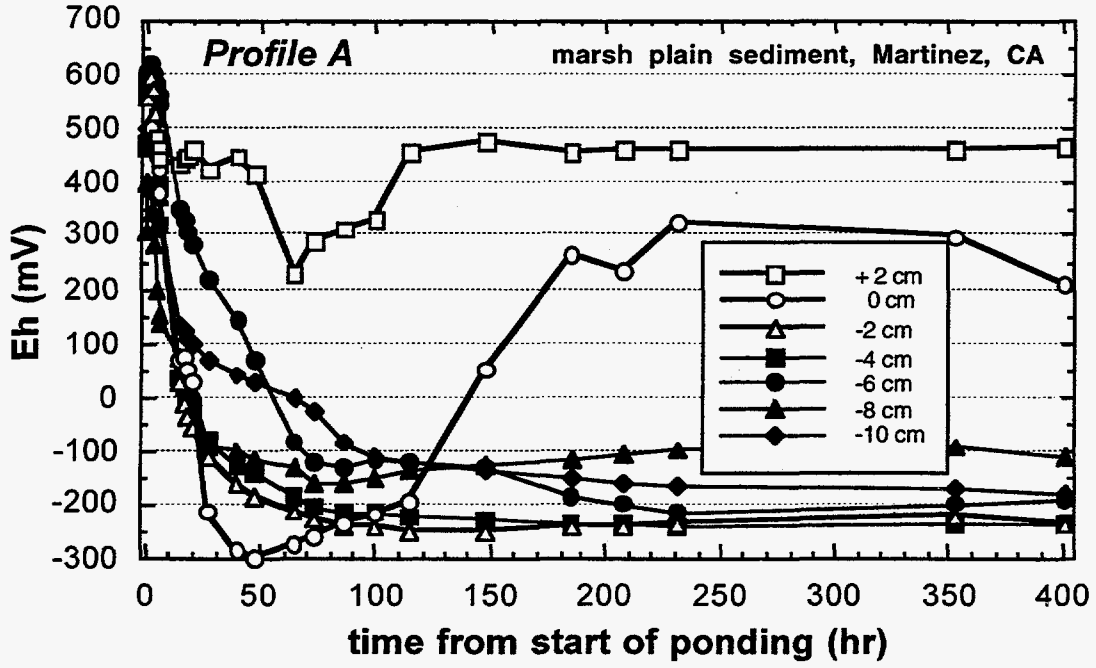

Figure 6.14 Redox potential trends in the sediments (depths < 0) and the overlying water (depths > 0), in the marsh plain microcosm ponded for 400 hours, Profile A.

An interesting departure from the general trend is observed in Profile A after 100 hours (Fig. 6.14). The Eh at the sediment-water interface increased from -200 mV to +300 mV over a period of approximately 100 hours and remained at that level until after 350 hr, after which it dropped slightly, to +200 mV at the conclusion of the experiment. This pattern is probably related to the fact that the depth of the ponded water, initially 10 cm, decreased during the course of the experiment due to removal of water during sampling and evapotranspiration. Therefore, at t = 100 hr, under these shallow water conditions, oxygen diffusion through the water column can affect redox conditions in the sediment. It has been found that under ponded conditions, the active reducing zone can migrate deeper into the sediment due to the rapid microbial consumption of soil organic carbon early on in the ponding (Tokunaga, 1997). Such depletion in nutrients would result in lowered respiration rates and the increased ability of oxygen diffusion to keep up with oxygen consumption, resulting in Eh increases.

The Eh of the overlying pond water at 2 cm above the sediment does not fall below +250 mV during the entire experiment, which may be related to the fact that the depth of the ponded water is decreasing, as described above.

6.2.4 EC and Se trends, Experiment II

In order to minimize the effects of drawing water out of the microcosm, only Profile B was sampled regularly, while the other profiles were sampled very sparsely. EC, pH, and Se were measured on all samples, though in cases where only a limited volume of sample was available, the measurement of EC was not possible. No trends in pH were observed and pH data is not shown. EC data collected over the course of 400 hours is shown in Fig. 6.15.

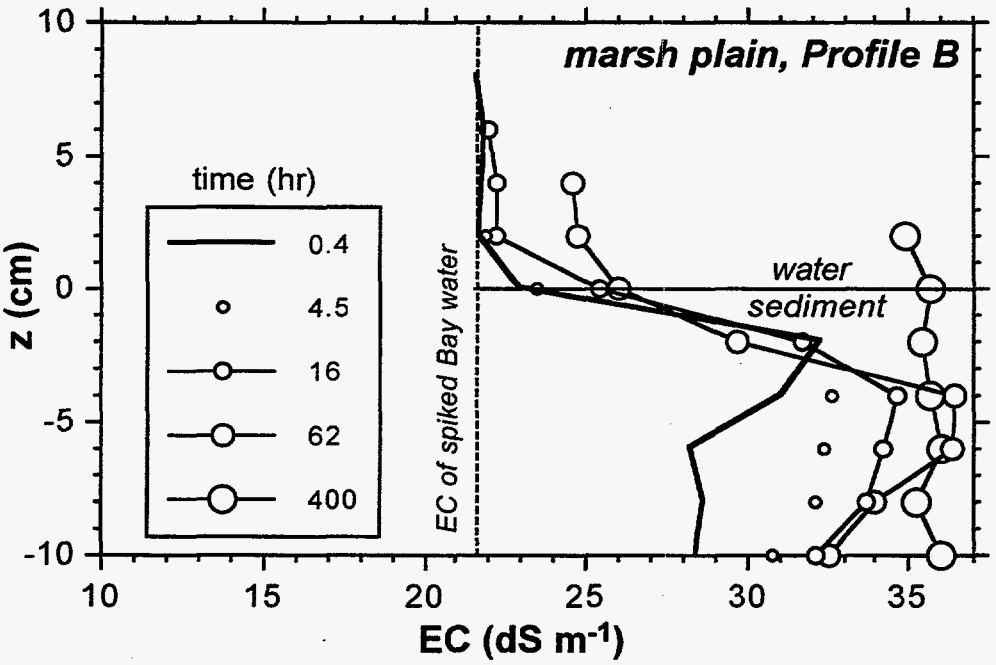

Figure 6.15 Electrical conductivity in ponded and pore water sampled from the marsh plain microcosm, Profile B, during the 400-hr ponding experiment.

There is a net increase in salinity in the aqueous phase, indicating that evapotranspirative losses of water were significant. Recall that this microcosm contained live plants and at least some of the salinity increase in the sediment can be attributed to transpiration. On the other hand, the increase in salinity in the overlying water can be due to two processes: evaporation and upward diffusion of salts across the sediment-water interface. Although the evaporation rate was not measured, it can be estimated based on the changes in the height of the ponded water and the amount of water removed via sampling. The average evapotranspiration rate was 0.1 mm hr^{-1} or 2.4 mm d^{-1} which accounts for the loss of approximately 50% of the ponded water.

Assuming a linear relationship between EC and salinity, this should have resulted in an EC of 43 dS m^{-1} compared with the final EC of 36 dS m^{-1}. However, EC is not linear with respect to salinity over this wide a range, and assuming a power dependence of EC on salinity, with 0.89 being a commonly used exponent, EC should have increased to 39.8 dS m^{-1}, fairly close to the observed value. This strongly supports the idea that most of the observed increase in EC is due to evaporative concentration.

As water was collected from soil water samplers embedded in the sediment, the water level dropped slightly, and there was a small downward displacement of water. Generally, this effect is not apparent in the EC data, since at most points in the sediment EC increased, but at the depth of 2 cm, slight decreases were observed between 0.4 and 62 hours. It is, therefore, clear that such vertical displacement needs to be considered in the evaluation of Se data.

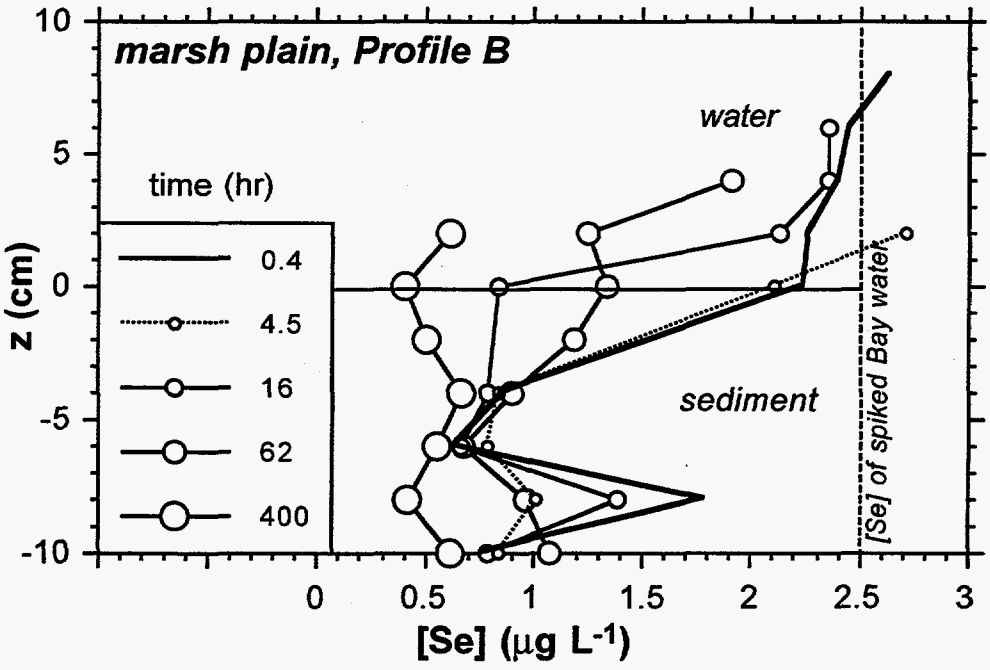

Figure 6.16 Total dissolved Se in ponded and pore water sampled from the marsh plain microcosm, Profile B, during the 400-hr ponding experiment.

Total dissolved Se is shown in Fig. 6.16 and selenite (Se(IV)) data is shown in Fig. 6.17. In agreement with the results of Experiment I, no significant changes in Se concentrations, or speciation, occur during the first 4.5 hours of ponding, with the exception of the 8 cm depth in the sediment, where the data is noisy and is probably a reflection of the spatial variability of Se concentrations. In concurrence with Eh

measurements, the first substantial changes occur at the sediment-water interface, where the Se concentration drops from about 2 μg L^{-1} to less than 1 μg L^{-1} after 16 hours of ponding, while Se concentrations at other depths remained unchanged. All of the observed decrease can be attributed to the decrease in Se(IV), either due to adsorption or reduction to Se(0). It is not until the 62 hour sample that a decline in Se concentrations in the ponded water are observed. However, Eh was stable in the ponded water, generally at around +500 mV (c.f. Fig. 6.12). Therefore, much of this loss is a result of Se(IV) diffusion out of the ponded water and into the sediment, due to Se(IV) reduction and depletion at the sediment-water interface. This type of effect has been observed and confirmed via x-ray absorption spectroscopy in similar microcosm experiments albeit using much higher Se concentrations (Tokunaga et al., 1996).

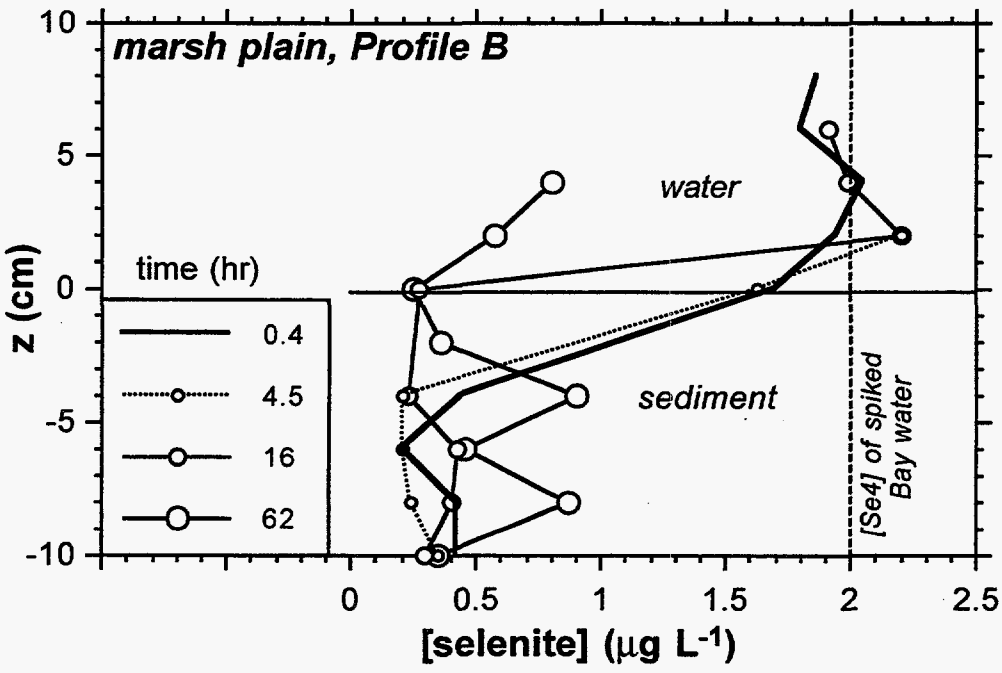

Figure 6.17 Dissolved selenite in ponded and pore water sampled from the marsh plain microcosm, Profile B, during the 400-hr ponding experiment.

6.3 Summary

The microcosm experiments described above provide preliminary evidence that immobilization of Se from the water column occurs only under infrequent conditions characterized by extended ponding of the intertidal environment, either during very high

tide or as a result of stagnant conditions in topographic lows. Such reduction is far more likely in the marsh where organic carbon is abundant at the sediment-water interface, as is plant litter which may provide additional sorption and/or reducing sites. Although the exact rates of Se reduction and immobilization under these conditions are extremely difficult to measure due to the very low fluxes over a tidal cycle, it is likely that this is a process of secondary importance in terms of Se input into the sediments, as compared with particulate-Se fluxes.

Several problems were encountered during the course of the experiments. The most significant was the displacement of water in the sediments due to sampling. Since the Eh and Se time trends can now be anticipated, future experiments will require far less sampling. Furthermore, the analysis of organic-rich water samples needs to be improved in order to reduce the volume of sampled water. Finally, Se diffusion out of the sediment was not studied, partly because it was difficult to isolate from other processes, and partly because the diffusive flux would be expected to be very small over the course of a single tidal cycle. Therefore, field measurements may be the best way to characterize this process, using some variant of benthic chambers, specifically adapted for use in an intertidal zone.

7 Stable Isotope Methods

Selenium stable isotope ratios have the potential to distinguish anthropogenic Se from other sources, and to provide information about the chemical cycling of Se. This segment of the project focused on developing methods to measure the $^{80}Se/^{76}Se$ ratio and generating an initial database. Because measurements of this type had never been made before, pioneering work was required to develop methods for mass spectrometry and purification of Se.

7.1 Stable Isotope Ratios as Environmental Tools

Isotope ratios have been used as environmental tools with increasing frequency in recent years, as measurement techniques have improved and environmental studies have become more complex. A common use of isotope ratios is as a "fingerprinting" tool. For example, natural lead (Pb) dissolving from a soil usually has $^{207}Pb/^{204}Pb$ and $^{206}Pb/^{204}Pb$ ratios that are distinct from those of industrial Pb. Studies of Pb isotope ratios have succeeded in calculating the relative contributions of the two sources to Pb in stream water (Bullen et al., 1994; Bacon and Bain, 1995). Similarly, nitrogen and oxygen isotope ratios have been used to examine sources of nitrate in groundwater (Kendall et al., 1994).

In addition to distinguishing sources, isotope ratios can also give information concerning chemical transformations. Sulfur isotope ratio variations have been used extensively to investigate sources of sulfur and chemical processes in ore deposits (Ohmoto, 1986; Faure, 1986), sedimentary rocks (e.g., Zaback et al., 1993; Tuttle and Goldhaber, 1993), and groundwater systems (e.g., Van Stempvoort et al., 1994; Van Stempvoort et al., 1992; Fontes et al., 1989; Dowouna et al., 1993). Stable isotope variations are often expressed as deviations in parts per thousand, or per mil, from a standard material. For example, the $^{34}S/^{32}S$ ratio can be expressed as follows:

$$\partial^{34}S = 1000\left[\frac{^{34}S/^{32}S_{sample} - ^{34}S/^{32}S_{std.}}{^{34}S/^{32}S_{std}}\right]$$

$\delta^{34}S$ values observed in nature can be used to distinguish sources of sulfur in groundwater (e.g., Dowouna et al., 1993) because $\delta^{34}S$ of sulfide minerals is often 20 to 50 per mil lower than that of sulfate minerals. Evidence of reduction of sulfate to sulfide, which can decrease $\delta^{34}S$ by 20 to 70 per mil, has been documented in sediments and sedimentary rocks (e.g., Tuttle and Goldhaber, 1993).

7.2. Selenium Isotope Ratios

Selenium has six stable isotopes, with masses 74, 76, 77, 78, 80 and 82 (see Fig. 7.1), and the kinetic properties and chemical bond strengths of the isotopes vary slightly according to mass. Accordingly, chemical reactions fractionate the isotopes; decreases of as much as a few percent in the $^{82}Se/^{76}Se$ ratio have been observed in Se that has passed through reduction reactions (Krouse and Thode, 1962; Rashid et al, 1978; Webster, 1972). This phenomenon is similar to fractionation observed for sulfur, oxygen, carbon, nitrogen, and hydrogen. This mass-dependent fractionation is a fundamental cause of isotopic variations which have been widely used in geological, oceanographic, and hydrologic studies (Faure, 1986). The other major source of isotope ratio variation, radioactive decay, is not a factor in stable Se isotope studies.

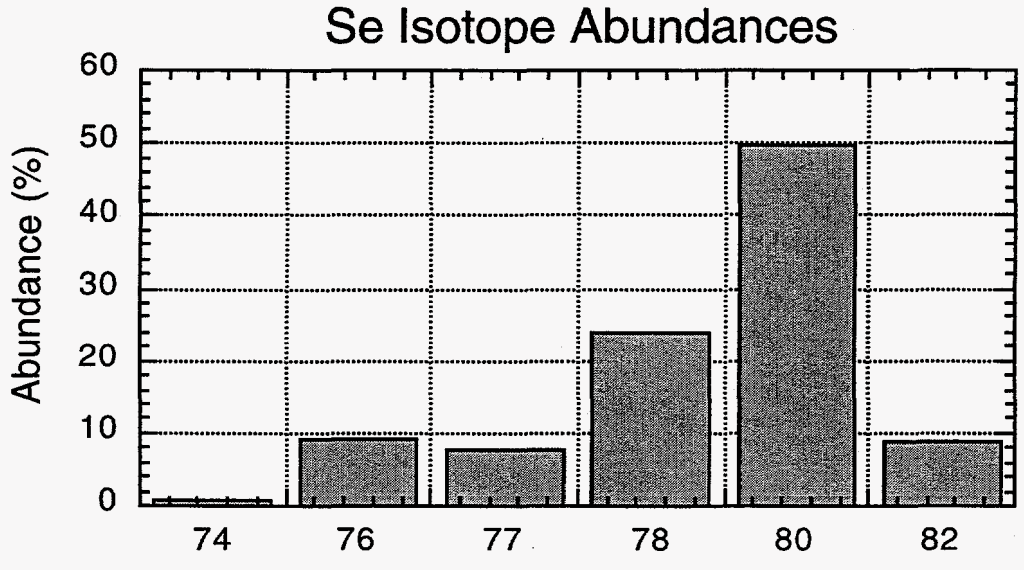

Figure 7.1 Abundance of stable Se isotopes.

Very little previous work has been done on the natural variation of Se isotope ratios. The initial work, done over thirty years ago, employed analytical techniques that were modified from those used for sulfur. Se was converted to SeF_6 gas and measurements were made using gas-source mass spectrometry. This method is problematic for several reasons. It involves difficult sample preparation, the SeF_6 is highly toxic, and large amounts (>50 μg) of Se are required. Krouse and Thode (1962) made theoretical predictions of Se isotope fractionation and performed $^{82}Se/^{76}Se$ measurements on several natural samples, finding variations of 15 per mil in plant samples (Fig. 7.2). Very little variation was found in sulfide samples from ore deposits. Rashid et al. (1978) measured shifts of up to 40 per mil in $^{82}Se/^{76}Se$ caused by bacterial reduction. Webster (1972) reported variations of 150‰ in the $^{74}Se/^{80}Se$ ratio at a former groundwater reduction zone associated with a roll-front uranium deposit.

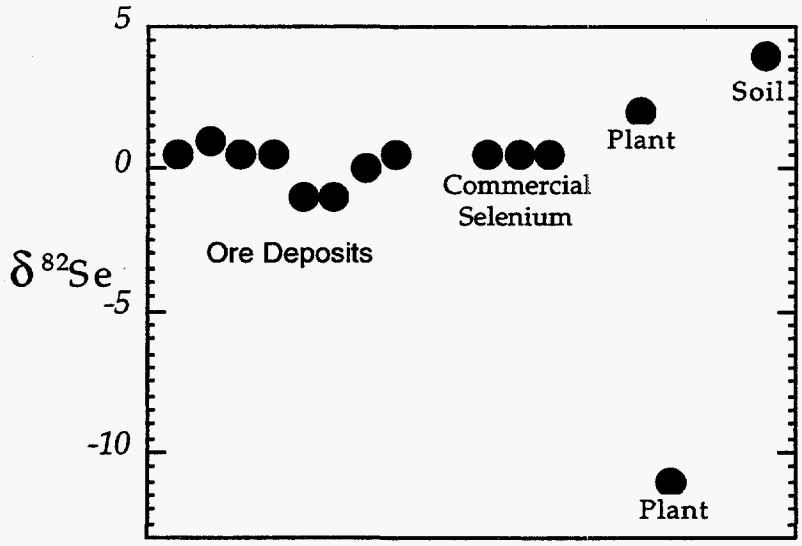

Figure 7.2 Data from Krouse and Thode (1962), given in per mil deviations from the $^{82}Se/^{76}Se$ ratio of Se extracted from troilite from the Canyon Diablo Meteorite. Uncertainties are given by the sizes of the circles.

Se isotope ratio measurements have the potential to give key information about sources of Se and chemical processes that control its fate and mobility. Chemical

reactions alter the relative abundance of the six stable Se isotopes. For example, chemical reduction of Se is known to increase the abundance of the lighter isotopes relative to the heavier isotopes. Accordingly, the $^{80}Se/^{76}Se$ ratio reflects the chemical history of a Se sample.

There are two ways in which Se isotope data may be used. Because Se occurring in oil refinery wastewater has a very different chemical history from Se in river or sea water, it was hoped that its $^{80}Se/^{76}Se$ ratio would be distinct from those of other sources. The isotope ratio would thus be useful as a tool for distinguishing refinery-source Se from Se of other origins. Perhaps more importantly, $^{80}Se/^{76}Se$ measurements provide a tool for studying the chemical processes that affect Se mobility. In field investigations, the relative values of $^{80}Se/^{76}Se$ in the various forms of Se (dissolved, adsorbed, precipitated Se^0, pyrite Se) give indications of the pathways through which those fractions were formed. In general, the isotope ratios give information that complements the concentration measurements that are performed. Concentration data give the sizes of the various pools of Se, while the isotope ratios give information about their sources and/or the reactions that transfer Se between them.

7.3 Methods

Mass spectrometry and chemical purification techniques were developed simultaneously. Unforeseen difficulties with the mass spectrometry led to development of a "double spike" procedure for Se. Extraction and purification of microgram quantities of Se from aqueous and solid samples were carried out using a variety of techniques developed for the various sample types.

7.3.1 Mass Spectrometry

A technique recently developed by Wachsmann and Heumann (1992) enables Se isotope ratio measurements on 0.5 μg of Se using thermal ionization mass spectrometry (TIMS), the method used for isotope ratio measurements of strontium, neodymium, lead, and other heavy elements. While most TIMS analysis is done on elements that easily produce positive ions, and most machines are configured to analyze only positive ions, interest has recently increased in elements that produce negative ions (e.g., Os and B). Wachsmann and Heumann (1992) used this negative ion technique to decrease the sample size needed for TIMS analysis. However, their method has been applied only to isotope dilution measurements of Se concentration and no studies on natural isotopic variations have been published.

Raw TIMS measurements usually differ from the true ratios in the sample material, and this bias, or discrimination, must be minimized or compensated for in order to obtain highly precise ratios. Before the beginning of the present study, minor discrimination was expected. However, despite numerous attempts in this study, it was found that the discrimination during Se isotope ratio measurements is large and variable, presumably because of the semi-volatile behavior of Se and the complex chemical transformations that result in the formation of Se^- ions from SeO_2. A "double spike" routine was developed to compensate for the discrimination, as has been done previously for barium and calcium isotope ratio measurements (Eugster et al, 1969; Russell et al., 1978). With this technique, two stable isotopes, ^{82}Se and ^{74}Se, are added to the sample. The $^{82}Se/^{74}Se$ ratio of the added Se is known, and the measured $^{82}Se/^{74}Se$ ratio can be used to evaluate the discrimination. Calibration of the double spike and development of software to calculate sample $\partial^{80}Se$ values from raw $^{82}Se/^{80}Se$, $^{80}Se/^{76}Se$, and $^{76}Se/^{74}Se$ ratios were carried out.

An internal standard, MH495, was analyzed with each batch of 2 to 8 samples. Long-term precision of ±0.2‰ was observed on the standard. This represents the precision that can be obtained with complete purification of at least 0.5 μg of Se. In practice, contaminants in the Se purified from natural samples and limitations in the amount of Se that could be extracted from reasonable samples sizes decreased the intensity of the ion beams in the mass spectrometer and thus introduced greater uncertainty into the measurements.

7.3.2 Purification Chemistry

The separation of microgram quantities of Se from concentrated solutions such as Bay water and sediment extracts presents a significant challenge. Only small amounts of chlorine, sulfur and other elements can be tolerated in the final purified Se solution, and in saline waters, sulfur and chloride are more than one million times more abundant than Se.

Concentration of selenite via ferric hydroxide co-precipitation

A ferric iron hydroxide $Fe(OH)_3$ co-precipitation procedure was modified from one reported by Chau and Riley (1965) to concentrate Se from large volumes of water. The procedure involves adding Fe^{3+} to the solution, adjusting the pH, filtering to recover the precipitate, dissolving it in acid, and removing the Fe^{3+} with cation exchange resin. This leaves selenite and a few other weak acid anions in the final solution. The $Fe(OH)_3$

co-precipitation scrubs selenite from solution without a reduction step, has a yield between 95% and 100%, and can be carried out with very large volume samples.

Purification of selenite via anion exchange

Phosphate and organic acid anions brought with the selenite through the $Fe(OH)_3$ precipitation procedure can interfere with the measurements, so an anion chromatography procedure was developed. The solution was passed through a column of anion exchange resin, followed by a known amount of dilute acid. The selenite was separated from the other anions because it moves at a different rate through the column. This technique yielded a sufficiently pure Se solution which can be used for mass spectrometry, and we have found that at least 90% of the Se is recovered. Analysis of the final product of an extraction of one microgram Se from one liter Bay water spiked with 30 μg P (as phosphate) yielded the results given in Table 7.1. The process is effective at removing Cl and P and retains a high percentage of the Se.

Table 7.1 Results of chemical purification of Se

Element	Amount in final solution (μg)	Percent recovered
Se	0.91	91%
P	1	3%
Cl	10	0.00001%

Pre-concentration of selenate and selenite in river water via anion exchange

Additional techniques were developed to recover selenate from large volumes of water. With brackish or saline samples, the volume of the sample was reduced by evaporation and selenate was converted to selenite by adding large amounts of concentrated hydrochloric acid and heating. The solution was then neutralized and the selenite recovered in the usual way. Unfortunately, these steps consume huge quantities of time and reagents, and are not desirable for larger-scale processing of samples.

Pre-concentration of selenate by adsorption onto anion exchange resin is effective for the dilute waters of the upper parts of the bay system; all of the anions in one liter of water were adsorbed onto a small column (several cubic centimeters) of anion exchange resin. This procedure could ultimately be carried out in the field concurrent with filtration of the samples. After collection of all anions, they were removed from the

column by 30 mL of hydrochloric acid and this small volume was then processed via the usual methods.

Hydride generation as a purification procedure

Hydride generation was avoided as a purification method early in this project because the rapid reduction inherent in the method could greatly alter the isotope ratios of the processed samples. However, after the double spike technique was developed, use of hydride generation became a viable option again. As long as the spike is introduced before purification procedures, alteration of the Se isotope ratios during purification can be corrected for along with the mass spectrometry bias.

The hydride generation method is similar to that used for low-level Se analysis, and will enable relatively rapid processing of sediment extracts and digests. The sample solution is mixed with hydrochloric acid, sodium borohydride is added, and the evolved hydrogen selenide is swept from the solution by a carrier gas. For isotope ratio analyses, the hydrogen selenide is absorbed in nitric acid, according to the method of Tanzer and Heumann (1992). This solution is then easily prepared for mass spectrometry because there are few other elements other than Se in it.

An absorption tube, in which the carrier gas and hydrogen selenide are bubbled through the nitric acid, was fabricated and was tested to verify that complete absorption was obtained. Then, the MH495 standard was spiked and processed through the hydride apparatus and analyzed on the mass spectrometer. As expected, the double spike method successfully compensated for any alteration of the $^{80}Se/^{76}Se$ ratio, and the correct value was obtained for the standard.

7.4 Results

A total of 18 samples were analyzed, including duplicates and samples that did not yield reliable data (Table 7.2). Twelve samples yielded precise values and are plotted in Fig. 7.3. The first group of samples consisted of water and refinery effluent, and were chosen to evaluate the potential for distinguishing refinery-related Se from the riverine inputs. The water samples from Antioch, Tracy, and Kesterson Reservoir give a preliminary characterization of Se input from the San Joaquin river into the Bay. The Martinez sample probably represents some mixture of San Joaquin River, oil refinery, and possibly other inputs. Unfortunately, the oil refinery effluent $\partial^{80}Se$ values are not distinct from those obtained for the San Joaquin River system. Thus, based on these

limited data, it appears that ∂^{80}Se does not provide a tracer of refinery-related Se in this system.

Table 7.2. Results of δ^{80}Se measurements

Sample	δ^{80}Se	standard error	estimated uncertainty
OHx SHB T1S1G + T1S2F compos	0.72‰	±0.53‰	
OHx MRP T1S1B + T1S3G compos	0.62‰	±1.06‰	
Root, MRP CT-5b	-0.13‰	±0.55‰	
Root, MRP SC-2a	2.21‰	±0.33‰	
TAD SHB T1S1 E	1.64‰	±1.20‰	
TAD SHB T1S3 D	-0.65‰	±0.37‰	
Sulfite extract MRP composite	2.02‰	±0.45‰	
Dx, SHB Cattail #4	2.26‰	±0.13‰	
Martinez Water	3.18‰	±0.31‰	
Tracy Water	2.63‰		±1.00‰
Antioch Water	5.48‰	±0.40‰	
Kesterson Water	3.60‰	±0.3‰	
Chevron effluent	4.36‰	±1.3‰	
Shell Effluent	4.90‰		±0.70‰
Shell Effluent	4.30‰	±0.5‰	
UNOCAL Effluent	4.25‰	±0.2‰	
UNOCAL Effluent	3.20‰	±0.2‰	
Exxon Effluent	5.30‰	±0.1‰	
Hydride fractionation experiment	4.35‰	±0.57‰	

The second group of samples consisted of various extracts and digests of sediment components. The results (Fig. 7.3) show a systematic difference between dissolved ∂^{80}Se in Bay water and ∂^{80}Se in marsh sediments and plants. Such a difference was expected, because Se in the sediments and plants tends to be chemically reduced (predominantly organic Se and elemental Se). It is known that "open-system" chemical reduction of selenite to more reduced forms results in a shift in ∂^{80}Se toward lower

values. A marsh system that extracts Se from overlying bay waters would be considered an open system. Thus, the observation that ∂^{80}Se values are lower in the sediment components is not surprising. However, this difference is not as large as would be expected for open system reduction of Se. The work Krouse and Thode (1962) and Rashid and Krouse (1978) suggests that a much larger difference of roughly 10 per mil should be observed.

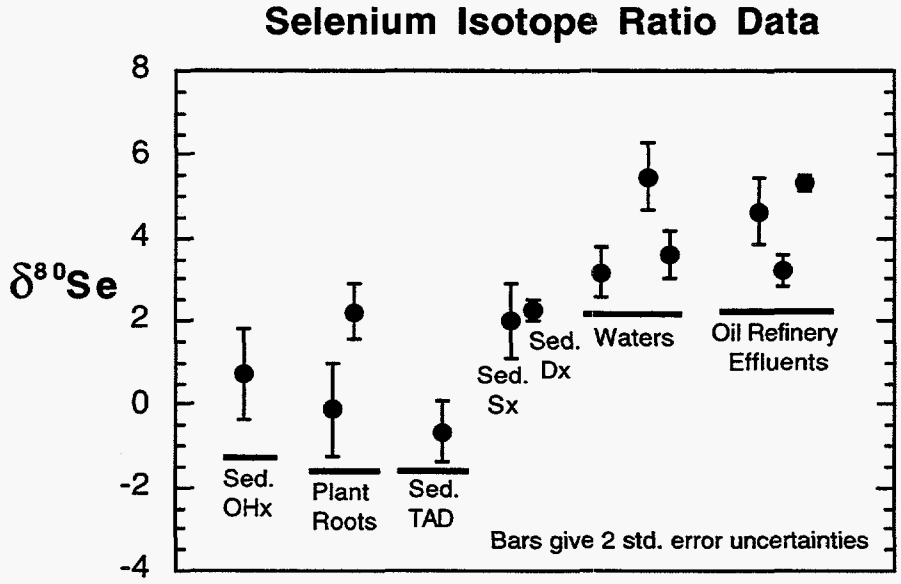

Figure 7.3 Results of Se stable isotope ratio measurements. Dx indicates a distilled water extract of a sediment core; Sx, sulfite extract; TAD, total acid digest; OHx, hydroxide extract.

An alternative model better explains the small offset between water and solid phases. If Se is concentrated in the marshes not by open-system chemical reduction, but by sedimentation effects, the offset could be quite small. The processes by which Se becomes bound to sediment and then deposited in marsh and mud flat sediments need not fractionate the isotopes. For example, simple adsorption probably would not fractionate them appreciably. Thus, the isotope ratio results support the conclusions of other parts of this study, which suggest that sedimentation is the dominant mode of Se deposition in the marshes.

7.5 Conclusions

The above data are the first application of environmental Se isotope ratios in the world. The procedures developed in this study will enable further application of this technique toward increased understanding of Se cycling in various systems. The groundbreaking work needed to make this first set of measurements consumed most of the effort allocated to this part of the project, and thus only a reconnaissance data base was collected. However, this data base provides a needed feasibility test for isotope tracing of Se in the bay and an encouraging first look at how $^{80}Se/^{76}Se$ measurements may help in studies of the biogeochemical cycling of Se.

8 *In-Situ* Se Speciation and Distribution in Bivalves

Selenium uptake by bivalves is an important process in the accumulation of selenium in the biological system, especially as a key element of the diet of diving ducks. The process is poorly understood, primarily because the speciation of Se in bivalve tissues was, until recently, not available. In this chapter, the first ever in-situ speciation and spatial distribution in bivalve organs, using X-ray absorption spectroscopic methods, are presented. Comparisons to speciation in sediments help draw preliminary conclusions on the biogeochemical conversions of selenium in bivalves.

8.1 Introduction

The bio-accumulation of selenium (Se) and several other trace elements in different bird and invertebrate species in the San Francisco Bay has been well documented (SFBRWQCB, 1992). The tentative pathways of Se mobilization from water and sediments into the higher organisms are thought to be through algae and filter-feeding invertebrates such as bivalves (Luoma et al., 1992; Besser et al., 1993). However, the bioavailability of different Se redox species and the Se species being accumulated are poorly understood. Insufficient knowledge on Se speciation and its redox equilibria in the sediments, and in the biota of the San Francisco Bay sediments has become the potential barrier for investigating these issues. This suggests that a more fundamental investigation of the Bay water and sediment Se geochemistry is essential to the understanding of different Se bioaccumulation pathways. While other chapters of this report have shown Se speciation in surface waters, suspended particulates and sediments, this chapter focuses mainly on indirect Se speciation in Bay sediments and direct Se speciation of bivalve tissues using in-situ X-ray absorption spectroscopic (XAS) methods. Since bivalves are the principal organisms acting as Se conveyors for higher organisms, such as diving ducks, we focused our study on Se speciation in bivalves and the material they ingest.

In nature, Se occurs in both inorganic (+VI, +IV, 0, -II) and organic forms [seleno-methionine (-R-Se-R), seleno-cystine (-R-Se-Se-R-), seleno-cysteine (R-Se-H)]. The higher valent inorganic forms and all the organic forms are relatively more bio-

available. In biota, all of the above mentioned organo-Se forms have been reported to occur as the structural components of amino acids and proteins (Ganther, 1974; Bottino et al., 1984; Stadtman, 1990). Other organo-Se compounds such as seleno-urea, -inosine, -guanosine in which Se forms double bonds with C, which in turn is linked to amine or amide groups have been synthesized, but their occurrences in the biological systems have not been reported so far. While the main Se contributors to the San Francisco Bay are from both natural sources (primarily as SeO_4^{2-} through rivers receiving drainage from agricultural lands of the San Joaquin Valley, California (Presser and Ohlendorf, 1988)), and anthropogenic sources (as SeO_3^{2-} from local oil refinery discharges (Cutter, 1989)), Se in the surface water occurs in a number of forms, including dissolved species, species adsorbed onto suspended particulate matter, and phytoplankton-Se. Particle-adsorbed Se(VI) and Se(IV) may undergo modifications by reacting with the unsaturated C-O bonds and by displacing S from -SH groups of the dissolved and particle bound humic substances, and also by reacting with similar functional groups within the algal cells (Bottino et al., 1984; Luoma et al., 1992; Besser et al., 1993; Amarathunga and Milne, 1994). Such reactions can transform inorganic Se into organo-Se forms mentioned above, and although direct speciation is not possible, the presence of organo-Se compounds has been suggested in Bay waters, based on indirect methods (Cutter, 1989). Given this preliminary information, it may be hypothesized that the particulate-adsorbed inorganic Se is deposited with the sediment, and transformed according to the redox conditions in the sediments before it is ingested by the bottom dwellers. While direct particulate ingestion by bivalves and fish is also an important pathway through which Se is incorporated into the food web (Luoma et al., 1992, Besser et al., 1993), the deposit feeders, such as some of the bivalve species, are exposed to the sediment Se for a longer time. Since bivalves residing at the sediment-water interface of the intertidal zone constitute a significant part of the diet for diving ducks and other birds that inhabit the Estuary, Se mobilization from the sediment and into the bivalves may be a critical pathway.

In this chapter we present the in-situ Se speciation of bivalve tissue collected from different locations in the San Francisco Bay. The low sediment Se concentrations are not accessible for direct speciation by any spectroscopic technique, and so we have used indirect methods to identify Se speciation in intertidal wetlands sediments. In this method, sediment redox conditions were obtained by evaluating the sediment major element redox couples with XAS. The underlying assumption is that the redox couples of the major elements (e.g. Fe, S) and the organic matter act as sediment redox buffers

and the minor elements, such as Se, follow the redox trend set by these dominant couples (Sposito, 1989; Morel and Hering, 1993). Using the Fe redox couple we predicted the sediment redox status, and assuming thermodynamic equilibrium in the system we extrapolated this information to predict sediment Se speciation. In a separate laboratory study, we have evaluated these equilibria assumptions by examining Se speciation and redox kinetics in the presence of dissolved Fe(II), and Fe(II,III) oxides (green rust, magnetite). The sediment microbes may also modify the reaction rates, and their influence on the major and trace elements can be different. However, such disequilibrium reactions and their energetics, can be interpreted from accurate estimates of the ratios of redox couples (e.g. Fe(II)/FE(III), Morel and Hering, 1993). Using this in-situ spectroscopic information on sediments and bivalve tissue, we postulated some of the probable reactions that might be causing Se bioaccumulation.

8.2 Experimental Methods

8.2.1 Sediment Se Speciation

Using sequential extraction procedures, Se speciation in the intertidal sediments from San Francisco Bay was conducted previously and the results are summarized in Chapter 2. However, the chemical treatment associated with extraction procedures may alter the chemical states of Se and hence the obtained results are inconclusive. Se redox speciation of the sediment may also be estimated indirectly from sediment Eh-pH and from the redox equilibria of major elements, which can be evaluated accurately using in-situ XANES spectroscopy. This methodology assumes thermodynamic equilibrium between Se and major element redox couples in the sediment. In this study we used these indirect methods, since Se concentration in the Bay sediments is small (~ 25 mM kg^{-1}) and is well below the detection limits of any direct physical methods. Also our recent studies have shown that Se(VI) could be reduced rapidly by Fe(II) above pH of 5.0 (Myneni et al., 1996).

For sediment Se fractionation and Fe speciation, fresh, undisturbed, 20 cm-deep mudflat sediment cores were collected from the Carquinez Strait at a very low tide. The cores were sealed in airtight polypropylene cylinders and were transferred in frozen condition to the synchrotron facilities for analysis. XANES spectroscopy measurements were made within 24 hours of collection. The redox potentials and pH of the sediment were measured at different depths using Pt and Sb electrodes, respectively, as described in Chapter 2. Later Fe(II)/Fe(III) ratios in the sediment were

evaluated using Fe-XANES features. If thermodynamic equilibrium exists, the ratios of Fe(II)/Fe(III) are directly related to the sediment redox potentials (Morel and Hering, 1993).

8.2.2 Bivalve Collection and Gut Evacuation

Three different species of bivalves, *Corbicula fluminea*, *Macoma balthica*, and *Potamocorbula amurensis*, representing the inter-tidal regions were sampled from the San Francisco Bay. The collected samples were from 2-6 cm deep sediment, and the sampling was done while the tide was receding. Sample cleaning, gut evacuation and preservation procedures were described previously by Luoma et al. (1992). The gut evacuated bivalves were frozen (≈ 0°C) before the shells were separated and analyzed using the in-situ XANES spectroscopy. The low temperatures killed the organisms and, when thawed, the tissue could be separated easily from the shells. Redox transformations at these low temperatures are extremely slow and hence changes in clam Se speciation during sample storage and transport to the synchrotron facilities is negligible.

8.2.3 Fe and Se XANES Spectroscopic Data Collection and Analysis

Frozen sediment core samples were thawed just before the XANES data collection, and the innermost part of the core was used in the analysis. Sediment Fe XANES were collected at the beamline 4-2, Stanford Synchrotron Radiation Laboratory (SSRL, Stanford, CA). The beamline has Si(111) double crystal monochromator, with the beam size approximately 12mm x 2mm before the monochromator crystals. The XANES spectra were collected in fluorescence mode using a Lytle detector, and the sample Fe-absorption edge position were calibrated against iron foil [Fe(0), 1s→4s transition in the white line was set to 7106 eV]. The sample spectra were compared with Fe model compounds of different oxidation states (0: Fe-film, II: FeSO4•7H2O, III: FeOOH) to evaluate Fe(II) fraction in the sediment.

For the XANES spectra of the bulk bivalve tissue, the samples were positioned between two Mylar windows and mounted on a hollow polypropylene slide frame. Se K-edge XANES spectra were collected in fluorescence mode (13-element Ge array detector) at the SSRL, on Beamline 4-3. For better spectral resolution at the Se edge, we used Si (220) monochromator crystals and a 12mm x 2mm slit opening before the monochromator. The X-ray beam was also detuned by 50-70% to remove the higher order harmonics. The spectral resolution at the Se K-edge was better than 2.5 eV. However, edge shifts as small as 0.5 eV could be detected accurately. The scan energy

range was 12430 to 12770 eV, with a 0.2 eV step size adjacent to the edge region. XANES Spectra were also collected for different inorganic and organic Se model compounds [Se(VI), Se(IV), Se(0), Se(-II), seleno-cystine, seleno-methionine), and the sample and model compound energy positions were calibrated against Se(0) foil (12658 eV). Spectra were processed for background subtraction in the pre-edge region and also ≈20 eV above the absorption edge separately, by fitting a first order polynomial. The extremely dilute tissue sample spectra were very noisy, and these were smoothed using Savitzky-Golay convolution function (13 points, 2nd order polynomial).

The micro-XANES studies were conducted at the National Synchrotron Light Source (NSLS; Brookhaven National Laboratory, Upton, NY) on a synchrotron X-ray microprobe beamline X26A. The operating characteristics of this facility are described in Sutton et al. (1995). For the present work, synchrotron X-rays were passed through a channel-cut monochromator and ellipsoidal focusing mirror which rejects higher order harmonics, without additional collimation. The effective beam size was about 0.3 mm. The monochromator was tuned from about -50 eV to about +100 eV relative to the Se(0) K absorption edge (taken as 12658 eV), in steps ranging from 0.3 eV (in the near-edge region) to 9 eV (above and below the edge). The spectra were also compared with different inorganic and organic Se model compounds discussed above.

8.2.4 Synchrotron X-ray Microprobe Data Collection and Analysis

Selenium and other trace element relative-concentration maps for the bivalve-tissue were prepared using the X-ray microprobe (X26A, NSLS), with monochromatic X-rays tuned 100 eV above the Se K-edge. A stepper motor-driven x-y stage was used to scan the sample in front of the stationary X-ray beam, and fluorescent X-rays emitted from the targeted spot were detected with an energy-dispersive detector. The beam characteristics have been described previously. The elemental map was generated by scanning across a 16 x 13 mm area in a 0.5 mm grid, counting for 40 s at each spot. The normalized trace element Kα-fluorescence count intensities (proportional to detected trace element 2p to 1s electronic transitions) were collected, and relative concentration contour maps were prepared for each element. It should be noted that variations in sample thickness and matrix composition also contribute to the apparent concentration contrasts, and such effects are expected to yield up to about 5-fold differences within this sample.

8.3 Results

8.3.1 Sediment Redox Equilibria and Sediment Se Speciation

Although the Bay surface waters are oxidizing, sediment Eh measurements indicate that the redox conditions vary with the energy of the depositional environment (sediment depositional rate and size). Surficial mudflat sediments are coarse, have relatively higher Eh, and different Eh-depth profiles as compared to the marshes. These results are shown in Chapter 2, specifically in Figs. 2.9 and 2.10. All the mudflat sediments collected from two intertidal wetlands in the Bay exhibit a decreasing Eh trend with depth. The sediment Eh values ranged from 350 mV at the surface at the Martinez site to as low as -100 mV at 17.5 cm below the surface at the Southampton Bay site. The sediment pH values are the same as the sea water pH (~ 8.0), except for a few deeper samples where pH was 9.5 - 10.5. Although, SO_4^{2-} reduction can result in pH increases, such high values were not found in inter-tidal sediments. Results from a representative core from the Martinez site are shown in Table 8.1. In these sediment Eh-pH regimes, sediment Se should be present predominantly as SeO_3^{2-} with some conversion to Se(0) a few centimeters below the surface (Masscheleyn et al., 1990). In addition, these Eh-pH measurements also predict that sediment Fe should be predominantly in +III oxidation state.

The sediment redox potentials obtained from sediment Fe(II)/Fe(III) ratios (from Fe XANES spectroscopy) were quantitatively inconsistent with direct Eh measurements. Since the sediment Eh-depth profiles were very similar in the mudflat samples collected from different locations in the Bay (Zawislanski et al., 1995), Fe-XANES study was focused on a mudflat sediment column collected from the Martinez site, the same core as summarized in Table 8.1. Fe-XANES spectroscopic studies indicate that the energy position of the Fe K-absorption edge (1s→4s transitions), and its small pre-edge (1s→3d transitions) increases with increases in Fe oxidation state (Bajt et al., 1994; Westre et al., 1997). Since the pre-edge feature of the sediment samples was broad due to the presence of a mixture of oxidation states in a variety of structural environments, its energy shifts could not be used for Fe(II)/(III) estimation. However, the main absorption edge energy shifts were distinct with that of Fe(II) and Fe(III) at 7112.8, and 7116 eV, respectively. When compared to these two Fe oxidation states, all the sediment samples exhibit intermediate values (Table 8.1). As the sample depth increases, Fe K-edge position shifts to lower energies (from 7114.8 eV at the top to 7113.6 eV ~ 12 cm below sediment-water interface), indicating increased Fe(II)

concentration at greater depths. When these edge positions were transformed into concentrations, Fe(III) at the top of the core was 60-65 % of total iron, and the bottom-most part of the core had only 25 % Fe(III). While these distinct changes in the relative concentrations of Fe redox species with depth are consistent with measured sediment Eh, its magnitude is at least 150 mV higher than those predicted from XANES Fe(II)/Fe(III) ratios (-150 to -300 mV, Table 8.1). If Se redox speciation is at equilibrium with that of Fe, then Se should either be in elemental or selenide form.

Table 8.1. Solid-phase Fe speciation and Eh and pH measurements on a mudflat sediment core from the Martinez Regional Park.

Sample depth (cm) (± 0.2)	Measured pH (Sb-electrode)	Measured Redox Eh (mV) (Pt-electrode)†	Edge Position‡ (eV)	Estimated Fe(III) (%)¥
0.5	7.4	367	7114.8	63
1.5	7.6	414	7114.6	56
2.5	8.5	339	7114.3	47
4	8.2	173	7114.2	44
6.3	8.6	136	7114.1	41
8.8	7.6	32	7113.9	34
12.5	7.8	115	7113.6	25
Fe (II) in $FeSO_4 \cdot 7\ H_2O$	-	-	7112.8	-
Fe (III) in FeOOH	-	> 0 at pH 7.0	7116	100

† Estimated Eh from Fe redox couple are less and are in the range of -150 to - 300 mV
‡ Edge position was calibrated against Fe-foil (1s→4s transitions) at 7106 eV.
¥ Predicted concentrations are not corrected for ligand effects, for e.g. OH- versus S^{2-}.

Although the sequential extraction studies of the mudflat samples indicated that Se is predominantly present in the elemental form (≈50%), other, more oxidized species, such as Se(IV), are also present. "Organically-associated" Se is the second most common fraction, and, as described in Chapter 2, it is operationally-defined and may include both organic and inorganic Se species. This suggests that sediment Se speciation estimated using different methodologies is inconsistent, and the observed variation in Se speciation may be due to extraction of more than one type of Se species

during a given sequential extraction step, and/or inaccurate redox potentials measured with a Pt-electrode, which may be due to its poor sensitivity to sulfide-rich sediments. Although in-situ XANES spectroscopy provided information on Fe redox couples and inferences were made on Se speciation in the sediments, the influence of structure (mineral type), and ligand effects on Fe K-edge shifts have to be considered for predicting the percentage of each Fe valence state accurately. However, these features do not shift the edge by a large magnitude and hence the predicted Fe(II)/Fe(III) ratios may not significantly deviate from the true values. Recent kinetic studies on Se(VI) reduction in the presence of Fe(II) indicated that it converts Se(VI) to Se(0) within 4 days (Myneni et al., 1996), though the effects of complexation with and onto solid and organic surfaces were not considered. In summary, XANES studies predict that Se is present in the sediments as Se(0), with probably some Se(-II) in the deeper sediments. Since most of the bivalve samples were collected from the upper sediment layers, it is expected that the organisms may have been predominantly exposed to Se(0), smaller concentrations of Se(IV), and possibly some organo-Se species as well.

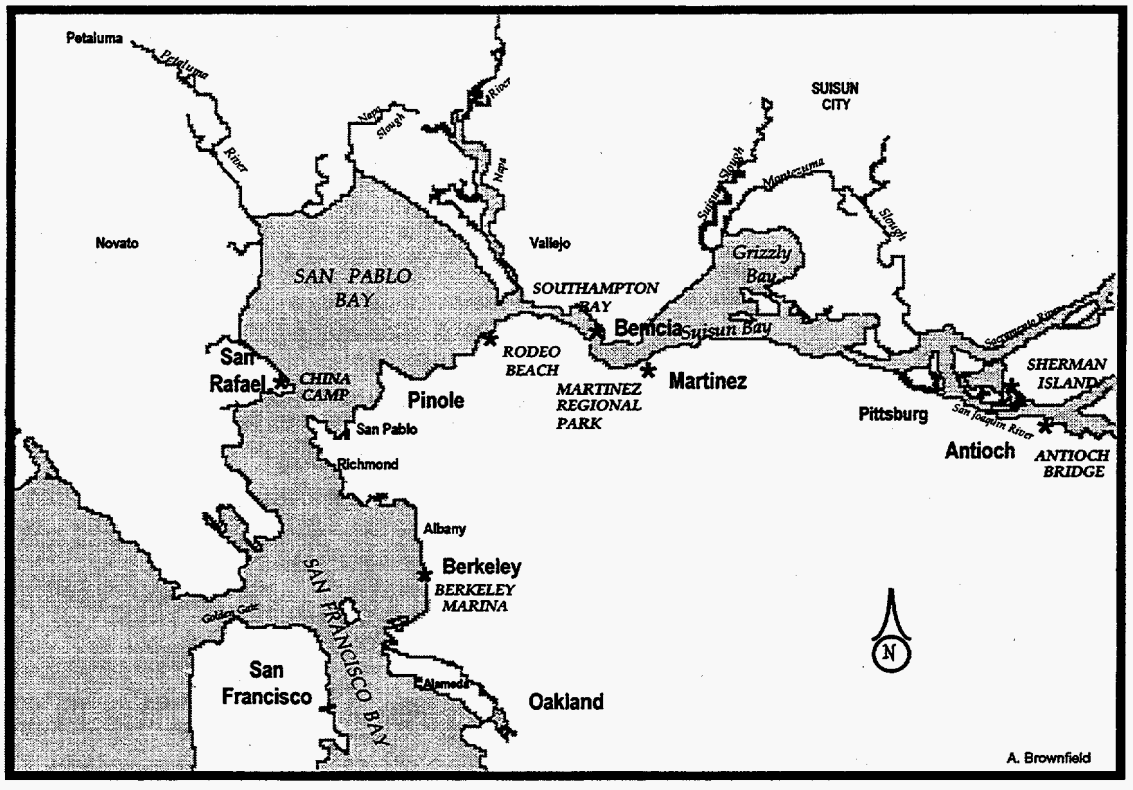

Figure 8.1 Bivalve sampling locations in the central and northern reaches of the San Francisco Estuary.

8.3.2 Bivalve Se Speciation

Se speciation in the bivalves was examined for *Corbicula fluminae*, *Macoma balthica*, and *Potamocorbula amurensis*. During sample collection at each location in the San Francisco Bay (Fig. 8.1), only the dominant bivalve species inhabiting that location were sampled. The spatial distribution of bivalve species across the Bay is controlled by water salinity and sediment load. The total Se concentrations in bivalve tissue samples ranged from 1.6 to 7.9 mg kg^{-1} (dry weight basis), with the highest concentrations recorded in the bivalve tissues of Southampton, San Pablo and Grizzly Bays (Luoma et al., 1996).

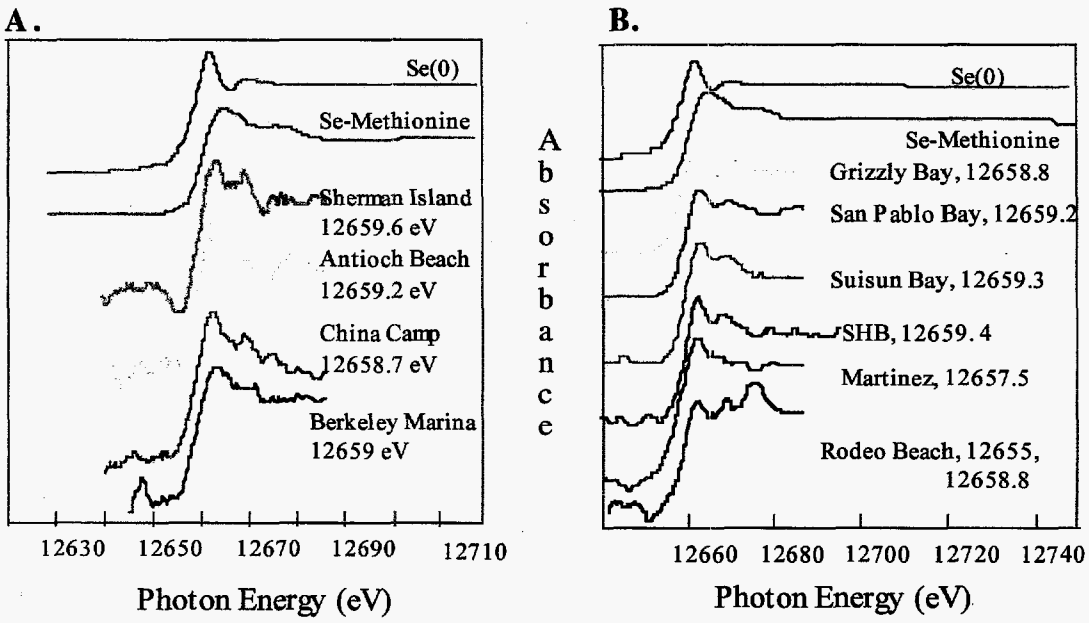

Figure 8.2. In-situ *XANES speciation of Se in the bivalve tissues collected across the San Francisco Bay. Samples from areas more distant from refinery outfall are shown in A, and samples collected adjacent to the refinery outfalls are shown in B. Elemental selenium and seleno-methionine are shown for comparison.*

Like the Fe K-absorption edge, Se K-edge XANES spectra (1s→4p transitions) linearly shifts to higher energy as the Se oxidation state increases (Pickering et al., 1995). Among the examined model compounds, Se(-II) and Se(VI) have the lowest (12656 eV) and highest (12665 eV) energies, respectively, with the other oxidation state Se K-edges in between these two. Organo Se compounds, such as seleno-cystine and -methionine have absorption edges at 12659 and 12660 eV, respectively. In addition to the edge-energy shifts, the XANES spectra 10 eV above the main absorption edge also exhibit structure, which is a function of the local coordination

around Se atoms. When compared to these Se-models, the bivalve tissue Se-edge spectra are noisy due to the low Se concentration, but exhibit a clear Se-absorption edge (Fig. 8.2). The edge position of tissue-Se is distinctly different from that of inorganic Se compounds examined. Excepting the clam tissue collected from the Martinez Bay, all of the other samples exhibit absorption edges at least 1-1.6 eV higher than Se(0). The *Macoma balthica* tissue collected from the Martinez site exhibits Se absorption edge at 12657.3 (±0.5) eV.

The spectral deconvolution of bivalve tissue samples suggests that seleno-cystine and seleno-methionine are the predominant species. Since the spectra were noisy, the relative percentages of these two organo-Se compounds are difficult to estimate. Samples with edges closer to 12659 (±0.2) eV may be enriched in Se-cystine with relatively minor Se-methionine, and the samples with absorption edges at approximately 12659.5 eV may have significant Se-methionine. The presence of minor concentrations of inorganic Se species and other organo-Se compounds with structures similar to seleno-urea, -inosine and -purine can not be ruled out. However, Se directly links to a C atom either through single or double bonds in all these organic compounds. Although the local coordination around Se bonded C varies slightly, Se oxidation state may be closer to that of Se-methionine. The oxidation state of Se in the Martinez sample is interesting because only this sample showed much smaller values for the absorption edge and the spectra were similar for the samples collected during different times, which indicates that the sample Se edges are consistently below 12658 eV. This suggests that the formal oxidation state of Se in these samples may be less than 0 but greater than -I, and such Se species is expected to be in forms such as R-Se-H (R: linking organic molecule). Since "H" attains a formal oxidation state of +I in similar compounds, the nature of "R", i.e. the electron withdrawing or donating tendency controls the overall formal oxidation state on Se. This study suggests that the dominant Se fraction in these samples is in Se-H type. However, this does not rule out the possibility of other Se forms (Se-methionine, -cystine) which may be present in significant concentrations.

Micro-XANES spectra were collected on clam guttural portions in which more than ≈90% of the total clam Se was concentrated. Although, the Se K-edge was clearly discernible in the micro-XANES scan, the experimental problems associated with the monochromator energy calibration prohibited accurate Se oxidation state determination. An energy uncertainty of about 0.5 eV was noted based on periodic energy calibration using elemental Se. These results suggest that clam Se-edge is at 12658.5 (±0.5) eV

(Fig. 8.3). This finding definitely rules out the presence of inorganic SeO_3^{2-} or SeO_4^{2-} in large concentrations (>10 %).

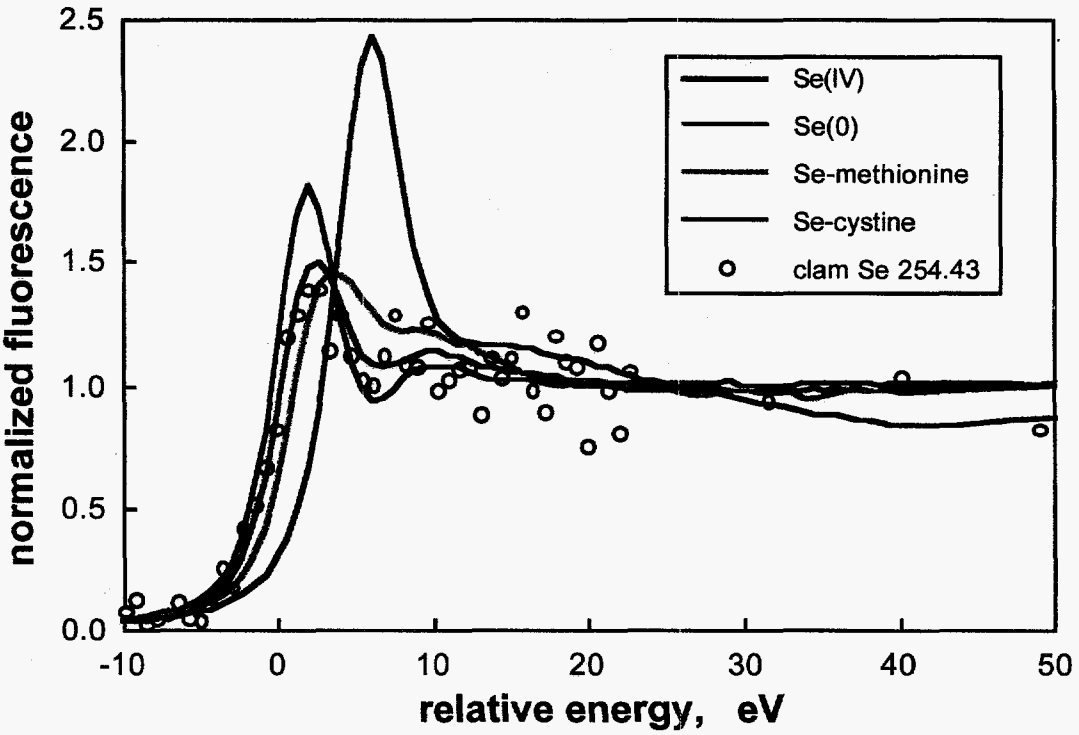

Figure 8.3 Se micro-XANES spectra of Potamocorbula amurensis *collected from the Southampton Bay. The spectra were collected for the Se content in the gut, and were normalized with respect to the absorption edge of elemental Se (12658 eV). Se XANES spectra of other compounds are also shown for reference.*

8.3.3 Se and Other Trace Element Spatial Distribution

Relative concentration maps were prepared for Cu, Zn, As, Se, Cr, Ti, Ca and Fe in a bivalve tissue sample of *P. amurensis*. The results indicate that Zn, Ca, Cu, Se, and As are concentrated both in the stomach and also in the intestinal tract, while Fe, Ti, Mn, and Cr are concentrated only in the intestinal tract region (Fig. 8.4). Overall, the mantle has much smaller trace element accumulation. This clearly indicates that trace element accumulation is dominant in certain organs of the clam and such distribution may depend on trace element biogeochemical factors such as speciation in the environment, residence time and the clam food ingestion processes and their rates.

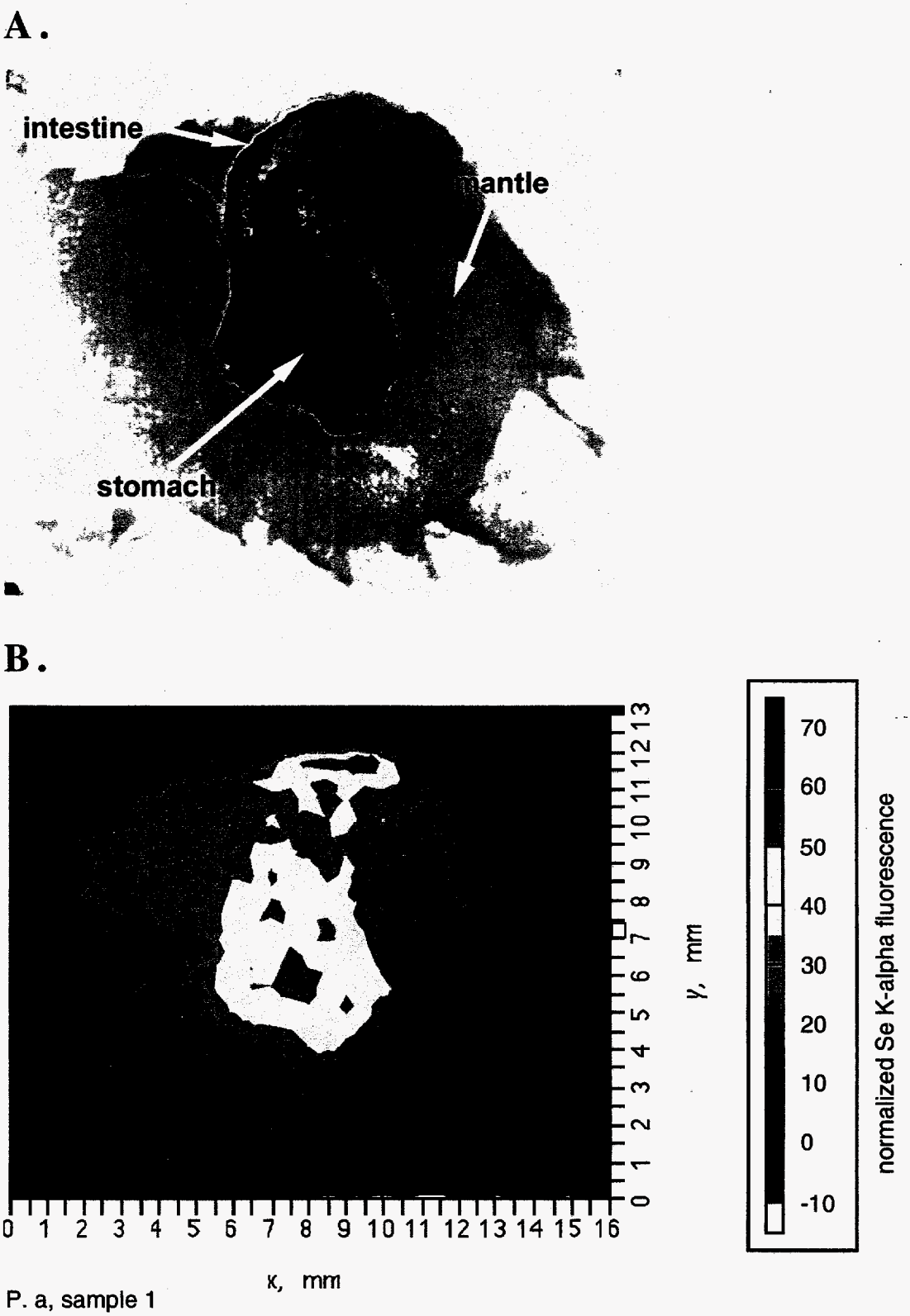

Figure 8.4 (A) Optical micrograph, and (B) X-ray microprobe Se mapping of Potamocorbula amurensis.

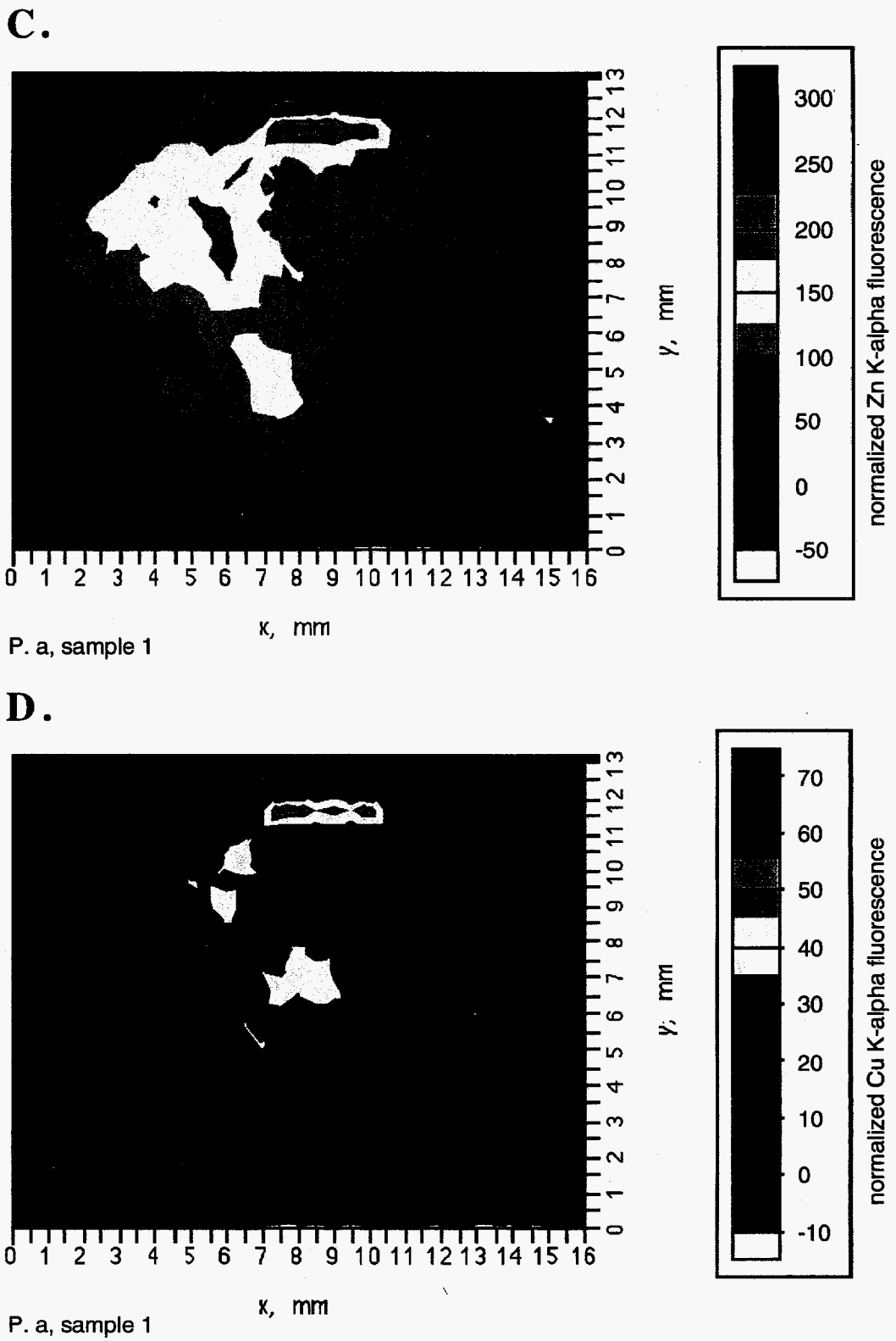

Figure 8.4 (C) X-ray microprobe Zn, and (D) Cu mapping of Potamocorbula amurensis.

E.

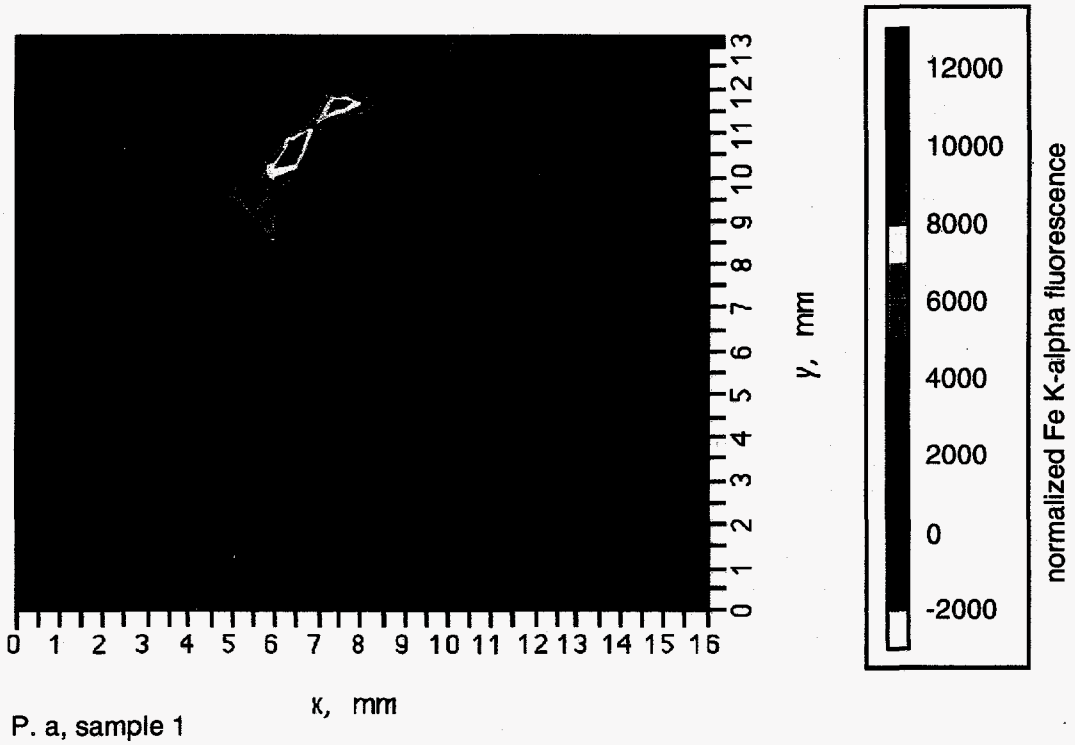

F.

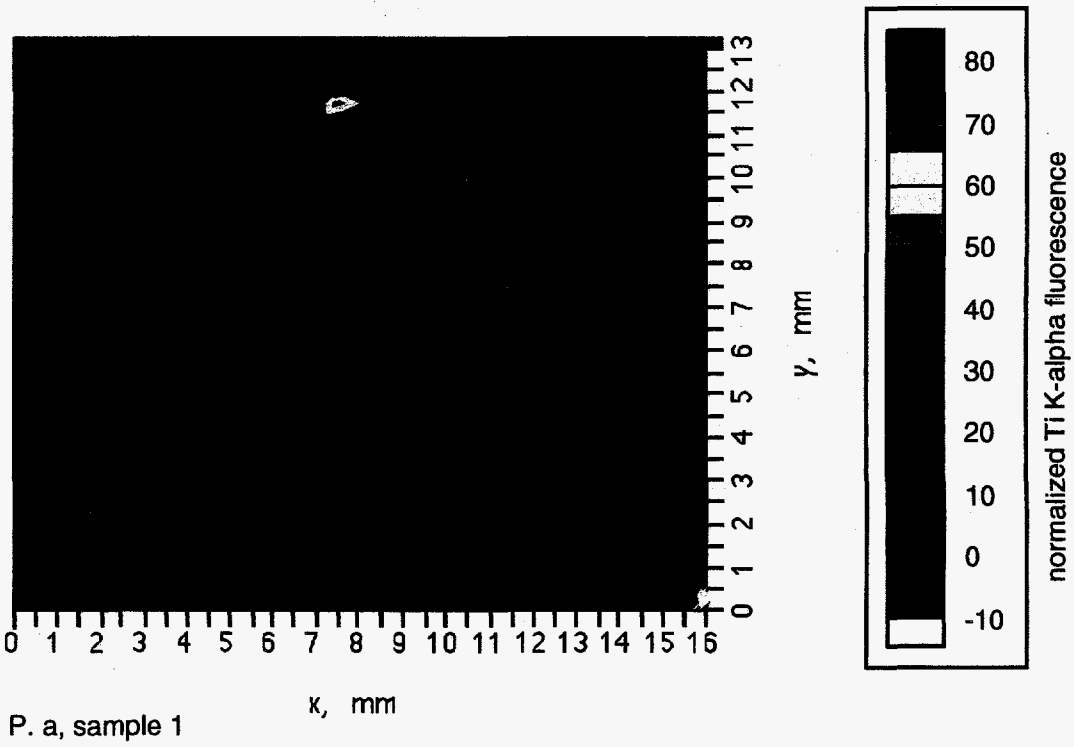

Figure 8.4 (E) X-ray microprobe Fe, and (F) Ti mapping of Potamocorbula amurensis.

8.4 Discussion and Conclusions

The results of this study demonstrate that synchrotron XANES and X-ray microprobe analyses can serve as useful tools for studying trace element uptake and transformations in different organisms. The examined trace elements are non-uniformly distributed in the examined bivalve tissue central organs, and these clearly reflect different micro-scale bio-geochemical processes. For several of the examined elements, the dominant accumulation was in the visceral mass as compared to the mantle or other soft body tissue. Previous controlled experiments on metal uptake by bivalves have indicated that soluble ion uptake produced high metal concentrations in the mantle, whereas metal uptake through sediment ingestion and filter feeding processes produced metal accumulations in the visceral portions (Fowler and Benayoun, 1974; Campbell and Evans, 1991; Winter, 1996). An extremely high accumulation of Se in the gut and the intestinal tract of the bivalve tissue suggests that Se accumulates predominantly from ingestion processes rather than from the consumption of dissolved Se species. Further, the results indicate that Se accumulated in the tissue is present in organic forms, such as Se-cystine, and Se-methionine. Overall, Se speciation of the bivalve tissue does not vary as a function of the type of bivalve species and their location in the Bay (except for the Martinez clams).

Both direct and indirect sediment Se speciation studies indicate that Se(0) is the predominant Se species in the Bay sediments. Even if some organo-Se species are accumulated in the sediment through the deposition of particulates and algal cells, they can be rapidly converted to Se(0) in the presence of Fe(II). For example, recent studies have indicated that seleno-methionine conversion was rapid in anoxic soils, with an apparent first order rate constant of 3.0×10^{-2} day^{-1} (Sarkar and Vance, 1997). Our Se(VI) reduction experiments with Fe(II) and humic acid have also showed no organo-Se species as the predominant products of reduction reaction (Myneni et al., 1996). Hence bivalves dwelling a few centimeters below the sediment-water interface are exposed primarily to inorganic Se, which is later converted to organo-Se compounds after ingestion.

Conversion of Se(0) to organo-Se forms may occur through its substitution reactions for S in amino acids and proteins. Since Se-cystine and Se-methionine appear to be the dominant species in the tissue, Se(0) may directly interact with their S-analogues through an oxidative pathway (Amarathunga and Milne, 1994).

Research is currently in progress to evaluate Se speciation in algae and fish tissue. We expect that in-situ speciation information on the naturally occurring algae in the San Francisco Bay may help provide more conclusive evidence on Se bioaccumulation pathways. This study will help evaluate the relative importance of dissolved species uptake versus sediment ingestion.

9 Analytical Methods

Three variants of hydride-generation atomic absorption spectrometry were used to analyze selenium in surface water, pore water, and variable-matrix liquid extracts of soils and sediments. The methods were compared to each other and the strenghts and weaknesses of each method identified.

9.1 Introduction

The objective of this work was to evaluate a potentially better way of analyzing for ultra-trace level selenium. The liquid nitrogen-hydride generation-atomic absorption spectrometry (LN-HG-AAS) method (Cutter, 1978) is reliable, but has two major drawbacks. These drawbacks are the treatment of glassware to ensure selenium is not absorbed into the glass, the accumulation of water within this system, which leads to Se adsorption, and the small number of samples that can be analyzed in one day. Presently, using the LN-HG-AAS method, a maximum of ten samples can be analyzed in a day. The need for analyzing hundreds of samples for low levels of selenium meant that this would be a significant, labor intensive undertaking. Work by Tao and Hansen (1994) demonstrated an alternative method for analyzing for selenium at low levels. The method could give the same detection limits as the LN-HG-AAS method, but samples could be run by an autosampler. This would allow for samples to be run overnight and up to fifty samples could be run in one day. Therefore, if the Hansen method proved able to handle a seawater matrix, it would be the preferred method for analyzing selenium in the parts-per-trillion range. In this section, the two methods are discussed and results are compared.

9.2 LN-HG-AAS Method

The LN-HG-AAS system developed by Cutter (1978) involves reacting selenium with sodium borohydride in a closed system and analyzing the hydrogen selenide by a flame atomic absorption spectrometer (FLAA). The hydrogen selenide is stripped from the water using helium as a carrier. The helium then travels through two traps. The first trap, a coil, is in isopropanol with dry ice. This trap removes all of the water, hydrochloric acid, and unreacted sodium borohydride that travels on the helium stream,

but is not cold enough to trap the hydrogen selenide. The second trap, U-tube with silanized glass wool, is in liquid nitrogen. This will trap everything, except for the helium, which was not captured in the first trap. After waiting for the selenium to completely react with the sodium borohydride, the U-tube is removed from the liquid nitrogen trap and allowed to warm to room temperature. While the trap comes to room temperature, the hydrogen selenide is liberated from the glass wool and travels to the FLAA. The concentration of selenium is then recorded on an integrator and the concentration is calculated verses a calibration curve in a spreadsheet. This method has a detection limit of 5.0 ng/L for a 100 mL sample. A sketch of the apparatus is included in Fig. 9.1.

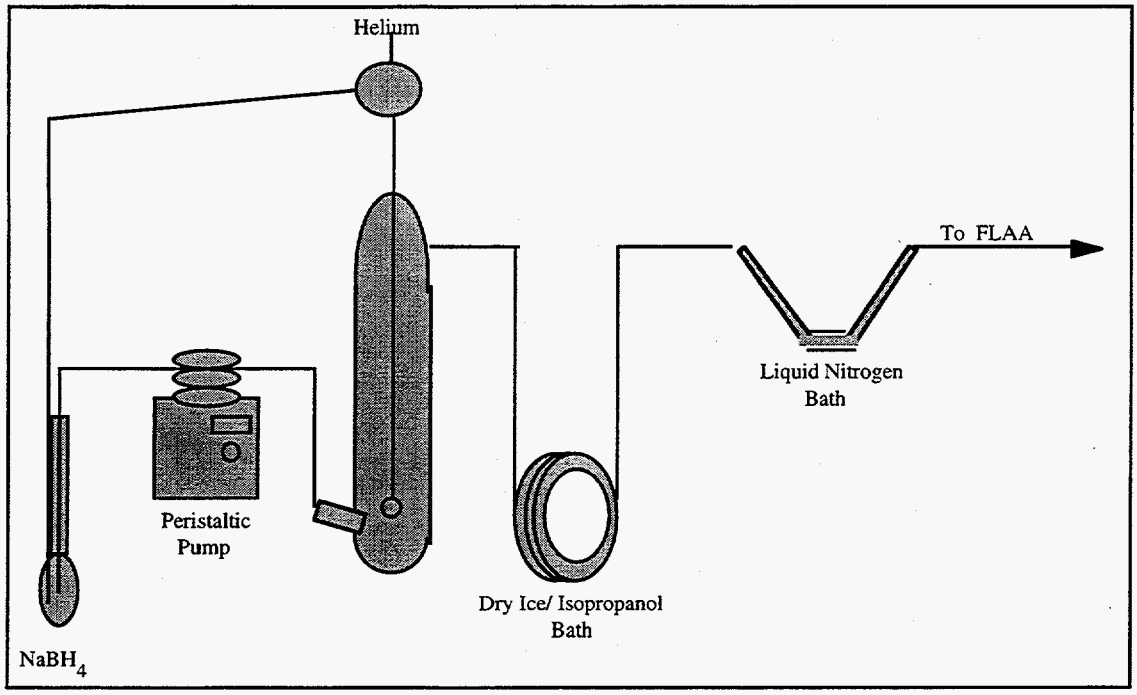

Figure 9.1 Schematic of apparatus for hydrogen selenide trapping (Cutter, 1978).

For a series of samples that have been analyzed, using the LN-HG-AAS method, the reproducibility has been very good. A sample from the Carquinez Strait was analyzed five times. The average for the sample was 1.06 ng of selenium with a standard deviation of 0.05 ng.

A method detection limit study was performed using Carquinez Strait water spiked with 1.0 ng of selenite. The method detection limit calculations was performed following the procedure outlined by the California Department of Health Services. The

method detection limit for seawater is 0.16 ng based on a five sample set. This calculates to a concentration of 4.5 pptr for a 35 mL sample. This does not reflect the actual detection limit but the theoretical detection limit based on the calculation. The reporting detection limit for a 50 mL sample is 10 pptr. This reflects interference that may arise because of medium to high levels of sulfur in the sample.

9.3 Lanthanum Co-Precipitation Method

Tao and Hansen (1994) used an in-line co-precipitation of selenium (IV) with lanthanum hydroxide, and found this method very effective for analyzing low levels of selenium. This method was expected to give detection limits close to the LN-HG-AAS method and allow for more samples to be analyzed using less sample volume and time. The method is based on concentrating selenium (IV) by co-precipitating the selenite with $La(OH)_2$ and collecting the precipitate in a series of knots, called a knotted reactor. Reaction equations for this process are:

$$La(NO_3)_2 + NH_4OH \longrightarrow La(OH)_2 + NH_3 + H^+ + NO_3^-$$

$$2\,La(NO_3)_2 + 2\,NH_4OH + SeO_3^{2-} \longrightarrow La_2(OH)_2(SeO_3) + NH_3 + H^+ + NO_3^-$$

The knotted reactor is then back-flushed with hydrochloric acid. The concentrated selenite reacts with sodium borohydride to form hydrogen selenide. The hydrogen selenide then is analyzed by a flame atomic absorption spectrometer. A Perkin Elmer Flow Injection Accessory, FIAS, controls the peristaltic pumps and a 5-way valve. Fig. 9.2 shows the co-precipitation setup when the system is forming and collecting the $La_n(OH)_m(SeO_4)_o$ precipitate. Fig. 9.3 shows the system back-flushing the reaction coils. The general run conditions for the co-precipitation method are: sample load time of 50 sec, three 1 meter knotted reactors, buffer pH of 9.10, and an argon flow rate of 75 mL/min.

A method detection limit study was performed where deionized water contained 100 ng/L of selenite. The method detection limit calculations was performed following the procedure outlined by the California Department of Health Services. The method detection limit for water was 0.042 ng (3σ). This does not reflect the actual detection limit but the theoretical detection limit based on the calculation. The reporting detection limit for a sample of 9.5 mL is 0.295 ng of selenium. This reflects interference that may arise because of medium to high levels of anions in the sample.

The effect of anions is a very significant and potentially problematic if not corrected for in the final concentration. Correction factors for different anion concentration levels are shown in Table 9.1.

Table 9.1 Correction factors for anion interference in Se analysis using the lanthanum co-precipitation method.

Anion	Correction Factor $(mmol/L)^{-1}$
Chloride	0.0074 %
Sulfate	0.7000 %
Nitrate	0.0300 %
Phosphate	84.000 %

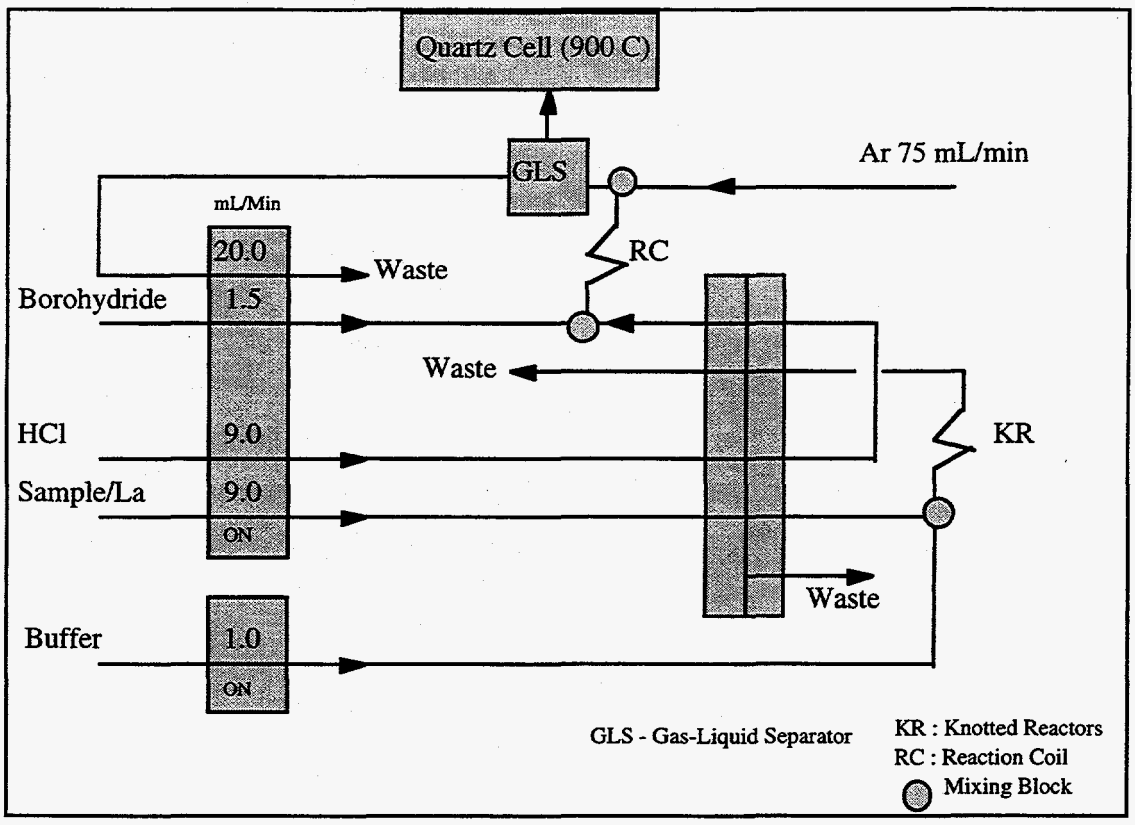

Figure 9.2 Schematic of lanthanum co-precipitation FIAS system during the forming and collecting of the $La_n(OH)_m(SeO_4)_o$ precipitate.

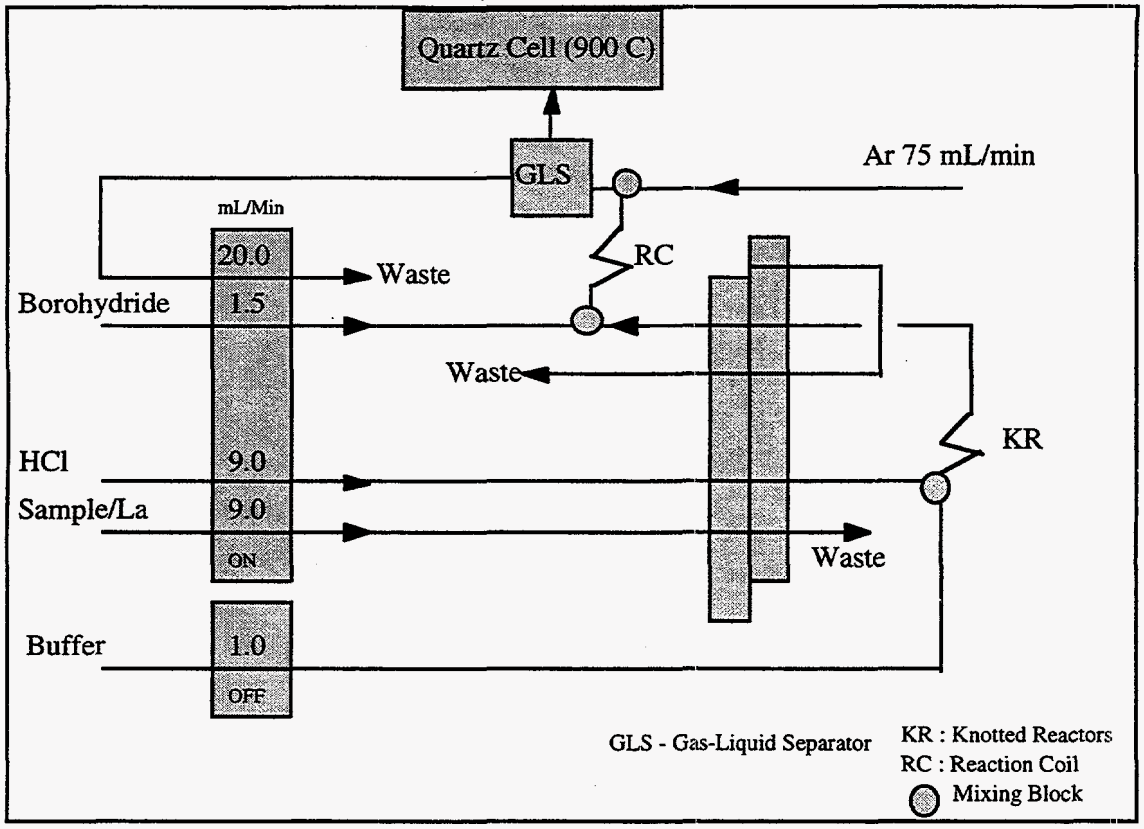

Figure 9.3 Schematic of lanthanum co-precipitation FIAS system during the back-flushing of the reaction coils with HCl.

These values were determined by spiking solutions with known levels of selenite with each of these anions. The amount the signal was suppressed determined the correction factor for that particular anion. Therefore, if 1.0 mmol/L of chloride is present in the sample, then the selenium value was corrected by +0.0074%. This means all samples need to be examined for anion concentrations prior to analysis. From the table, it is apparent that if phosphate is present, selenium cannot be analyzed using this method.

9.4 LN-HG-AAS vs. Co-Precipitation

A direct comparison between the LN-HG-AAS and co-precipitation methods has been performed. Several surface waters were collected over a period of eleven months. Table 9.2 summarizes the data.

Based on this data the two methods generally agree with each other. The co-precipitation data reflects adjustments made after ion chromatography was performed

on the samples. The anions present are chloride and sulfate. A DIONEX HPLC with a suppresser and conductivity detector was used to perform the ion chromatography. Other anions which were analyzed for were: fluoride, nitrite, bromide, nitrate, and phosphate.

Table 9.2 Comparison of Se analysis results obtained using the lanthanum co-precipitation and LN-HGAAS methods.

Sample ID	[Se] via co-precipitation ($ng\ L^{-1}$)	*[Se] via LN-HG-AAS* ($ng\ L^{-1}$)	RPD
11/17/95 MRP Pier	341	254	29
12/12/95 MRP	77	73	5
12/20/95 MRP	306	208	38
1/3/96 MRP	171	102	51
3/20/96 SPM	347	232	40
4/8/96 SPM	223	273	20
5/1/96 SPM	256	241	6
6/3/96	218	196	11
9/19/96	208	219	5
10/9/96 San Joaquin	619	420	38
10/16/96 MRP	218	218	0

MRP: Martinez Regional Park
SPM: Suspended Particulate Matter
RPD: Relative Percent Difference

9.5 HG-AAS vs. Co-Precipitation

As part of a microcosm experiment, a set of sediment pore waters and surface waters was collected just above the sediment and were analyzed by hydride-generator-flame atomic absorption spectrometry, HG-AAS, and the La co-precipitation method. The results of these analyses are shown in Table 9.3.

It is apparent the two methods are not in agreement for all the mudflat samples and most of the upper marsh samples. The comparison is somewhat suspect because the detection limit for the HG-AAS method is 0.32 mg/L for a simple matrix. Therefore, for a better evaluation some of the samples above need to be analyzed by the LN-HG-AAS method to determine if whether HG-AAS values or the co-precipitation method numbers are correct. If the LN-HG-AAS method agrees with the co-precipitation

method then it would be definitive proof that the co-precipitation method is capable of handling a seawater matrix.

Table 9.3 Comparison of Se analysis results obtained using the lanthanum co-precipitation and HGAAS methods.

Sample ID	*[Se] via co-precipitation* ($\mu g\ L^{-1}$)	[Se] via HG-AAS ($\mu g\ L^{-1}$)	RPD	Type
2	0.284	1.012	112.3	2
3	0.149	0.836	139.5	2
4	0.112	0.902	155.8	2
5	0.142	1.100	154.3	2
11	0.410	0.924	77.1	2
13	0.127	0.528	122.4	2
6	0.120	0.924	154.0	1
7	0.492	1.364	94.0	1
9	0.463	0.902	64.3	1
10	0.418	1.034	84.8	1
12	0.343	0.528	42.5	1
14	0.209	0.440	71.2	3
16	0.559	0.418	28.9	3
17	0.336	0.396	16.4	3
18	0.426	0.506	17.2	3
20	0.471	0.660	33.4	3
21	0.478	0.550	14.0	3
22	0.426	0.418	1.9	3
23	0.471	0.616	26.7	3

Types are defined as:
1: Pore/surface water from the upper marsh,
2: Pore water from the mudflats, and
3: Pore water from the upper marsh.

9.6 Summary

After careful examination of two methods for low level selenium analysis, certain advantages and disadvantages of the LN-HG-AAS and co-precipitation methods become apparent. The LN-HG-AAS method is not affected by high salt content and is

accepted as a method for measuring selenium in seawater matrices. The disadvantages of the LN-HG-AAS method is the length of time required to analyze a sample and the need to frequently treat glassware because of heavy exposure to hydrochloric acid. The advantages of the co-precipitation method are that many samples can be analyzed in a day, using a small sample size, and it can be easily set up and maintained. The disadvantages are the interference of high salt concentration with the co-precipitation and the need to perform ion chromatography on every sample prior to analysis. Both methods have very good sensitivity and reproducibility. The need to reanalyze the pore water samples with the LN-HG-AAS method is critical to complete the evaluation of the co-precipitation method. Samples from an agricultural region may contain phosphate and are therefore not analyzable using the co-precipitation method. Otherwise, both methods have been demonstrated to be able to measure low levels of selenium in a seawater matrix.

10 Summary, Implications, and Future Work

Research described in this report was designed to address questions regarding processes which affect the biogeochemical cycling of Se in estuarine wetlands. As is commonly the case, it has given rise to a number of new questions and identified areas which require further investigation. Nonetheless, our understanding of the Se cycle in this environment has been significantly enhanced.

10.1 Summary of Findings

- Total sediment Se concentrations are highest in the marsh plain, the most inland part of the system, which is inundated for the shortest amount of time per day, on the order of 4 hr. The lowest concentrations were observed in the mudflats, or the part of the system which is most frequently flooded, as much as 18 hr each day. Se concentrations in the marshes are generally between 1 and 1.25 mg/kg, while those in the mudflats are between 0.5 and 1 mg/kg. The most notable feature of this distribution is that sediment Se concentrations in the mudflats are lower than Se concentrations on suspended sediments in the water column while those in the marshes fall in the SPM-Se range.

- In all environments elemental Se (Se(0)) is the predominant species (47 to 53%). Residual Se is relatively high in the marsh plain (26%) but declines to 7% in the mudflats; this decline is correlated with the decline in C, suggesting that residual Se may in fact be associated with complex organic matter, probably more resistant plant components, such as lignin. The organically-associated Se fraction is not species-specific, in that it could represent any type of Se association with soil organic matter, even adsorption. It comprises between 23% and 32% of total. Of particular interest are the relatively low concentrations of soluble Se, at or below 1% of total.

- Se concentrations in interstitial water found near the sediment-water interface exceed those found in overlying waters by 1 to 2 orders of magnitude, with the highest values in the top 1-2 cm of the mudflat sediment and in the marsh plain. Together with the speciation results from suspended sediments, this suggests that Se is being

solubilized *in-situ*. Such an upward soluble Se gradient may cause Se to diffuse into the overlying Bay water. A rough estimate of potential Se loss due to diffusive flux, based on Fick's Law, falls in the range of 0.3-0.4 $mg/m^2/yr$ which is about a half to one order of magnitude less than the sedimentary Se input.

- Concentrations of Se associated with suspended particulates (SPM-Se) agree with previous measurements for surface water sampled in the Carquinez Strait, with most values between 1 and 1.5 mg/kg. Total Se in SPM increases with decreasing SPM concentration. SPM-Se is moderately well correlated with carbon, suggesting that the biological component of SPM, such as plankton, may play an important role in Se sequestration. Surprisingly, adsorbed Se was found to be a minor fraction (<5%) of SPM-Se. Preliminary results show that SPM-Se is inefficiently extracted by the sequence developed for soils (78% residual Se). While the reasons for such low efficiency are under investigation, one could hypothesize that it is due to the inability of the procedure to disrupt live cells. If this is the case, then biogenic-Se may dominate SPM-Se.

- Preliminary data collected from sediment traps shows that sedimentation rates are highest in the mudflats and at the mudflat/lower marsh boundary. Se concentrations show the opposite trend, with concentrations above 1 mg/kg in the marsh plain and around 0.5 mg/kg in the mudflats, concentrations which coincide with sediment core data. The marked increase in total C in the particulates trapped in the marsh plain indicates a high organic component. The landward increase in Se concentration on trapped sediments may be indicative of a size-separation of particulates in the wetlands system. As seen from the sedimentation/erosion patterns, the mudflats are a high-energy regime in which tidal action and wind gusts can produce resuspension and also maintain coarser particles in suspension. Ongoing work on the size-composition of particulates trapped in different regimes will shed further light on this issue. On the other hand, the low marsh and marsh plain environments are lower and lowest energy environments in the wetlands, respectively. A comprehensive set of samples collected over at least a 12 month period is needed for a complete interpretation of sediment-Se dynamics, but the implication so far is that sediment deposition patterns are very important in Se distribution.

- A preliminary estimate of the sediment-Se flux into the marsh can be made. Based on the range of sedimentation rates observed in the marsh, and the concentration of Se on the settling particulates, sediment-Se deposition in the marsh ranges from less than 1 mg m^{-2} yr^{-1} in the most upland parts of the marsh plain, to 7 mg m^{-2} yr^{-1} in the lower marsh, although most values fall at or below 3 mg m^{-2} yr^{-1}. Even though the marsh is much less dynamic than the mudflats, there is the possibility of sediment redistribution at different times of year, and this analysis will not be complete until 12 months of data are collected and processed.

- Aboveground plant tissue generally contains low Se concentrations, approximately 0.1 μg g^{-1}, while belowground concentrations are up to an order of magnitude higher. Combined with the fact that the belowground biomass is likely much greater than the aboveground biomass, especially in the marsh plain, roots and rhizomes may be important links in the Se cycle, especially in the redistribution of dissolved Se in the root zone and incorporation of selenate and selenite into plant tissue. Such incorporation undoubtedly leads to the formation of organo-Se compounds, thereby affecting the overall speciation and bio-availability of Se in the marsh sediment. The litter bag study has identified decaying plant litter as a surface for Se immobilization, probably due to adsorption. Further work is needed to quantify this process, its kinetics, and its long-term effects on Se accumulation in the marsh. It may be difficult to estimate the degree to which the decomposed plant material is incorporated into the underlying sediment.

- Microcosm experiments provide evidence that immobilization of Se from the water column occurs only under conditions characterized by extended ponding of the intertidal environment, either during very high tide or as a result of stagnant conditions in topographic lows. Such reduction is far more likely in the marsh where organic carbon is abundant at the sediment-water interface, as is plant litter which may provide additional sorption and/or reducing sites. Although the exact rates of Se reduction and immobilization under these conditions are extremely difficult to measure due to the very low fluxes over a tidal cycle, it is likely that this is a process of secondary importance in terms of Se input into the sediments, as compared with particulate-Se fluxes.

- Development of purification and analytical techniques has resulted in the first ever application of environmental Se isotope ratios. The procedures developed in this study will enable further application of this technique toward increased understanding of Se cycling in various systems. Small isotopic differences observed between Se in Bay water and Se on marsh sediments can be explained by a cycling model in which Se is concentrated in the marshes not by open-system chemical reduction, but by sedimentation effects. The processes by which Se becomes bound to sediment and then deposited in marsh and mudflat sediments need not fractionate the isotopes. Thus, the isotope ratio results support the conclusions of other parts of this study, which suggest that sedimentation is the dominant mode of Se deposition in the marshes.

- Synchrotron XANES and X-ray microprobe analyses have proven to be useful tools for studying Se uptake and transformations in clam tissue. An extremely high accumulation of Se in the gut and the intestinal tract of the bivalve tissue suggests that Se accumulates predominantly from ingestion processes rather than from the consumption of dissolved Se species. Further, the results indicate that Se accumulated in the tissue is present in organic forms, such as Se-cystine, and Se-methionine. Overall, Se speciation of the bivalve tissue does not vary as a function of the type of bivalve species and their location in the Bay. Both direct and indirect sediment Se speciation studies indicate that Se(0) is the predominant Se species in the Bay sediments. Hence bivalves dwelling a few centimeters below the sediment-water interface are exposed primarily to inorganic Se, which is later converted to organo-Se compounds after ingestion.

10.2 Implications

All of the available data tend to favor a Se cycling hypothesis in which the accumulation of Se in estuarine wetlands is influenced by sedimentation dynamics, suspended particulates, diffusive fluxes, and to a lesser degree, reduction-oxidation cycles in very shallow soils and sediments. This hypothetical cycle does not address the fate of Se in geologic time, i.e., changes resulting from diagenesis, although the effect of diagenetic processes on present-day Se concentrations, specifically in interstitial water, should not be disregarded. The predominant processes are shown schematically in Fig. 10.1.

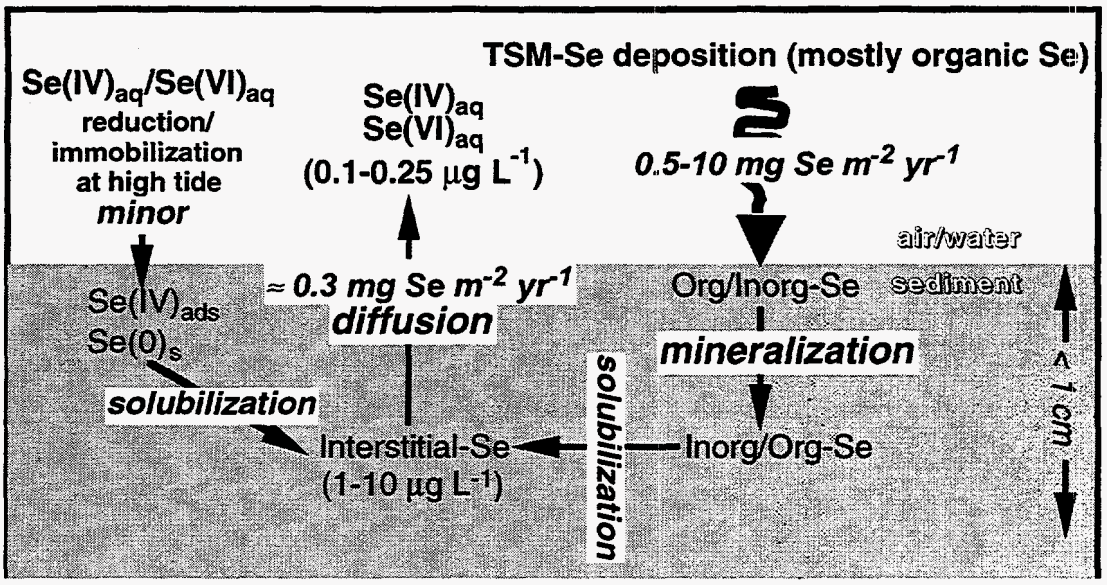

Figure 10.1 Conceptual diagram of the selenium cycle near the water-sediment interface in an estuarine environment. Ranges of measured Se concentrations and estimates of Se fluxes are shown.

The ecological significance of such a cycle in an anthropogenically-affected environment is considerable, given the primary exposure pathways with respect to Se in estuarine wetlands. As discussed earlier, tissue-Se concentrations in bivalves, which are a major part of waterfowl diet, are closely related to particulate-Se levels. The relatively lower sediment-Se concentrations in mudflats are encouraging, since the mudflats are primary feeding grounds for wading birds. Given the relatively slow mean sedimentation rates, it is doubtful that changes in Se levels in the Carquinez Strait waters would result in a noticeable decrease in sedimentary-Se in estuarine wetlands over periods of 10 to 50 years. Therefore, benthic organisms which are primarily sediment filter-feeders are likely to be subjected to similar Se concentrations over fairly long periods of time, regardless of Se level in ambient water. On the other hand, organisms which feed primarily on phytoplankton would be subjected to lower Se in their diet should Se concentrations in the Carquinez Strait water decline.

Finally, the implications of an upward gradient in soluble Se from the interstitial water into Bay water need to be considered. If Se is continually solubilized in the sediment column, there appears to be a long-term source for soluble-Se to the overlying water. The assumptions made in the hypothesis discussed herein are rather conservative, as no advective mixing of tidal waters with interstitial waters was assumed. Inasmuch as some mixing is inevitable in this highly dynamic hydrologic

system, exchange of soluble Se may occur on a more rapid scale and diffusion may be a flux of secondary importance. The overall net flux to the water column may be small in comparison to fluxes of SPM-Se, but the effect on Se concentrations at the sediment-water interface may be significant. Since much of the biological activity of concern transpires at the sediment-water interface, it is there that Se levels need to be monitored, in order to assess the effects of changes in dissolved- and particulate-Se levels in the Carquinez Strait.

10.3 Future Work

The results presented herein provide a framework for both a Se cycling model and future studies to refine that model. It is necessary to improve the existing semi-quantitative notion of an estuary-scale Se mass balance, and quantify the fraction of the Se influx which remains in the Bay. In order for this to be possible, the magnitude and direction of Se fluxes into and out of sediments need to be established, especially since processes at the sediment-water interface are of biological importance. Further laboratory work on Se mineralization and solubilization in the sediment could shed light on the time scales required to effectively reduce Se concentrations at the interface. The bio-availability of Se on suspended particulates as well as the ecological risks associated with observed Se concentrations on sediment need to be established.

11 References

Amarathunga W., and Milne J. 1994. Studies on the interaction of selenite and selenium with sulphur donors. Part 2. A kinetic study of the reaction with mercaptoethanol. Can. J. Chem. 72:2506-2515.

Anderson, J.U. 1963. An improved pretreatment for mineralogical analysis of samples containing organic matter. Clays and Clay Minerals. 10:380-388.

Bacon, J.R., and D.C. Bain. 1995. Characterization of environmental water samples using strontium and lead isotope compositions. Environ. Geochem. Health. 17:39-49.

Bajt S., Sutton S. R., Delaney J. S. 1994. X-ray microprobe analysis of iron oxidation states in silicates and oxides using X-ray absorption near edge structures (XANES). Geochim. Cosmochim. Acta 58, 5209-5214.

Balistrieri L.S. and T.T. Chao. 1987. Selenium adsorption by goethite. Soil Sci. Soc. Am. J. 51:1145-1151.

Bellis, V.J., and A.C. Gaither. 1985. Seasonality and aboveground and belowground biomass for six salt marsh species. J. Elisha Mitchell Sci. Soc. 101:95.

Besser J.M., Canfield T.J., and La Point T. W. 1993. Bioaccumulation of organic and inorganic selenium in a laboratory food chain. Environ. Toxicol. Chem. 12:57-72.

Bohn, H.L. 1971. Redox potentials. Soil Science. 112:39-45.

Bottino N. R., Banks C. H., Irgolic K. J., Micks P., Wheeler A. E., Zingaro R. A. Selenium containing amino acids and proteins in marine algae. 1984. Phytochemistry. 23, 2445-2452.

Brown, C.L. and S.N. Luoma. 1995. Use of the euryhaline bivalve *Potamocorbula amurensis* as a bioessential species to assess trace metal contamination in San Francisco Bay. Mar. Ecol. Prog. Ser. 124:129-142.

Brown Jr. G.E., G. Calas, G.A. Waychunas, and J. Petiau. 1988. In Spectroscopic Methods in Mineralogy and Geology. Ed. F.C.Hawthrone. Rev. in Mineral. 18, Mineral. Soc. Am. 431-512.

Bullen, T.D. and J.B. Shanley. 1994. Sr and Pb isotopes as surrogate tracers of water flowpaths in a forested catchment. EOS, Transact., Amer. Geophys. Union. 75:144.

Campbell, J. and Evans D. 1991. Cadmium concentrations in the fresh water mussel (*Ellipto complanata*) and their relationship to water chemistry. Arch. Environ. Contam. Toxicol. 20: 125-131.

CDFG: California Department of Fish and Game. 1988. Selenium Verification Study. 1986-1987. (CDFG, Sacramento, CA).

CDFG. 1989. Selenium Verification Study. 1987-1988. (CDFG, Sacramento, CA).

Chau, Y.K., and Riley, J.P. 1965. The determination of selenium in sea water, silicates, and marine organisms. Anal. Chim Acta. 33:36-49.

Childers, D.L., F.H. Sklar, B. Drake, and T. Jordan. 1993. Seasonal measurements of sediment elevation in three mid-Atlantic estuaries. Jour. of Coastal Res. 9:986-1003.

Cutter, G.A. 1978. Species determination of selenium natural waters. Analytica Chimica Acta, 98: 59-66.

Cutter, G.A. 1985. Determination of selenium speciation in biogenic particles and sediments. Anal. Chem. 57:2951-2955.

Cutter, G.A. 1989. The estuarine behaviour of selenium in San Francisco Bay. Estuar. Coast. Shelf. Sci. 28:13-34.

Cutter, G.A., and T.J. Oats. 1987. Selenium speciation in estuarine waters. Analytical Chemistry 59: 717-720.

Cutter, G.A., and M.L.C. San Diego-McGlone. 1990. Temporal variability of selenium fluxes in San Francisco Bay. Sci. Total Environ. 97/98:235-250.

Dixon, J.B. and S.B. Weed. 1989. Minerals in Soil Environments. Soil Science Society of America, Madison, WI.

Dowouna, G.N., A.R. Mermut, and H.R. Krouse, Stable isotope geochemistry of sulfate in relation to hydrogeology in southern Saskatchewan, Canada, Appl. Geochem, 8, 255-263, 1993.

Eugster, O., F. Tera, and G.J. Wasserburg. 1969. Isotopic analyses of barium in meteorites and in terrestrial samples. J. Geophys. Res. 74:3897-3908.

Faure, G. 1986. Principles of isotope geology. John Wiley and Sons, New York, 589 pp.

Fontes, J.-C., Fritz, P., Louvat, D., Michelot, J.-L. 1989. Aqueous sulphates from the Stripa groundwater system, Geochim. Cosmochim. Acta, 53:1783-1789.

Fowler S.W., and Benayoun G. 1976. Accumulation and distribution of selenium in mussel and shrimp tissues. *Mar. Biol.* **37**. 59-68.

Ganje and Page. 1974. Rapid acid dissolution of plant tissue for cadmium detrmination by atomic absorption spectrometry. Atomic Absorb. Newsl. 13:131-134.

Ganther H. E. 1974. Biochemistry of selenium. In: Zingaro RA and Cooper WC (Eds). Selenium. Van Nostrand Pub. New York.546-614.

Gilbert, G.K. 1917. Hydraulic mining debris in the Sierra Nevada. U.S.G.S. Professional Paper 105.

Gissel-Nielsen, G. 1979. Uptake and translocation of ^{75}Se in *Zea mays*. In, Isotopes and radiation in research on soil-plant relationships. IAEA Vienna. 427-436.

Gruebel, K.A., J.A. Davis, and J.O. Leckie. 1988. The feasibility of using sequential extraction techniques for arsenic and selenium in soils and sediments. Soil Sci. Soc. Am. J. 52:390-397.

Harrison, E.Z. and A.L. Bloom. 1977. Sedimentation rates on tidal salt marshes in Connecticut. Journal of Sedimentary Petrology. 47:1484-1490.

Hayes, M.H.B. 1994. Chapter 2, Methods for the extraction of humic substance. *In* Humic substances II, (M.H.B. Hayes Ed.). Marcel Dekker, London, pp. 845.

Hayes, K.F., A.L. Roe, G.E. Brown, Jr., K.O. Hodgsen, J.O. Leckie, and G.A. Parks. 1987. In situ x-ray absorption study of surface complexes: Selenium oxyanions on α-FeOOH. Science 238:783-786.

Johns, C., S.N. Luoma, and V. Elrod. 1988. Selenium accumulation in benthic bivalves and fine sediments of San Francisco Bay, the Sacramento-San Joaquin Delta, and selected tributaries. Estuarine, Coastal and Shelf Science 27:381-396.

Kendall, C., S.R. Silva, C.C. Chang, D.H. Campbell, D.A. Burns, J.B. Shanley. 1994. Use of oxygen and nitrogen isotopes to trace sources of nitrate in hydrologic systems. EOS, Transact., Amer. Geophys. Union. 75:144.

Krouse, H.R. and H.G. Thode. 1962. Thermodynamic properties and geochemistry of isotopic compounds of selenium. Canad. J. Chem. 40:367-375.

Lavkulich, L.M. and J.H. Wiens. 1970. Comparison of organic matter destruction by hydrogen peroxide and sodium hypochlorite and its effects on selected mineral constituents. Soil Sci. Soc. Amer. Proc. 34:755-758.

Light, T.S. 1972. Standard solution for redox potential measurement. Anal. Chem. 44:1038-1039.

Lipton, D.S. 1991. Associations of selenium with inorganic and organic constituents in soils of a semi-arid region. Ph.D. thesis. University of California at Berkeley.

Luoma, S., C. Johns, N. Fisher, N. Steinberg, R. Oremland, and J. Reinfelder. 1992. Determination of selenium bioavailability to a benthic bivalve from particulate and solute pathways. Environ. Sci. Tech. 26:485:491.

Luoma, S.N., R. Linville, G. Cutter, L. Cutter, B.-G. Lee, C. Brown. 1996. Distribution, fate and effects of selenium and related contaminants in North San Francisco Bay/Delta and its benthic food web. Progress Report to San Francisco Bay Regional Water Quality Control Board. November 1996.

Masscheleyn, P.H., R.D. Delaune, and W.H. Patrick. 1990. Transformations of selenium as affected by sediment oxidation-reduction potential and pH. Environ. Sci. Technol. 24:91-96.

McNaughton, S.J. 1966. Ecotype function in the *Typha* community type. Ecol. Monogr. 36:297.

Morel F. and Hering J.G. 1993. Principles and Applications of Aquatic Chemistry. Wiley Inter Science.

Myneni S.C.B., Brown Jr., G.E., Tokunaga T.K. 1996. Heterogeneous redox chemistry in the presence of Fe(II,III) oxides and Fe(0). SSRL Activity Report. (In print).

Neal, R.H. and G. Sposito. 1989. Selenate adsorpiton on alluvial soils. Soil Sci. Soc. Am. J. 53:70-74.

Neal, R.H., G. Sposito, K.M. Holtzclaw, and S.J. Traina. 1987. Selenite adsorption on alluvial soils: I. Soil composition and pH effects. Soil Sci. Soc. Am. J. 51:1161-65

Ogden Beeman and Associates, Inc. 1992. Sediment budget study for San Francisco Bay. Prepared for Corps of Engineers, San Francisco District.

Ohmoto, H., Stable isotope geochemistry of ore deposits, in Stable Isotopes in High Temperature Geological Processe, J.W. Valley, H.P. Taylor, Jr., and J.R. O'Neil, eds., Reviews in Mineralogy, Vol. 16, Mineralogical Society of America, Washington, D.C., 1986.

Orson, R.A., R.L. Simpson, and R.E. Good. 1990. Rates of sediment accumulation in a tidal freshwater marsh. J. Sed. Petrol. 60:859-869.

Pethick, J.S. 1981. Long-term accretion rates on tidal salt marshes. Journal of Sedimentary Petrology, 1981. 51:571-577.

Pethick, J.S. 1992. *in* Saltmarshes: Morphodynamics, Conservation, and Engineering Significance, J.R.L. Allen and K. Pye eds., Cambridge, Cambridge University Press.

Pickering, I. J., G.E. Brown Jr., and T.K. Tokunaga. 1995. Quantitative Speciation of Selenium in soils using X-ray Absorption Spectroscopy. Env. Sci. Tech., V 29, 2456-2459.

Presser, T.S., and H.M. Ohlendorf. 1988. Biogeochemical cycling of selenium in the San Joaquin Valley, California, USA. Environ. Management. 11:6.

Rajan, S.S.S., and J.H. Watkinson. 1976. Adsorption of selenite and phosphate on an allophane clay. Journal of the Soil Science Society of America. 40: 51-54.

Rashid, K., H.R. Krouse, and R.G.L. McCready. 1978. Selenium isotope fractionation during bacterial selenite reduction. In Fourth Intl. Conf., Geochron., Cosmochron., Isotope Geol., U.S. Geol. Survey Open-file Rep., 78-701:347-348.

Russell, W.A., D.A. Papanastassiou, and T.A. Tombrello. 1978. Calcium isotope fractionation on the earth and other solar system materials. Geochim. Cosmochim. Acta, 42:1075-1090.

Sarkar S., and Vance G. F. 1997. Kinetics of selenomethionine disappearance from reclaimed coal mine soils of Wyoming, U. S. A. Environ. Geol. 29:203-208.

Schaller, G., and W.R. Fischer. 1981. The use of antimony electrodes for pH measurements in soils. Z. Pflanzenernaehr. Bodenk. 144:197-204.

Schnitzer, M. 1982. Organic matter characterization. p.581-594. In A.L. Page et al. (ed.) Methods of soil analysis. Part 2. 2nd ed. Agron. Monogr. 9 ASA and SSSA, Madison, WI.

Schoellhamer, D.H. 1996. Factors affecting suspended-solids concentrations in South San Francisco Bay, California. Jour. Geophys. Res. 101:12,087-12,095.

Schubauer, J.P. and C.S. Hopkinson. 1984. Above- and belowground emergent macrophyte production and turnover in a coastal marsh ecosystem. Georgia. Limnol. Oceanogr. 29:1052.

Schuler, C.A., G.R. Anthony, and H.M. Ohlendorf. 1990. Selenium in wetlands and waterfowl foods at Kesterson Reservoir, California, 1984. Arch. Environ. Contam. Toxicol. 19:845-853.

SFBRWQCB (San Francisco Bay Regional Water Quality Control Board). 1992. Mass emissions reduction strategy for selenium. Staff report.

Smith, C.S., M.S. Adams, T.D. Gustavson. 1988. The importance of belowground mineral element stores in cattails (*Typha latifolia* L.). Aquat. Bot. 30:343.

Sposito, G. 1984. The surface chemistry of soils. Oxford University Press, New York. pp. 234.

Sposito, G. 1989. The chemistry of soils. Oxford University Press, New York. pp. 277.

Stadtman T. C. 1990. Selenium biochemistry. Annu. Rev. Biochem. 59. 111-127.

Stoddart, D.R., D.J. Reed, and J.R. French. 1989. Understanding salt-marsh accretion, Scolt Head Island, Norfolk, England. Estuaries 12:228-236.

Stumpf, R.P. 1983. The process of sedimentation on the surface of a salt marsh. Estuar. Coast. Shelf Sci. 17:495-508.

Stumm, W. and J.J. Morgan. 1981. Aquatic Chemistry. Second Addition. Wiley-Interscience, New York, NY.

Sutton, S.R., S. Bajt, J. Delaney, D. Schulze, and T. Tokunaga. 1995. Rev. Sci. Instrum. 66. 1464-1467.

Tanzer, D., and K.G. Heumann. 1991. Determination of dissolved selenium species in environmental water samples using isotope dilution mass spectrometry. Anal. Chem. 63:1984-1989.

Tao, G. and E. H. Hansen. 1994. Determination of ultr-trace amounts of selenium (IV) by flow injection hydride generation atomic absorption spectrometry with on-line preconcentration by coprecipitation with lanthanum hydroxide. Analyst, 119: 333-337.

Tessier, A., P.G.C. Campbell, M. Bisson. 1979. Sequential extraction procedure for the speciation of particulate trace metals. Analytical Chemistry. 51(7): 844-851.

Toivonen, H., and T. Lappalainen. 1980. Ecology and production of aquatic macrophytes in the oligotrophic, mesohumic lake Suomunjarvi, eastern Finland. Ann. Bot. Fennici. 17:69.

Tokunaga, T.K. 1997. Selenium partitioning in ephemeral pools: A laboratory study. Submitted to Soil Sci. Soc. Am. J.

Tokunaga, T.K., D.S. Lipton, S.M. Benson, A.Y. Yee, J.M. Oldfather, E.C. Duckart, P.W. Johannis, and K.H. Halvorsen. 1991. Soil selenium fractionation, depth profiles and time trends in a vegetated site at Kesterson Reservoir. Water, Air, and Soil Pollut. 57-58:31-41.

Tokunaga, T.K, P.T. Zawislanski, P.W. Johannis, S. Benson, and D.S. Lipton. 1994a. Field investigations of selenium speciation, transformation, and transport in soils from Kesterson

Reservoir and Lahontan Valley. In, Selenium in the Environment. W.T. Frankenberger and S. Benson, eds. Marcel Dekker. New York. pp. 119-138.

Tokunaga, T.K, S.R. Sutton, and S. Bajt. 1994b. Mapping of selenium concentrations in soil aggregates with synchrotron X-ray fluorescence microprobe. Soil Science. 158:421-434.

Tokunaga, T.K, I.J. Pickering, and G.E. Brown. 1996. Selenium transformations in ponded sediments. Soil Sci. Soc. Am. J. 60:781-790.

Tuttle, M.L. and M.B. Goldhaber, Sedimentary sulfur geochemistry of the Paleogene Green River Formation, western USA: Implications for interpreting depositional and diagenetic processes in saline alkaline lakes, Geochim. Cosmochim. Acta, 57, 3023-3039, 1993.

Van Stempvoort, D.R., P. Fritz, and E.J. Reardon, Sulfate dynamics in upland forest soils, central and southern Ontario, Canada: Stable isotope evidence, Appl. Geochem., 7, 159-175, 1992.

Van Stempvoort, D.R., M.J. Hendry, J.J. Schoenau, H.R. Krouse, Sources and dynamics of sulfur in weathered till, Western Glaciated Plains of North America, Chem. Geol., 111, 35-56, 1994.

Velinsky, D.J. and G.A. Cutter. 1990. Determination of elemental Se and pyrite-Se in sediments. Analytica Chimica Acta, 235:419-425.

Vymazal, J. 1995. Algae and Element Cycling in Wetlands. Lewis Publishers. Boca Raton,.Florida. 689 pp.

Wachsmann, M., and K.G. Heumann. 1992. Negative thermal ionization mass spectrometry of main group elements. Part 2. 6th group: sulfur, selenium, tellurium. Intl. J. Mass Spectrom. Ion Proc. 114:209-220.

Webster, C.L., Selenium isotope analysis and geochemical applications, unpublished Ph.D. Dissertation, Colorado State University, Fort Collins, CO, 74 pp., 1972.

Weres, O., A.-R. Jaouni, and L. Tsao. 1989. The distribution, speciation and geochemical cycling of selenium in a sedimentary environment, Kesterson Reservoir, California, U.S.A. Applied Geochemistry 4:543-563.

Westre T.E., Kennepohl P., DeWitt J.G., Hedman B., Hodgson K.O., Solomon E.I. 1997. A multiplet analysis of Fe K-edge 1s→3d pre-edge features of iron complexes. J. Am. Chem. Soc. 119. 6297-6314.

White, D.A, T.E. Weiss, J.M. Trapani, and L.B. Thien. 1978. Productivity and decomposition of the dominant salt marsh plants in Louisiana. Ecology. 59:751.

Whigham, D.F., and R.L. Simpson. 1978. The relationship between aboveground and belowground biomass of freshwater tidal wetland macrophytes. Aquat. Bot. 5:535.

White, D.A., and J.M. Trapani. 1982. Factors influencing the disappearance of *Spartina alterniflora* from litter bags. Ecology 63:242-245.

Winter, S. 1996. Cadmium uptake kinetics by freshwater mollusc soft body under hard and soft water conditions. Chemosphere 32: 1937-1948.

Zaback, D.A., L.M. Pratt, and J.M. Hayes, Transport and reduction of sulfate and immobilization of sulfide in marine black shales, Geology, 21, 141-144, 1993.

Zawislanski, P.T., and M. Zavarin. 1996. Nature and rates of selenium transformations in Kesterson Reservoir soils: A laboratory study. Soil Sci. Soc. Am. J. 60:791-800.

Zawislanski, P.T., A.E. McGrath, S.M. Benson, H.S. Mountford, T.M. Johnson, L. Tsao, J. Oldfather, A.F. Haxo, and T.C. Sears. 1995. Selenium Fractionation and Cycling in the Intertidal Zone of the Carquinez Strait. Annual Report, November 1995. Lawrence Berkeley National Laboratory Report 39515.

Zawislanski, P.T., A.E. McGrath, S.M. Benson, H.S. Mountford, T.M. Johnson, S. Myneni, L. Tsao, J. Oldfather, A.F. Haxo, and T.C. Sears. 1996a. Selenium Fractionation and Cycling in the Intertidal Zone of the Carquinez Strait. Quarterly Progress Report, January 1996. Lawrence Berkeley National Laboratory Report 39517.

Zhabina, N.N., and I.I. Volkov. 1980. Trace level sulfur measurements by cryogenic concentrating for HG-AAS. In Environmental Biogeochemistry and Geomicrobiology, W.E. Krumbein (ed.), Ann Arbor Sci., Ann Arbor, MI, 1980, p. 735-790.

Zhang, G.H., M.H. Hu, Y.P. Huang, and P.J. Harrison. 1990. Se uptake and accumulation in marine phytoplankton and transfer of Se to the clam Puditapes philippnarum. Marine Environmental Research, 30: 179-190.

Zwolsman, J.J.G., G.W. Berger, and G.T.M. Van Eck. 1993. Sediment accumulation rates, historical input, postdepositional mobility and retention of major elements and trace metals in salt marsh sediments of the Scheldt estuary, SW Netherlands. Mar. Chem. 44:73-94.

Appendix A.-- SOPs for Sediment Extraction

A.1 Interstitial Water Extraction and Sample Homogenization

Wetland soils and intertidal sediments have a high water content in the field, and therefore require de-watering before moisture content can be determined. The following method is used to extract interstitial water and leave sediments and soils at a constant water content.

OBJECTIVE

To remove excess interstitial water, and homogenize the soil sample.

APPARATUS

250 mL centrifuge bottles
High speed centrifuge
Milipore 0.45 µm filter cartridges
60 mL syringes
Metal bowl
Soil chopper

PROCEDURE

Mix sample to homogenize material. Weigh out 300 g of wet soil. Centrifuge at 10,000 rpm for 30 min and remove all of the supernatant solution. Filter the interstitial water using the syringe and 0.45 µm filter apparatus. If suspended sediments persist after initial centrifugation, samples should be centrifuged for additional time. Sediments should be rehomogenized, and pebbles and plant material greater in size than 0.5 cm should be removed.

A subsample of the homogenized soil (10.0 g) should be weighed into a tared soil can and dried at 104.5°C for 24 hr. Moisture content (θ) values are calculated from the oven-dry mass (OD) using the formula:

$$\theta = \frac{M_W}{M_{OD}},$$

where M_W is the mass of water removed from the soil by dessication (M_i - M_{OD}) and M_{OD} is the OD mass of the soil after dessication. θ can be used to determine the mass of residual water in the original homogenized sample, and determine the amount of OD soil in a specific mass of homogenized soil. To obtain the mass of OD, use the following formula:

$$M_{OD} = \frac{M_i}{(1+\theta)}$$

where M_i is the mass of homogenized moist soil, θ is the water content or theta value, and M_{OD} is the oven-dry mass of soil.

The supernatant solution is saved for Se analysis (selenite, selenite + selenate, and total selenium). Soils are frozen for use in sequential extractions, the final mass of the soil + residual water are recorded in order to correct subsequent sequential extractions (Distilled Water Extraction) for residual water extracted Se in the soils.

A.2 Distilled Water Extraction

OBJECTIVE

To extract free or unadsorbed Se from soils and sediments in wetland and intertidal areas.

APPARATUS

250 mL centrifuge bottles
High speed centrifuge
Milipore 0.45 µm filter cartridges
60 mL syringes
Distilled water
Reciprocating shaker

PROCEDURE

Weigh out 10.00 g (2.0 g) of dewatered-homogenized soil. Add distilled water to the soil at a soil:water ratio of 1:2 (if 2.0 g are used the ratio should be 4:1), accounting for the residual water calculated from the θ measurement. Shake samples on a reciprocating shaker for 1 hr, and centrifuge at 10,000 rpm for 30 min. Filter the supernatant solution using the syringe and 0.45 µm filter apparatus. If suspended sediments persist after initial centrifugation, samples should be centrifuged for additional time to minimize filtering time and loss of supernatant.

The supernatant solution is saved for Se analysis (selenite, selenite+selenate, and total selenium). If Se concentrations are too low for efficient quantification, the method of standard additions should be used to improve quantification. Soils are also saved for additional sequential extractions, the final mass of the soil+residual water are recorded in order to correct subsequent sequential extractions (Phosphate Extraction) for residual water extracted Se in the soils.

A.3 Phosphate Extraction

The phosphate extraction is used to remove adsorbed selenium, predominantly selenite, from colloid surfaces in soils. This method has been used extensively on Kesterson soils, but its applicability to bay-wetland soils and intertidal sediments is unknown. Phosphate is a strong ligand that forms inne-sphere complexes with hydroxyl groups displacing selenite on colloid surfaces. Selenate is a weaker ligand than selenite, and is therefore more easily removed from soils.

The principal problem with the use of phosphate extractions on bay sediments is the interference of organic matter (OM) in the adsorption of inorganic Se. In addition, phosphate solutions have a high pH (9.0) and therefore dissolve and release organic Se as well. This is not problematic because adsorbed Se includes both inorganic and organic, but it does reduce our total measurement of organic Se in the NaOH extract.

Also, OM can interfere with Selenite measurements, meaning that only total Se can be measured on extracts with high OM contents, and that adsorbed organic Se cannot be measured in these samples. Tests of OM interferences with spikes demonstrated that OM strongly adsorbs the selenite, removing significant amounts from solution.

OBJECTIVE

To determine the concentration of adsorbed Se remaining after distilled water extractions.

APPARATUS

250 mL centrifuge bottles
Reciprocating shaker
High speed centrifuge
Milipore 0.45 μm filter cartridges
60 mL syringes

REAGENTS

0.001 M Na_2PO_4

PROCEDURE

Usually this procedure is done sequentially after distilled water extraction of the soil. In the event that the procedure is done independently, weigh out the equivalent of 10.00 g of oven dried (OD) soil accounting for moisture contents measured from the OD weight of the soil (see procedure for obtaining θ values). Phosphate solution is added at a 5:1 ratio of solution to OD soil mass. Corrections for soil water are made using the θ values. After phosphate addition, the sample is shaken on the reciprocating shaker for 24 hr. The time the sample is placed on the shaker, and removed should be recorded. Samples are then centrifuged at 10,000 rpm for 30 min. and the supernatant solution filtered using a syringe and 0.45 μm filter apparatus. If suspended sediments persist after initial filtration, samples should be centrifuged for additional time.

The supernatant liquid is saved for Se analysis (selenite, selenite+ selenate, and total selenium). Soils are also saved for additional sequential extractions, final weight of the soil + residual phosphate solution are recorded in order to correct sequential extractions (Sodium Hydroxide Extraction) for residual phosphate extracted Se in the soils.

A.4 Sodium Hydroxide Extraction

Selenium is associated with organic fractions in sediments as covalently bound selenide (in proteins, amino acids, and humic and fulvic acids), and as adsorbed selenate and selenite. Quantification of organically bound Se (O-Se) is difficult because extraction techniques destroy Se-C bonds and turn O-Se into inorganic selenide or selenite and selenate. In addition, complete removal of organic matter is impossible in sediments without complete destruction of the OM into CO_2. Therefore, O-Se falls into four categories: protenaceous or amino acid-Se; humic and fulvic acid Se; and humin or residual O-Se. Dimethylselenide and other volatile species are assumed to be insignificant in these analyses, but measurements will be done to estimate their concentration.

Because of the difficulty of extracting organic Se from soils, several different techniques have been used to remove OM. Sodium hydroxide digestion (0.002 M NaOH at 85° C) is one of the more popular techniques, but it can oxidize OM and alter the chemical composition of the extract. It is also an ineffective extractant for OM in soil because most of the OM remains in the soil after extraction. In an attempt to address this problem Sodium hypochlorite digestion of soils is another technique developed by Lipton (1991) for the extraction of O-Se. Anderson (1963) and Lavkulich and Wiens (1970) demonstrated that hypochlorite is a more efficient technique for OM removal than peroxide, and is less likely to dissolve amorphous oxides associated with OM (Lavkulich and Wiens, 1970). Dimethylsulfoxide extraction has been proposed by Hayes (1994), but removal of DMSO from the extract is difficult, and makes further analysis of the mineral surfaces problematic. Pyrophosphate is often used, but it does not remove a sufficient amount of the OM, and still requires a more strongly basic solution.

Serious problems are associated with all methods. Transformation of O-Se to inorganic Se is predicted as a result of hydrolysis of C-Se bonds. No extraction technique has been demonstrated to completely remove OM from sediments without transforming the OM into carbon dioxide. Therefore precise quantification of Se in OM is impossible, and O-Se measurements will always be qualitative and dependent on method efficiency.

OBJECTIVE

To determine the concentration of organically-associated Se in soils and sediments that is not removed by distilled water and phosphate extractions.

APPARATUS

250 mL centrifuge bottles
Reciprocating shaker
High speed centrifuge
Milipore 0.45 µm filter cartridges
60 mL syringes

REAGENTS

0.02 M NaOH (or 0.50 or 1.0 M NaOH)

PROCEDURE

Usually this procedure is done sequentially after distilled water and phosphate extraction of the soil. In the event that the procedure is done independently, weigh out the equivalent of 10.00 g of oven dried (OD) soil accounting for moisture content (see procedure for obtaining θ values). Sodium hydroxide solution (0.02, 0.50, or 1.0 M) is added at a 10:1 ratio of solution to OD soil mass. Corrections for soil water are made using the θ values. The sample is heated in an 85°C bath for 2 h and shaken for 5 min every 30 min. Samples are then centrifuged at 10,000 rpm for up to 30 min or until all sediments have been removed from solution, and the supernatant solution is filtered using a syringe and 0.45 µm filter apparatus.

The supernatant liquid is saved for Se analysis (selenite+ selenate and total selenium). Soils are also saved for additional sequential extractions, final weight of the

soil + residual sodium hydroxide solution are recorded in order to correct sequential extractions (Acetate extraction) for residual sodium hydroxide extracted Se in the soils.

A.5 Sodium Hypochlorite Extraction (optional)

APPARATUS

250 mL centrifuge bottles
Reciprocating shaker
High speed centrifuge
Milipore 0.45 μm filter cartridges
60 mL syringes

REAGENTS

4-5 % NaOCl (pH adjusted to 9.5)

PROCEDURE

Usually this procedure is done sequentially after distilled water and phosphate extraction of the soil. In the event that the procedure is done independently, weigh out the equivalent of 10.00 g of oven dried (OD) soil accounting for moisture content (see procedure for obtaining θ values). Sodium hypochlorite solution (4-5 %) is added a 1:1 ratio of solution to OD soil mass. Corrections for soil water are made using the theta values. The sample is heated in a boiling water bath for 15 min. during each addition of hypochlorite. Samples are then centrifuged at 10,000 rpm for up to 30 min. or until all sediments have been removed from solution, and the supernatant solution is filtered using a syringe and 0.45 μm filter apparatus. Additional sodium hypochlorite is added and the soil is treated until no visible reaction occurs (up to 5 times). The supernatant is removed and collected after each treatment.

The supernatant liquid is saved for Se analysis (selenite + selenate and total selenium). Soils are also saved for additional sequential extractions, final weight of the soil + residual sodium hydroxide solution are recorded in order to correct sequential extractions (Acetate extraction) for residual sodium hypochlorite extracted Se in the soils.

A.6 Sodium Sulfite Extraction

The sodium sulfite extraction is used to remove elemental selenium in soils. This method was developed by Velinsky and Cutter (1990) for analysis of wetland soils. Sulfite forms a complex with elemental selenium which is soluble and can be removed from the soil solution.

The technique is ~90% effective at removing elemental Se from a sediment matrix when the pH is adjusted to pH 7.Interference is observed in both methods from the desorption of organic Se, and selenate and selenite, but at pH 7 only 11% of selenate and selenite is released (88% at pH 9). The problem of selenate + selenite interference can be reduced by extracting this fraction prior to sulfite extractions (see selenate-selenite extraction methods). The chemistry of this extraction is as follows:

$Sulfite_{(aq)} + Se_o$ ----> $Se\text{-}Sulfite_{(aq)}$.

Sulfite reacts with the elemental selenium forming a seleno-sulfite complex which solublizes the selenium.

Because of the difficulty of completely removing OM with preliminary extraction techniques (sodium hydroxide or sodium hypochlorite), interference from organic Se cannot be completely eliminated, but after removal of selenate and selenite, interferences should be minimal. Use of sodium hypochlorite to remove organic Se interferes strongly with elemental Se measurements because hypochlorite is a strong oxidizer that transforms all reduced Se species, including elemental Se.

OBJECTIVE

To determine the concentration of elemental Se in soils.

APPARATUS

50 mL centrifuge tubes
Sonicating bath
Ultrasonic Probe (with microprobe attachment)
Reciprocating shaker
High speed centrifuge
Milipore 0.45 µm filter cartridges
60 mL syringe

REAGENTS

1.0 M Na_2SO_3 (pH adjusted to 7.0 using concentrated HCl)
Concentrated Nitric acid
8 M Urea
4 M HCl

PROCEDURE

The oven-dried soil from the OHx is ground to a fine powder and 0.60 g is weighed into a 50 mL centrifuge tube. 3 mL of sulfite solution is added to the ground oven-dried soil mass. After sulfite addition, the sample is sonicated for one minute with the Ultrasonic probe (at a setting of 1.5) and then sonicated in the sonicating bath for 6 hr. Samples are then centrifuged at 10,000 rpm for 30 min. and the supernatant solution is filtered using the syringe and Millipore filter apparatus. Two 3 mL washes of of sulfite solution are used to rinse out the remaining sulfite extracted Se with a final 3 mL rinse of distilled water to remove the residual sulfite solution from the sample prior to drying. The rinses and the extract are combined and digested using nitric acid.

5 mL of extract is added to a 30 mL beaker and 1 mL of concentrated nitric acid is added to the beaker. The beaker is covered with a watch-glass and the solution is heated on a hot plate to reflux for 1 hr (set hot plate temperature to ~95° C). Uncover beakers after 1 hr and allow the sample to evaporate to near-dry. Add 0.5 mL and again allow the sample to reach near dryness before adding an additional 0.5 mL of water. If sample is to be stored for a significant period of time (> 2 days) add 10 mL of 4 M HCl to dissolve the sample, 0.5 mL 8 M urea (to remove residual nitric acid interference in analysis) and bring the volume up to 25 mL in a volumetric flask. If samples will be analyzed immediately (< 2 days), omit the 4 M HCl.

The supernatant solution is saved for Se analysis (total selenium) using an acid boil. Soils are also saved for additional sequential extractions, final weight of the soil +

residual phosphate solution are recorded in order to correct sequential extractions (pyrite extraction) for residual phosphate extracted Se in the soils.

A.7 Pyrite-Se Extraction (optional)

APPARATUS

Liquid Nitrogen Trapping Apparatus with Elution Column
High speed centrifuge
Milipore 0.45 µm filter cartridges
60 mL syringes

REAGENTS

Zn pellets
Conc. HCl
1.0 M $CrCl_3$ (in 1.0 M HCl)

PROCEDURE

Prepare extracting solution by placing Zn pellets into 100 mL of $CrCl_3$ solution. Allow to react until solution has turned from a green to a deep blue color indicating that Cr (III) has been reduced to Cr (II) chloride. Place 60 to 80 mg of the washed and dried soil sample from the sulfite extraction and suspend it in 15 mL of distilled water. Place solution in stripper and purge for 90 s. Turn six-way valve to allow carrier gases to vent and place trap in LN_2 bath. Add 5 mL HCl and 10 mL Cr (II) solution. After 25 min stirring, turn valve to direct carrier gas through the poropak PS (50/80 mesh) column. Retention time for the samples is approximately 1.8 min with an 80 cm column (200 mL/min flow rate). H_2S elute before H_2Se and can often cause detection problems with the samples. Quantification is done by peak integration of the absorbance peak detected on the AAS.

A.8 Total Acid Digestion (TAD) Procedure

OBJECTIVE

To determine the total Se content of soils and sediments from estuarine environments.

APPARATUS

balance--0.000g
50ml Teflon FEP centrifuge tubes
hot plate
aluminum digestion block
25 ml volumetric flasks
Milipore 0.45 µm filter cartridges

REAGENTS

conc. HNO_3
30% Hydrogen Peroxide
6M HCL

8M Urea

PROCEDURE

Oven dry at least 10 grams of soil from a pre-homogenized bulk sample at 104.5°C. Powder with a mortar and pestle, or ball mill sample to a fine matrix. Place 1 gram of soil into a teflon FEP tube. Add 2.0 ml of concentrated HNO_3 to each tube. Swirl gently. Add 1 ml of H_2O_2 to each tube. If vigorous effervescence occurs, mix and tap gently on the tube to prevent overflow. When the reaction has ceased, add additional hydrogen peroxide to those tubes in which the reaction has occurred (add enough so that the reaction subsides, not to exceed 10 mls). Insert tubes into the preheated digestion block (approximately 90 degrees celsius) for a period of 24 hours. Ensure that the tube caps are somewhat loosened to avoid excessive pressure build-up. Approximately 3 hours before the 24 hour period ends, i.e., at hour 21, remove the caps from the tubes and evaporate the nitric/h. peroxide mixture from the tubes. AVOID complete evaporation. When the liquid level has diminished so that the soil is damp, this process is complete. Do not let the soil go completely dry.

To each of the tubes, add 15 ml of 6M HCl. Sonicate samples for 3 minutes in a heated bath. Maximum temperature for the bath is 60°C. Return tubes to the digestion block for 24 hours. At the end of the 24 hour period, remove the tubes from the block and centrifuge them at 7000 rpm for 3-5 minutes. Be sure that the caps are tightened before centrifuging. Remove the tubes from the centrifuge and decant the supernatent solution into a 25 ml volumetric flask. Next, add 10 ml of 6M HCl to each tube. Sonicate the samples for 3 minutes in a 60°C. Put samples back on the digestion block and let them digest for 30 minutes at 90°C. Subsequently, centrifuge the tubes at 7000 rpm and decant the supernatent solution into 25 ml volumetric flasks. When warm, add 0.5 ml of 8M urea to each volumetric flask. Top-off with distilled water.

Appendix B. -- Quality Assurance and Control

The staff of the LBNL Earth Science Division (ESD) has been performing quality-controlled selenium analyses since 1987. The quality assurance program was established as a contract requirement with the U.S. Bureau of Reclamation and it has proven convenient to apply this program to all subsequent studies. Selenium analyses are performed by the staff of the Environmental Measurements Laboratory (EML).

B.1 Analytic Technique

Se analyses are performed on a Perkin-Elmer 3030 Atomic Absorption Spectrophotometer with a Varian Hydride Generator (HG-AAS). Selenite is analyzed by introducing the sample directly into the hydride generator. Total selenium is prepared for analysis by mixing 5.0 ml of a sample with an equal volume of concentrated (~37%) hydrochloric acid and between 0.2 and 0.5 ml of a 2% ammonium persulfate solution to oxidize any organic selenium compounds and other potentially interfering organic compounds. The mixture is heated at 98° C for 10 minutes to reduce all selenate to selenite, then allowed to cool and is introduced into the hydride generator for reading. The values reported to investigators are selenite and total selenium concentrations. Selenate concentration may be calculated from these values but is itself not directly subject to quality control because it is a derived quantity.

Analysis of ultra-trace levels of Se is performed using either a cold-trap HGAAS method or a La coprecipitation method, as described in Chapter 9. The same QA/QC procedures are applied to all types of analyses.

B.2 The Quality Control Process

Sample sets are assigned set numbers and tend to have 20 - 80 samples per set. Every seventh sample is a quality control, QC, sample. The QC coordinator will prepare the QC samples. The QC samples are used to track different aspects of the analysis. Once the sample set has been considered in control the results are sent to the analyst and requester. After this the sample sheets are stored in a binder for reference at a later date.

The different types of QC samples are a Blank, Matrix Spike, Standard and Duplicate. The blank represents any type of contamination that may occur during analysis. These can include: carry over on the instrument, contaminated reagents, contaminated glassware or pipettors, or improper hydride generation. The QC limit for blanks is the value must be less than the practical quantitation limit, PQL. Therefore if the samples are analyzed for selenite the blank must be less than 0.32 $\mu g\ L^{-1}$ if the samples were total acid digests, TADs, which are diluted 10.2 times, the blank must be less than 3.2 $\mu g\ L^{-1}$. Blanks are prepared by adding Nanopure water to an empty QC bottle.

Matrix spikes are used to determine if there is something in the sample suppressing or enhancing the results for the selenium analysis. The quality control limits for acceptance for matrix spikes is ± 25% or 75 to 125% recovery of the matrix spike. A matrix spike may be considered, "not statistically meaningful", NSM, if the sample is greater than three times the spike of selenium. The spiking solution contains both selenite and selenate. Since the main objective is to speciate the selenate and selenite the recovery of both of these compounds is tracked. There are two different spiking solutions. One is a high level solution, primarily meant for TADs. The second is for all other extraction methods and is at a much lower concentration. The high level spike contains 3030 $\mu g\ L^{-1}$ total selenium, presently, with 46% being selenite. The low-level spike contains 710 $\mu g\ L^{-1}$ total selenium, presently, with 29% being selenite. Matrix spikes are prepared by adding a known amount of the research sample to an empty QC bottle and spiking the solution with a know amount of selenium standard

Standards are meant to serve as a secondary check to verify the calibration curve, conversion of selenate to selenite, and technique of the analyst. A standard has a much tighter control limit of ± 15% or 85 - 115% recovery. The same spiking solution used for the matrix spike is used for the standard QC sample. Standards are prepared by adding Nanopure water and spiking the water with a known amount of selenium standard.

Duplicates are used to verify sample homogeneity, analyst technique, and instrument stability. A duplicate is considered in control when the relative percent difference, RPD, between the two samples are within 20 %. Where RPD is defined as

$$\frac{200 * |C_1 - C_2|}{(C_1 + C_2)}$$

C_1 and C_2 are the sample values. If the samples are below the lowest point of the calibration curve then the samples are considered NSM. Duplicate samples are prepared by pouring from the research sample bottle into a provided empty QC sample bottle

B.3 Measurements

A total of 1775 research samples were analyzed for total selenium with a QC load of 22.0%. Therefore 1455 samples were analyzed for total selenium. There were 9 different types of research samples. The types are total acid digests (TAD), sulfite extracts (Sx), solid particulate matter (SPM), sodium hydroxide extracts (OHx), phosphate extracts (Px), interstitial water (INT), water extracts (Dx), Microcosm experiment (Micro), and plant total acid digests (Plant).

Of the total research samples submitted the breakdown was as follows:

Table B.1 Summary of the types of analytical samples submitted for Se analysis and the number of corresponding QC samples.

Extract Type	Total Samples	QC Samples	Analytical Samples
TAD	423	85	338
Sx	114	26	88
SPM	60	10	50
OHx	151	34	119
Px	151	34	117
INT	518	66	451
Dx	135	24	111
Micro	104	19	85
Plant	119	23	96
Totals	1775	321	1454

B.3.1 Blanks

The practical quantitation limit, PQL, is a control limit for blanks. In conventional HG-AAS analysis for total selenium this is presently 1.02 ug/L. Looking at the concentrations of total selenium plotted vs. number of analysis (Fig. B.1), we can see that on five occasions the blank would appear out of control for a total of 70 blank QC

samples. In each case, the sample sets were diluted by a factor of 10.2 because of high selenium levels. The dilution factor therefore took the blank above the typical PQL.

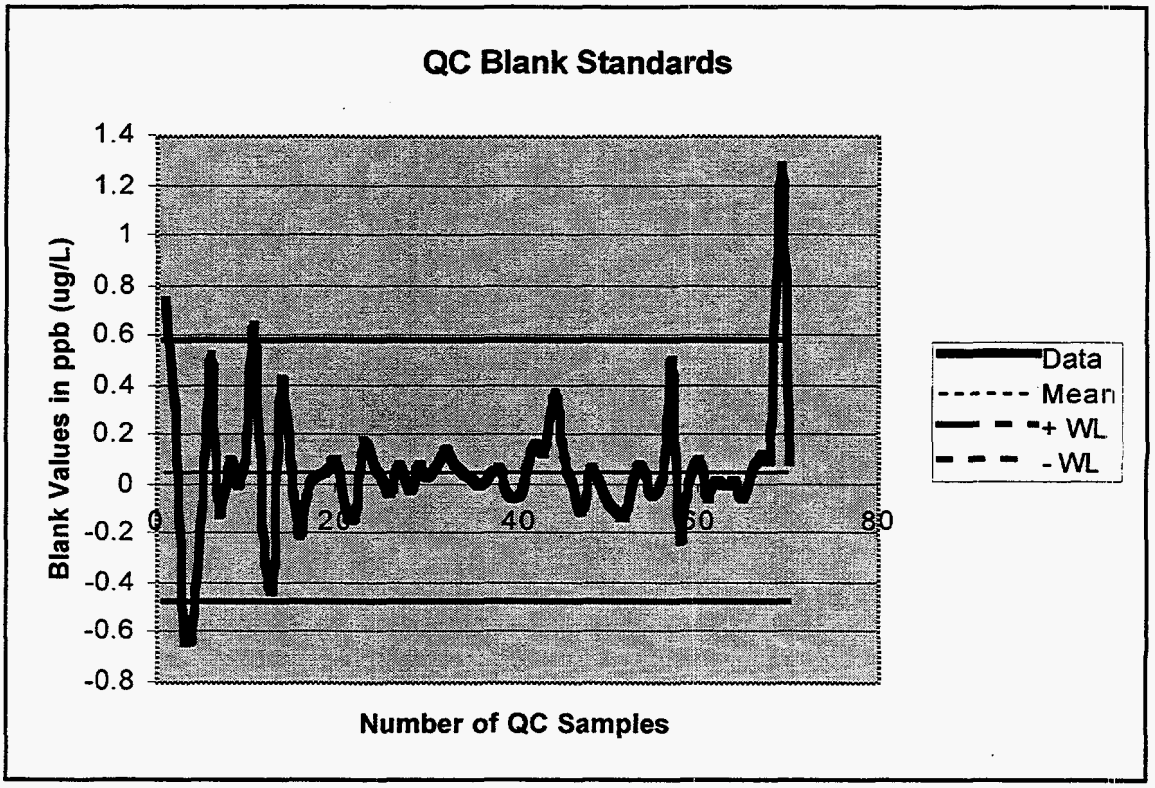

Figure B.1 Total selenium concentrations for Blank QC samples.

B.3.2 Matrix Spikes

A warning limit, WL, is considered to be two standard deviations from the mean value. In this case the warning limit range is 71 - 115 % recovery. Where the QC range is 75 - 125 % recovery. In Fig. B.2, we can see that the data except for five points are within the warning limits. In the case of the five outliers, the samples were reanalyzed and came back in control after the second analysis.

B.3.3 Standards

Standards tend to have a much tighter QC limit than matrix spikes because of the lack of matrix interference. In Fig. B.3, we can see that 101 standard QC samples were analyzed this year for total selenium. There were two samples outside of the warning limits. Both of these samples were at very low levels. Therefore the recovery of these samples will fluctuate significantly with small changes. Otherwise the data here reflects that the standards behaved as expected to validate the data represented by the

researchers in this report. The only outliers came during the analysis for INT extracts. In this case there was not enough sample for reanalysis.

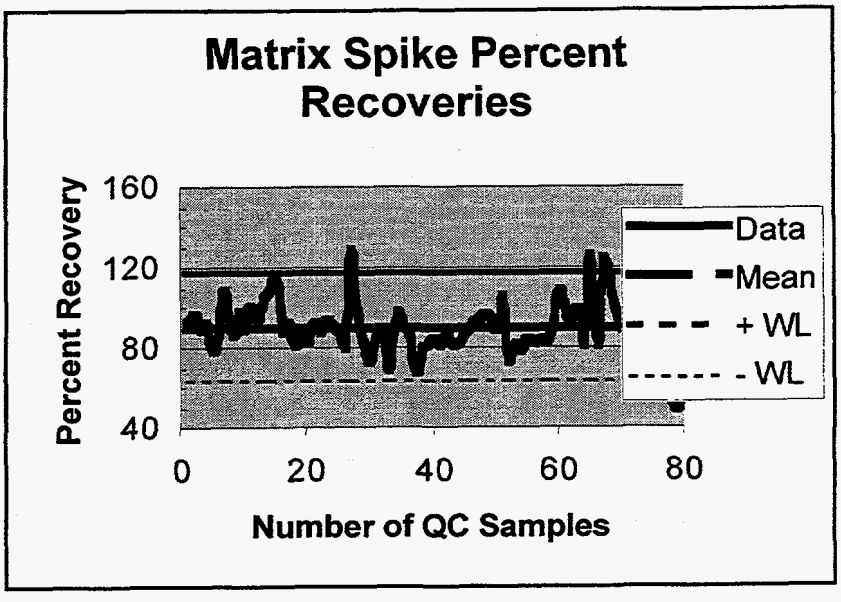

Figure B.2 Total selenium concentrations for Matrix Spike QC samples.

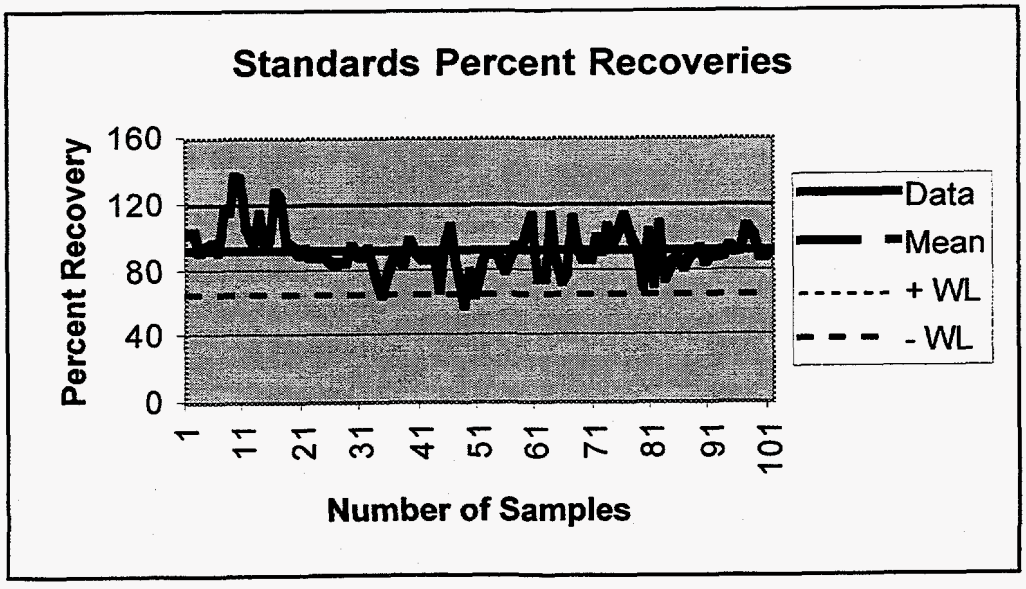

Figure B.3 Total selenium concentration for Standard QC samples.

B.3.4 Duplicates

A total of 88 selenium duplicate QC samples were analyzed. The range of RPD was from 0 to 35 with 16 samples being reanalyzed because they were above 20%.